

The tyrosine regulated DAHP synthase and the biosynthetic  
pathway of aromatic amino acids in *Saccharomyces cerevisiae*

Dissertation  
zur Erlangung des Doktorgrades  
der Mathematisch-Naturwissenschaftlichen Fakultäten  
der Georg-August-Universität zu Göttingen

vorgelegt von  
**Andrea Grzeganeck**  
**geb. Pfeil**  
aus Stade

Göttingen 2005

D7

Referent: Prof. Dr. G. Braus

Korreferent: PD Dr. Stefan Irniger

Tag der mündlichen Prüfung: 02.11.2005

Die vorliegende Arbeit wurde in der Zeit von Juni 2000 bis Juli 2004 im Institut für Mikrobiologie und Genetik der Georg-August-Universität zu Göttingen unter der Leitung von Prof. Dr. G.H. Braus angefertigt.

A little light in a dark room  
is still a great illumination.

Ernest Holmes

*Für meine Eltern  
und Peter*

# Table of contents

Abbreviations.....	4
Summary.....	7
Zusammenfassung.....	9
1. Introduction.....	11
1.1. Biosynthesis of Aromatic Amino Acids .....	11
1.1.1. The Shikimate Pathway .....	12
1.1.1.1. DAHP synthase (EC 2.5.1.54).....	16
1.1.1.1.1. TIM barrel.....	17
1.1.1.1.2. PEP utilizing enzymes .....	19
1.1.2. The phenylalanine-/tyrosine-branch.....	21
1.1.2.1. The chorismate mutase (EC 5.4.99.5).....	22
1.1.2.2. The prephenate dehydrogenase (EC 1.3.1.12) .....	23
1.1.2.3. The prephenate dehydratase (EC 4.2.1.51) and a regulatory domain .....	23
1.1.3. The tryptophan branch.....	24
1.1.3.1. The anthranilate synthase complex (EC 4.1.3.27) .....	25
1.1.4. Regulation of the aromatic amino acid biosynthesis of <i>S. cerevisiae</i> .....	25
1.1.4.1. Regulation of enzyme activities of aromatic amino acid biosynthesis .....	25
1.1.4.2. General control of amino acid biosynthetic pathway in fungi.....	26
1.1.4.3. Networks of regulatory pathways .....	28
1.2. Aim of this work .....	29
2. Materials and Methods.....	30
2.1. Materials .....	30
2.1.1. Chemicals .....	30
2.1.2. Strains and plasmids.....	30
2.2. Methods.....	34
2.2.1. Cultivation of cells .....	34
2.2.1.1. Cultivation of <i>E. coli</i> .....	34
2.2.1.2. Cultivation of <i>S. cerevisiae</i> .....	34
2.2.1.3. Cell storage .....	35
2.2.2. Nucleic Acid Methods.....	35
2.2.2.1. Isolation of plasmid DNA of <i>E. coli</i> .....	35

2.2.2.1.1. Quick-Prep.....	35
2.2.2.1.2. Qiagen plasmid-DNA-Midi-preparation.....	35
2.2.2.2. Isolation of chromosomal DNA from <i>S. cerevisiae</i> .....	35
2.2.2.3. DNA gel extraction.....	36
2.2.2.4. Determination of concentration of nucleic acids and purity control .....	36
2.2.2.5. Agarose gel-electrophoresis.....	36
2.2.2.6. Polymerase chain reaction (PCR) .....	36
2.2.2.6.1. Introduction of site-directed mutations .....	37
2.2.2.7. Enzymatical modification of nucleic acids .....	37
2.2.2.7.1. Restriction of DNA .....	37
2.2.2.7.2. Ligation of DNA fragments.....	37
2.2.2.7.3. DNA sequencing.....	37
2.2.2.8. Transfer of DNA to <i>E. coli</i> .....	38
2.2.2.8.1. Production of competent cells.....	38
2.2.2.8.2. Transformation of <i>E. coli</i> .....	38
2.2.2.9. Transfer of DNA to <i>S. cerevisiae</i> .....	38
2.2.2.10. Transfer of nucleic acids on membranes.....	39
2.2.2.10.1. Southern Blot .....	39
2.2.2.11. Radiolabeling of DNA-fragments with [ $\alpha$ - <sup>32</sup> P] dATP .....	39
2.2.2.12. Hybridisation of radioactive labeled probes.....	39
2.2.3. Protein Methods.....	39
2.2.3.1. Production of crude extracts of yeast cells.....	39
2.2.3.2. Purification of DAHP synthase .....	40
2.2.3.3. Purification of prephenate dehydratase.....	40
2.2.3.4. Gelfiltration .....	40
2.2.3.5. Concentration of enzyme solutions .....	40
2.2.3.6. Determination of protein concentration.....	40
2.2.3.7. Elektrophoretical methods .....	41
2.2.3.7.1. Discontinuous SDS-PAGE.....	41
2.2.3.7.2. Blue-Native PAGE .....	41
2.2.3.8. Transfer of proteins to membranes .....	42
2.2.3.9. Staining proteins.....	42
2.2.3.9.1. Coomassie staining.....	42
2.2.3.9.2. Silver staining.....	42
2.2.3.10. Determination of the molecular masses of proteins .....	43
2.2.3.11. DAHP synthase assay.....	43
2.2.3.12. Prephenate dehydratase assay.....	43

2.2.3.13. Evaluation of kinetic data.....	44
2.2.3.14. Sample preparation for mass spectrometry by tryptical restriction.....	44
2.2.3.15. Mass spectrometry .....	44
3. Results .....	46
3.1. The tyrosine-regulated DAHP synthase of <i>S. cerevisiae</i> .....	46
3.1.1. Catalysis and regulation.....	46
3.1.1.1. The substrate binding site of yeast Aro4p .....	46
3.1.1.2. Transmission of the inhibition signal within the tyrosine-regulated DAHP synthase .....	49
3.1.2. Tyrosine regulated DAHP synthase of <i>S. cerevisiae</i> is a dimer .....	57
3.1.2.1. Oligomeric status of Aro4p .....	57
3.1.2.2. The dimeric interface of tyrosine regulated DAHP synthase .....	59
3.2. The role of phenylalanine in the regulation of the biosynthetic pathway of aromatic amino acids.....	61
3.2.1. The phenylalanine branch.....	63
3.2.1.1. The prephenate dehydratase .....	63
3.2.1.2. The regulatory domain of the prephenate dehydratase of <i>S. cerevisiae</i> .....	66
3.2.2. Phenylalanine inhibition of <i>aro7<sup>c</sup> gcn4 S. cerevisiae</i> strains .....	70
3.2.2.1. The regulated Pha2p-Asp308Glu mutant does not restore growth of an <i>aro7<sup>c</sup> gcn4</i> strain in the presence of phenylalanine .....	70
3.2.2.2. Overexpression of the <i>TRP2/TRP3</i> genes encoding the anthranilate synthase complex suppress the growth inhibition by phenylalanine of the <i>aro7<sup>c</sup> gcn4</i> mutant strain.....	71
3.2.2.3. The tyrosine regulated DAHP synthase and the effect of phenylalanine .....	74
4. Discussion .....	79
4.1. Catalysis of DAHP synthase.....	79
4.2. Transmission of the inhibition signal within the DAHP synthase .....	83
4.2.1. The intramolecular transmission of the inhibition signal.....	84
4.2.2. The intermolecular transmission of the inhibition signal.....	85
4.3. Phenylalanine regulation of the aromatic amino acid pathway.....	90
4.3.1. The prephenate dehydratase of <i>S. cerevisiae</i> .....	90
4.3.2. The “phe-effect” of <i>aro7<sup>c</sup> gcn4 S. cerevisiae</i> strains .....	90
5. Conclusions.....	94
6. References .....	95

## Abbreviations

∅	diameter
°C	degree Celsius
A	adenine
A5P	D-arabinose 5-phosphate
ACT	<u>a</u> spartokinase, <u>c</u> horismate mutase, prephenate dehydrogenase (TyrA)
AMYME	<i>Amycolatopsis methanolica</i>
<i>A. nidulans</i>	<i>Aspergillus nidulans</i>
BACSU	<i>B. subtilis</i>
<i>B. subtilis</i>	<i>Bacillus subtilis</i>
BSA	bovine serum albumine
C	Cytosine
CDRP	carboxyphenylamino-1-deoxy-ribulose 5-phosphate
Da	Dalton
DAHP	3-deoxy-D- <i>arabino</i> -heptulosonate-7-phosphate
ddNTP	dideoxynucleosid-5-triphosphate
DHQ	3-dehydroquinate
DHS	3-dehydroshikimate
DMSO	dimethylsulfoxide
DNA	deoxyribonucleic acid
DNase	deoxyribonuclease
dNTPs	deoxyribonucleoside triphosphates
DTT	dithipthreitol
<i>E. coli</i>	<i>Escherichia coli</i>
ECOLI	<i>E. coli</i>
E4P	erythrose-4-phosphate
EAS	ethylaminosepharose
EDTA	ethylenediaminetetraacetate
EPSP	<i>enol</i> pyruvylshikimate-3-phosphate
FPLC	fast protein liquid chromatography
g	gram
G	guanine
GDP	guanosine diphosphate
GTP	guanosine triphosphate
h	hour
IGP	indole-3-glycerol-phosphate

k-	kilo
$K_{cat}$	catalytic constant
KDOP	3-deoxy-D- <i>manno</i> -2-octulosonate-8-phosphate
$K_i$	inhibition constant
$K_m$	Michaelis-Menten-constant
l	liter
$L^*$	loop with the number *
$\lambda$	wavelength
LACLA	<i>Lactococcus lactis</i>
LB	Luria-Bertani
m	meter
M	molar
m-	milli
$\mu$ -	micro
<i>MAT</i>	mating type
min	minute
MV	<u>m</u> inimal <u>y</u> itamins
n-	nano
$NAD^+$	nicotinamide adenine dinucleotide (oxidized form)
$NADP^+$	nicotinamide adenine dinucleotide phosphate (oxidized form)
<i>N. crassa</i>	<i>Neurospora crassa</i>
NEIGO	<i>Neisseria gonorrhoeae</i>
OD	optical density
ORF	open reading frame
p-	pico
PAGE	polyacrylamide gel electrophoresis
PCR	polymerase chain reaction
PDH	prephenate dehydrogenase
PDT	prephenate dehydratase
PEP	phospho <i>eno</i> lpyruvate
pH	potentia hydrogenii
PMSF	phenylmethylsulfonylfluorid
PPB	potassium phosphate buffer
P-protein	bifunctional prephenate dehydratase
PQQ	pyrrolo-quinoline quinone
PRA	phosphoribosylanthranilate
PTT	phenylalanine, tyrosine and tryptophan as supplements to MV medium

R <sub>f</sub>	migration distance of the protein/ migration distance of the dye
RNA, m, t	ribonucleic acid, messenger, transfer
RNase	ribonuclease
rpm	rotations per minute
<i>S. cerevisiae</i>	<i>Saccharomyces cerevisiae</i>
S3P	shikimate-3-phosphate
SCF	<u>S</u> kp1/ <u>c</u> ullin/ <u>E</u> -box protein
SDS	sodium dodecylsulfate
sec	second
STET	<u>s</u> odium chloride, <u>T</u> ris-HCl, <u>E</u> DTA, <u>T</u> riton X-100
T	temperature
T	thymine
TAE	<u>T</u> ris-HCl, <u>a</u> cetate, <u>E</u> DTA
TE	<u>T</u> ris-HCl, <u>E</u> DTA
TIM	triosephosphate isomerase
<i>T. maritima</i>	<i>Thermotoga maritima</i>
T-protein	bifunctional prephenate dehydrogenase
TSR	template suppression reagent
U	unit
U	uracil
uORF	upstream-located open reading frame
UV	ultraviolet
V	volt
v <sub>i</sub>	initial velocities
YEAST	<i>S. cerevisiae</i>
YEPD	<u>y</u> east <u>e</u> xtract, <u>p</u> eptone, <u>d</u> extrose

## Summary

3-Deoxy-D-*arabino*-heptulosonate 7-phosphate (DAHP) synthases (EC 2.5.1.54) catalyze the initial reaction of the aromatic amino acid biosynthetic pathway. Phosphoenolpyruvate (PEP) and erythrose-4-phosphate (E4P) are condensed to DAHP. There are two DAHP synthases in baker's yeast *Saccharomyces cerevisiae*, encoded by the genes *ARO3* and *ARO4*, that can be feedback-inhibited by phenylalanine and tyrosine, respectively. Crystal structures of the phenylalanine regulated DAHP synthase of *Escherichia coli* and of the tyrosine inhibitable isoenzyme of *S. cerevisiae* are available. With the help of amino acid substitutions at the catalytic center (Lys112Ala, Arg114Ala and Arg180Ala), the amino acid residues located in the loops L2 and L4 were shown to be essential for catalysis.

The structural elements of the allosteric site where the feedback-inhibitor tyrosine can be bound have to communicate to the catalytic center. Amino acid residue substitutions revealed that this communication includes a signal transduction pathway within the DAHP synthase monomer. Inhibitor binding results in a loss of contact between the loop L3 (Leu160) and loop L2 (Glu111). The inhibitor binding pulls the loop L3 in addition to the  $\beta$ -sheets  $\beta 0^*$ ,  $\beta 6a$  and  $\beta 6b$  towards the inhibitor molecule, which in turn destabilizes the catalytic site. In addition, inhibitor binding results in a crosstalk between the two monomers of a dimer because helix  $\alpha 4$  of one monomer (Gln185, Arg188, Glu189) loses intermolecular contacts in the form of hydrogen bonds to loop L2 of the second monomer (Arg114, Thr115, Lys120). This enhances the destabilizing effect on the catalytic center. The dual inhibitory pathways presumably result in reduced binding of substrates which reduces the activity of the enzyme. Native PAGE experiments suggest that the dimer is the preferred oligomerization state of Aro4p.

Phenylalanine is only known to feedback-inhibit the *ARO3* encoded DAHP synthase of yeast within the pathway. We analyzed whether the phenylalanine-specific branch in the aromatic amino acid biosynthetic pathway is also subject of phenylalanine regulation. Therefore the *PHA2* encoded prephenate dehydratase was expressed as *Strep-tag*<sup>®</sup> fusion protein and purified. The enzyme displayed an unregulated Michaelis-Menten-kinetic with a  $k_{cat} = 16 \text{ s}^{-1}$ . A single amino acid substitution in the NSRP (Asp308Glu) site of a domain with similarities to the ACT regulatory domain resulted in an enzyme with a significant reduced specific activity which can be feedback-inhibited by phenylalanine. These data suggest that the yeast Pha2 protein might be the derivative of a regulated ancestor which has lost the phenylalanine regulation during the course of evolution.

A yeast strain with an unregulated and constitutively active chorismate mutase activity which is also defective in the general control transcriptional network (*ARO7<sup>c</sup>*, *gcn4*) is impaired in

growth when phenylalanine is added to the cultivation medium. This so-called “phe-effect” can be suppressed when the genes *TRP2/TRP3* encoding the anthranilate synthase complex at the initial step of the tryptophan specific branch are overexpressed. Similarly, the addition of anthranilate or tryptophan can restore growth suggesting that the phe-effect is the result of tryptophan starvation. The *ARO4* gene encoding a tyrosine-inhibitable DAHP synthase at the initial step at the shikimate pathway is also but less effectively feedback-inhibited by phenylalanine. When we substituted the *ARO4* gene by an allele which results in an unregulated enzyme (Aro4p<sup>T162L</sup>) the phe-effect was lost and the resulting *ARO4*<sup>T162L</sup>, *gcn4*, *ARO7*<sup>c</sup> strain was able to grow in the presence of phenylalanine. Therefore the phe-effect is the result of an additional regulation of the *ARO4* gene product besides tyrosine also by phenylalanine which results in a diminished metabolic flux towards chorismate. A constitutively active chorismate mutase has to be counteracted under these conditions by the general control to prevent the phe-effect.

## Zusammenfassung

3-Deoxy-D-*arabino*-Heptulosonat 7-Phosphat (DAHP) Synthasen (EC 2.5.1.54) katalysieren die erste Reaktion des Biosyntheseweges. Das aus der Glykolyse kommende Phospho*eno*lpyruvat (PEP) und das aus dem Pentosephosphatweg stammende Erythrose-4-Phosphat (E4P) werden zu DAHP kondensiert. In der Bäckerhefe *Saccharomyces cerevisiae* liegen zwei DAHP Synthasen vor, die durch die Gene *ARO3* und *ARO4* kodiert werden und durch die Endprodukte Phenylalanin bzw. Tyrosin inhibiert werden können. Kristallstrukturen von der Phenylalanin regulierten DAHP Synthase aus *Escherichia coli* und dem Tyrosin inhibierbaren Isoenzym aus *S. cerevisiae* sind vorhanden. Mithilfe von Aminosäuresubstitutionen am katalytischen Zentrum (Lys112Ala, Arg114Ala and Arg180Ala) konnte die Bedeutung der für die Katalyse wichtigen Reste der Loops L2 und L4 gezeigt werden.

Die Strukturelemente, die wichtig für die Katalyse sind, kommunizieren mit dem Allosteriezentrum, an das der Inhibitor Tyrosin gebunden werden kann. Substitutionen von Aminosäureresten machen deutlich, dass diese Kommunikation einen Signaltransduktionsweg innerhalb des Monomers beinhaltet. Die Inhibitorbindung resultiert in dem Verlust des Kontaktes zwischen den Loops L3 (Leu160) und L2 (Glu111). Durch die Bindung des Inhibitors wird Loop L3 neben den  $\beta$ -Faltblattstrukturen  $\beta 0^*$ ,  $\beta 6a$  und  $\beta 6b$  zum Inhibitormolekül gezogen, wodurch das katalytische Zentrum destabilisiert wird. Außerdem führt die Bindung des Inhibitors zur Kommunikation zwischen den zwei Monomeren eines Dimers durch den Verlust von intermolekularen Kontakten in Form von Wasserstoffbrückenbindungen zwischen Helix  $\alpha 4$  des einen Monomers (Gln185, Arg188, Glu189) und Loop L2 des anderen Monomers (Arg114, Thr115, Lys120). Das verstärkt den destabilisierenden Effekt auf das katalytische Zentrum. Diese dualen inhibitorischen Wege resultieren vermutlich in einer reduzierten Substratbindefähigkeit, wodurch die Aktivität des Enzyms reduziert wird. Native PAGE Experimente deuten daraufhin, dass das Dimer der bevorzugte Oligomierzustand von Aro4p ist.

Phenylalanin ist nur bekannt als Rückkopplungsinhibitor der *ARO3* kodierten DAHP synthase der Hefe. Wir haben untersucht, ob der Phenylalanin spezifische Ast des aromatischen Aminosäure Biosyntheseweges ebenfalls Subjekt der Phenylalanin-Regulation ist. Hierfür wurde die durch *PHA2* kodierte Prephenat-Dehydratase als *Strep-tag*® Fusionsprotein exprimiert und aufgereinigt. Das Enzym zeigte eine Michaelis-Menten-Kinetik mit einem  $k_{cat}$  von  $16 \text{ s}^{-1}$ . Ein einziger Aminosäureaustausch in der NSRP-Region (Asp308Glu) der Domäne, die Ähnlichkeit zur regulatorischen ACT-Domäne hat, resultiert in einem signifikant in der spezifischen Aktivität reduzierten Enzym, welches Feedback-reguliert ist durch

Phenylalanin. Diese Daten deuten daraufhin, dass das Pha2-Protein einen regulierten Vorläufer hat, der im Laufe der Evolution seine Regulation verloren hat.

Ein Hefestamm mit einer unregulierten und konstitutiv aktiven Chorismat-Mutase Aktivität, der zusätzlich defekt im Transkriptionsnetzwerk der Allgemeinen Kontrolle der Aminosäurebiosynthese ist (*ARO7<sup>c</sup>*, *gcn4*), ist im Wachstum beeinträchtigt, wenn Phenylalanin ins Kultivierungsmedium gegeben worden ist. Dieser sogenannte „Phe-Effekt“ kann unterdrückt werden, wenn der durch *TRP2/TRP3* kodierte Anthranilat-Synthase-Komplex zu Beginn des Tryptophan-Wegs überexprimiert wird. Ebenso kann durch die Zugabe von Anthranilat oder Tryptophan das Wachstum wieder hergestellt werden, was daraufhin deutet, dass der Phe-Effekt durch eine Tryptophan-Verhungerung zustande kommt. Die durch das *ARO4*-Gen kodierte Tyrosin-regulierte DAHP Synthase zu Beginn des Shikimatwegs wird auch, jedoch weniger effektiv, durch eine Rückkopplung mit Phenylalanin inhibiert. Durch die Substitution des *ARO4*-Gens durch ein Allel, das für ein unreguliertes Enzym (*Aro4p<sup>T162L</sup>*) kodiert, wird der Phe-Effekt aufgehoben und der resultierende *ARO4<sup>T162L</sup>*, *gcn4*, *ARO7<sup>c</sup>* Stamm ist in der Lage in Anwesenheit von Phenylalanin zu wachsen. Der Phe-Effekt ist also das Resultat einer zusätzlichen Regulation des *ARO4*-Genproduktes durch Phenylalanin, was zu einem verringerten metabolischem Fluss zu Chorismat führte. Eine konstitutiv aktive Chorismat-Mutase muss unter diesen Umständen mithilfe der generellen Kontrolle entgegengewirkt werden, um dem „Phe-Effekt“ vorzubeugen.

# 1. Introduction

## 1.1. Biosynthesis of Aromatic Amino Acids

The aromatic amino acids phenylalanine, tyrosine and tryptophan are synthesized *de novo* by archaea, eubacteria, fungi and plants, respectively. Linking the carbohydrate metabolism with the biosynthesis of aromatic compounds (Herrmann and Weaver, 1999), biosynthesis of phenylalanine, tyrosine and tryptophan is associated with high metabolic costs. To synthesize one mole phenylalanine, tyrosine and tryptophan the cell has to invest 65, 62 and 78 mole ATP, respectively (Atkinson, 1977). This is probably the reason why animals lack this biosynthetic pathway of the three aromatic amino acids and are dependent on the uptake of these compounds with their diet (Davis, 1955; Sprinson, 1961; Gibson and Pittard, 1968). Animals have only the possibility to hydroxylate phenylalanine to tyrosine by hydroxylases. Therefore the biosynthetic pathway of aromatic amino acids is well studied in the last decades as possible point of attack for new antibiotics, antifungal agents or herbicides (O'Callaghan *et al.*, 1988).

This branched and highly regulated biosynthetic pathway is generally divided into the initial shikimate pathway as a stem yielding the last common intermediate chorismic acid and the two branches resulting in either tryptophan on one side or phenylalanine and tyrosine on the other (Figure 1) (Braus, 1991; Haslam, 1993; Herrmann and Weaver, 1999; Knaggs, 1999; Knaggs, 2001; Knaggs, 2003). Chorismic acid has a key position on aromatic metabolism and is a precursor to essential metabolites and cell components. These are routes to folate coenzymes via 4-aminobenzoic acid, ubiquinones via 4-hydroxybenzoic acid, menaquinones (vitamin K) via isochorismate and siderophores or the prototype enterobactin via 2,3-hydroxybenzoic acid (Haslam, 1993).

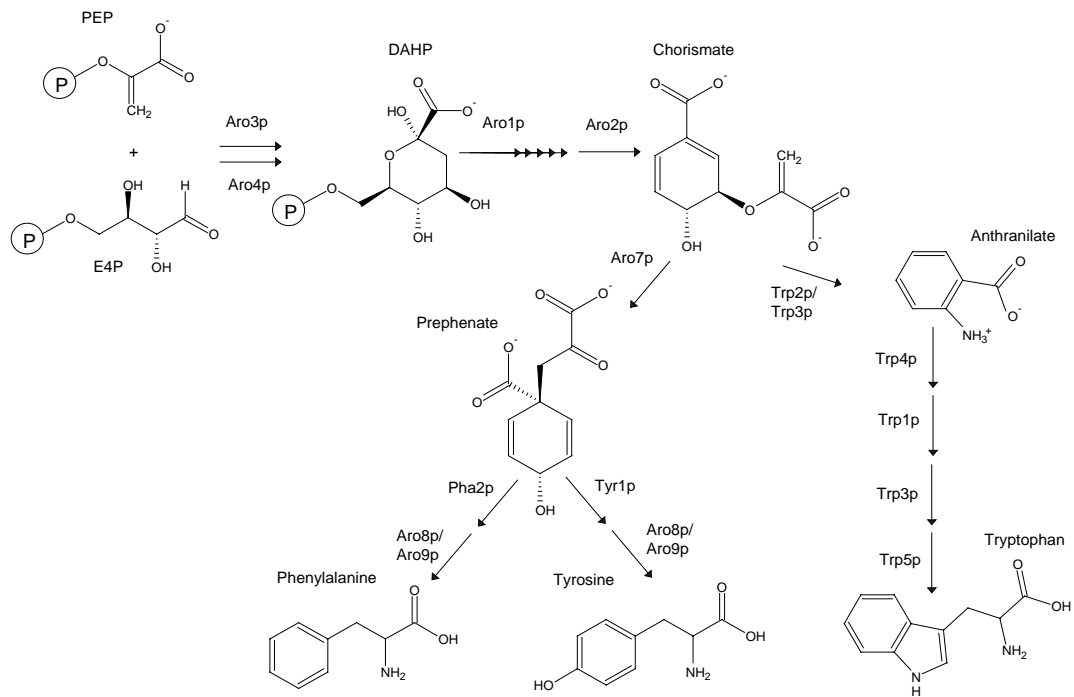


**Figure 1: Aromatic amino acid biosynthetic pathway of *Saccharomyces cerevisiae*.** The pathway starts with the condensation of phosphoenolpyruvate (PEP) and erythrose-4-phosphate (E4P) to 3-deoxy-D-arabino-heptulosonate-7-phosphate (DAHP) catalyzed by the DAHP synthase. DAHP is converted via six enzymatically catalyzed steps to chorismate. This last common metabolite of the shikimate pathway is the initial intermediate of the two branches leading to tryptophan on one side and to phenylalanine and tyrosine on the other side. In the scheme above the enzyme names are deduced from the names of the encoding genes.

### 1.1.1. The Shikimate Pathway

The main trunk of the aromatic amino acid biosynthetic pathway is named after the organic acid shikimate, which was first isolated from the fruits of the anis tree *Illicium religiosum* (shikimi-no-ki) and *Illicium anisatum*, where it is present in large quantities (up to 20%) (Eykmann, 1891). The common pathway for aromatic amino acids, leading to the branch point intermediate chorismate, starts with the condensation of the two carbohydrates phosphoenolpyruvate (PEP) derived from glycolysis and erythrose-4-phosphate (E4P) derived from pentosephosphate pathway to 3-deoxy-D-arabino-heptulosonate-7-phosphate (DAHP) with the release of the phosphate group of PEP as inorganic phosphate by the DAHP synthase (EC 2.5.1.54; Figure 2). More detailed information to the DAHP synthase are given in chapter 1.1.1.1.

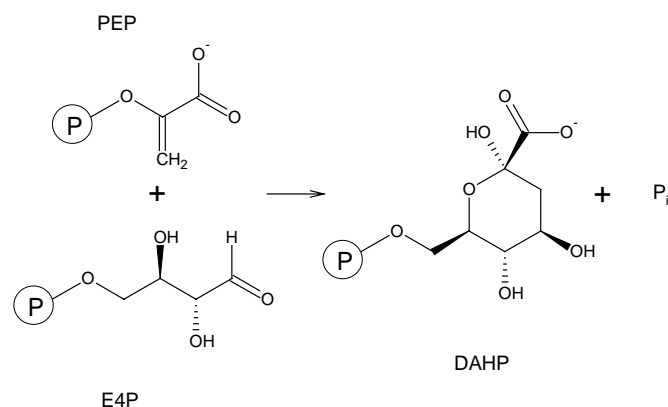


**Figure 2: DAHP synthase (EC 2.5.1.54) catalyzes the condensation of PEP and E4P yielding DAHP and inorganic phosphate.**

DAHP is converted via 3-dehydroquinate (DHQ), 3-dehydroshikimate (DHS), shikimate and shikimate-3-phosphate (S3P) to *enol*pyruvylshikimate-3-phosphate (EPSP). These conversions are catalyzed by the pentafunctional AROM protein in *S. cerevisiae* and other fungi (i.e. *Aspergillus nidulans*, *Neurospora crassa*) (Coggins *et al.*, 1985). The AROM protein is harboring the activities of DHQ synthase (EC 4.2.3.4), DHQ dehydratase (EC 4.2.1.10), DHS dehydrogenase (EC 1.1.1.25), shikimate kinase (EC 2.7.1.71) and EPSP synthase (EC 2.5.1.19), while these five enzymes are separate in bacteria (Bentley, 1990).

The enzymes of the AROM complexes are not arranged in the same order as reactions of the pathway. The domains of DHQ synthase and EPSP synthase are located at the N-terminus followed by the domains of the shikimate kinase, DHQ dehydratase and the shikimate dehydrogenase at the C-terminus (Hawkins and Smith, 1991).

With a complex multi-step mechanism the conversion from DAHP to DHQ is catalyzed by the DHQ synthase. Included in this reaction are alcohol oxidation, phosphate  $\beta$ -elimination, carbonyl reduction, ring opening and intramolecular aldol condensation (Figure 3).

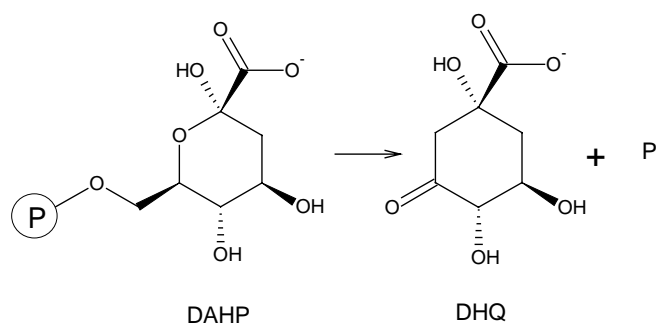


**Figure 3: DHQ synthase (EC 4.2.3.4) catalyzes the conversion from DAHP to 3-dehydroquinate (DHQ).**





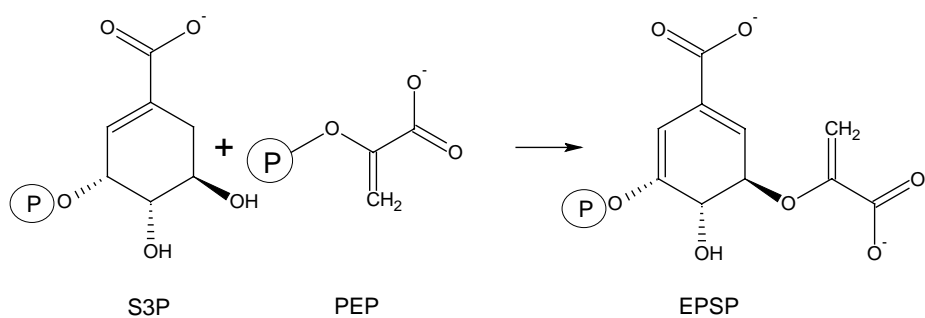


**Figure 7: Condensation of S3P and PEP to *enol*pyruvylshikimate-3-phosphate (EPSP) catalyzed by the EPSP synthase (EC 2.5.1.19).**

The final reaction of the shikimate pathway from EPSP to chorismate is catalyzed by the chorismate synthase (EC 4.2.3.5). Bacterial and plant chorismate synthases are monofunctional enzymes and require the addition of reduced flavine, while the fungal form is bifunctional and supplies itself with reduced flavines by the flavine reductase domain of these chorismate synthases. Crystal structures of the FMN-bound and FMN-free chorismate synthase of *Helicobacter pylori* have been determined (Ahn *et al.*, 2004).

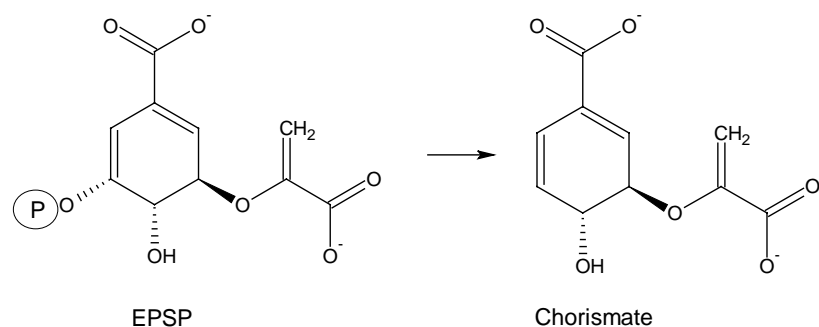


**Figure 8: Chorismate synthase (EC 4.2.3.5) catalyzes trans-1,4-elimination of EPSP to yield chorismate.**

#### 1.1.1.1. DAHP synthase (EC 2.5.1.54)

DAHP synthases catalyze the initial step of the aromatic amino acid pathway. The two carbohydrates PEP, derived from glycolysis, and E4P, derived from pentose phosphate pathway, are condensed to DAHP, a precursor of biologically synthesized aromatic compounds.

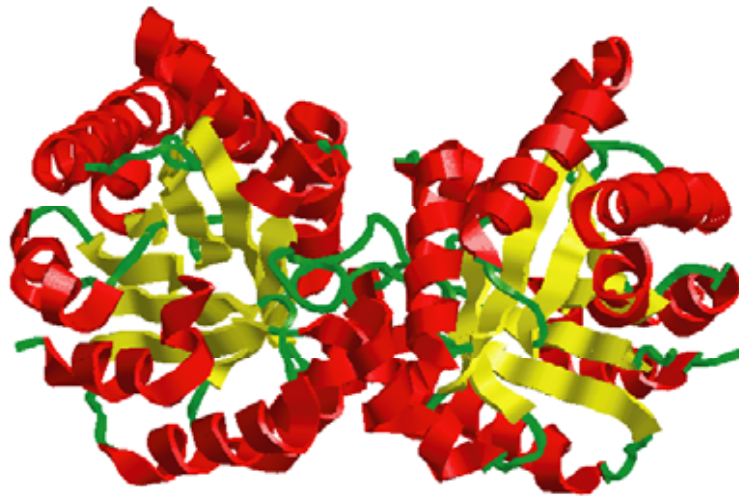
DAHP synthases can be grouped into different classes, I $\alpha$ , I $\beta$  and II. The class II DAHP synthases are described as 54 kDa enzymes and are represented by several higher-plant DAHP synthases, which are encoded by homologous genes (Walker *et al.*, 1996). The

class I enzymes correspond to the three paralogues for the DAHP synthases of *E. coli* with a resulting molecular mass of about 39 kDa. This class is divided into two subclasses the *E. coli* paralogues ( $1\alpha$ ) and the *Bacillus subtilis* paralogues with the 3-deoxy-D-manno-2-octulosonate-8-phosphate (KDOP) synthases ( $1\beta$ ) (Subramaniam *et al.*, 1998; Jensen *et al.*, 2002). Class I and II DAHP synthases show no similarities at the level of primary sequence (Jensen *et al.*, 2002).

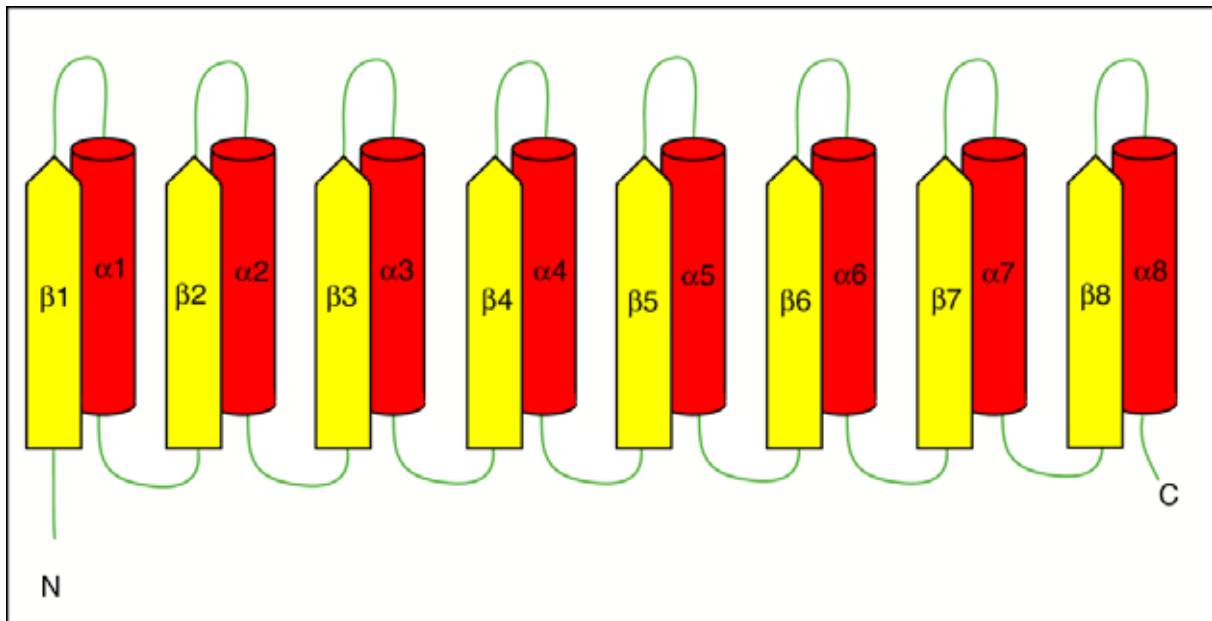
The DAHP synthases of different organisms vary in size, regulation and structural extras. Within the class I these enzymes show similarities in sequence, in the core a TIM barrel or  $(\beta/\alpha)_8$  barrel fold with the catalytic site at the c-terminal end of the  $\beta$ -sheets and probably in the mechanism of catalysis. The TIM barrel fold is described in detail in the following chapter. Kinetic parameters of DAHP synthases of several prokaryotic and eukaryotic organisms have been determined. Crystal structures were solved of the phenylalanine regulated DAHP synthase of *E. coli* (Shumilin *et al.*, 1999; Shumilin *et al.*, 2002; Shumilin *et al.*, 2003), the tyrosine regulated DAHP synthase of *S. cerevisiae* (Hartmann *et al.*, 2003; König *et al.*, 2004) and the DAHP synthase of *Thermotoga maritima* (Shumilin *et al.*, 2004), regulated by phenylalanine and tyrosine.

#### 1.1.1.1.1. TIM barrel

Class I DAHP synthase are  $(\beta/\alpha)_8$ -barrel or TIM barrel enzymes with extra parts. With the excursus to TIM barrels basic principles of this fold are shown. The TIM-barrel fold, which was first observed in the triosephosphate isomerase (TIM) of glycolysis, possesses alternating  $\beta$ -strands and  $\alpha$ -helices. The eight  $\beta$ -strands build a barrel, which is surrounded by the eight  $\alpha$ -helices (compare to Figure 9). The topology of all TIM barrels is  $(\beta\alpha)_8$  (= 8 repeats of a  $\beta$ -sheet followed by an  $\alpha$ -helix) except for the family of enolases, where the order of structural elements differ  $(\beta\beta\alpha\alpha(\beta\alpha))_6$  = 2  $\beta$ -sheets, 2  $\alpha$ -helices and 6 repeats of a  $\beta$ -sheet followed by an  $\alpha$ -helix (Babbitt *et al.*, 1996).



A



B

**Figure 9: TIM barrel structure of proteins.** **A** Dimer of the first crystallized triosephosphate isomerase of chicken (*Gallus gallus*) breast muscle (Banner *et al.*, 1976). The eight  $\beta$ -sheets surrounding the catalytic center are given in yellow, the eight  $\alpha$ -helices surrounding the  $\beta$ -barrel are shown in red and the loops are displayed in green. **B** Topology plot of the typical TIM barrel or  $(\beta/\alpha)_8$  fold. The eight  $\beta$ -sheets are given in yellow, the eight  $\alpha$ -helices are colored in red and the loops shown in green.

The most hydrophobic region of this fold is the core region between  $\beta$ -strands and  $\alpha$ -helices (Nagano *et al.*, 1999). A hydrogen bonding network is spanned through the complete molecule, to connect the N-terminal end of the barrel with the C-terminal end (Wierenga, 2001). Furthermore the active sites are located at the C-terminal ends of the  $\beta$ -sheets,

surrounded by the residues of the loops between the  $\beta$ -strands and the  $\alpha$ -helices (Wierenga, 2001). As shown for TIM as well as the histidine biosynthetic enzymes of *T. maritima* HisA and HisF, the loops between the  $\beta$ -strands and  $\alpha$ -helices tend to be larger than between the  $\alpha$ -helices and the  $\beta$ -strands (Maes *et al.*, 1999; Lang *et al.*, 2000). These flexible loops between the  $\beta$ -strands and the  $\alpha$ -helices, which bind the substrate, protect the catalytic site from solvents (Wierenga, 2001). Besides, there is a positive electrostatic potential at the C-terminal end of the barrel at the active site, which is consistent with the preference of TIM barrel enzymes for negatively charged substrates like phosphate groups (Raychaudhuri *et al.*, 1997; Copley and Bork, 2000; Wierenga, 2001).

The similarities in sequences and structures of TIM barrel enzymes are discussed to be the result of divergent evolution of a common ancestor. Three general routes of enzyme evolution are described (Wise and Rayment, 2004): substrate specificity, conserved reaction mechanism and conserved active site architecture. An example for the evolutionary division by substrate specificity are the homologues enzymes catalyzing successive steps in the biosynthesis of tryptophan and histidine (Henn-Sax *et al.*, 2002). Furthermore the investigation of the sequences and structures of HisA and HisF suggest, that both  $(\beta\alpha)_8$ -barrels are the result of a gene duplication (Fani *et al.*, 1994; Lang *et al.*, 2000).

#### **1.1.1.1.2. PEP utilizing enzymes**

PEP as one of the substrates of DAHP synthases is also used in several additional biochemical steps, which play key roles in cellular energy metabolism and biosynthesis (Anderson, 1999). Only five enzymes found till now are able to catalyze the unusual C-O bond cleavage of PEP and can be grouped into two types of PEP utilizing enzymes (Haslam, 1993). The first group transfers the *enol*pyruvoyl moiety of PEP to the alcohol as co-substrate with the formation of an *enol* ether linkage, while the second group is coupling the C3 atom of PEP with the aldehyde as co-substrate with the formation of a net aldol condensation product (Anderson, 2005).

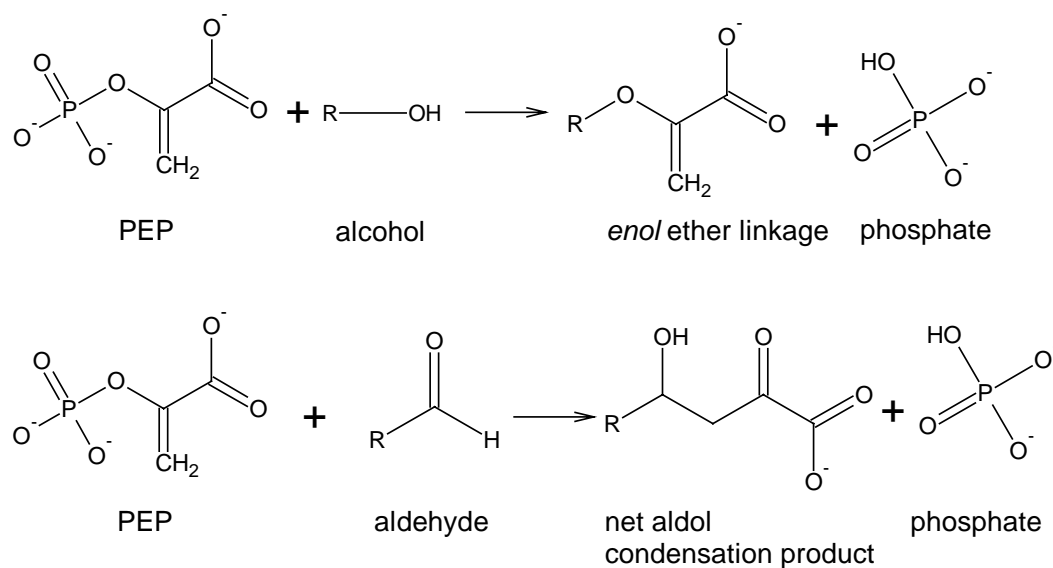


**Figure 10: Two types of unusual C-O bond cleavage of PEP catalyzed by the two types of PEP utilizing enzymes.** In the first reaction the *enol*pyruvoyl moiety of PEP is transferred to the alcohol-co-substrate with the formation of an *enol* ether linkage and in the second reaction the C3 atom of PEP is condensed with the aldehyde-co-substrate (Anderson, 2005).

The EPSP synthase of the shikimate pathway (compare chapter 1.1.1.) and the UDP-GlcNAc *enol*pyruvoyl transferase, an enzyme which is involved in peptidoglycan biosynthesis (Kahan *et al.*, 1974), belong to the first group. The KDOP synthase, taking part in the lipopolysaccharide formation in most Gram-negative bacteria, the DAHP synthase (compare chapter 1.1.1.1.) and the N-acetyl-neuramic acid (NeuAc) synthase, which is part of the polysaccharide cell wall biosynthesis, catalyze the second type of reaction.

The condensation of the KDOP synthase is stereospecific and PEP attacks with the *si*-site the *re*-site of D-arabinose 5-phosphate (A5P) (Dotson *et al.*, 1993; Kohen *et al.*, 1993). The mechanism of enzyme catalysis of KDOP synthase was analyzed by real-time monitoring the catalysis. The semiketal phosphate intermediate of the catalysis was found with the help of electrospray ionization mass spectrometry (Li *et al.*, 2003).

KDOP synthase folds in an  $\beta/\alpha$  barrel like the DAHP synthase, which is metal-independent in *E. coli* (Wagner *et al.*, 2000; Asojo *et al.*, 2001) and metal dependent in *Aquifex aeolicus* (Radaev *et al.*, 2000; Duewel *et al.*, 2001; Wang *et al.*, 2001). The only differences between these enzymes are the extra-parts to the  $\beta/\alpha$  barrel, which are required for regulation, in the DAHP synthase. The coordination of the divalent metal ion and the substrate PEP in both enzymes are similar (König *et al.*, 2004).

### 1.1.2. The phenylalanine-/tyrosine-branch

In three enzymatic steps chorismate is formed via prephenate, the last common intermediate, to phenylalanine and tyrosine, respectively. The first step is the conversion from chorismate to prephenate and is catalyzed by the chorismate mutase. Prephenate is converted to phenylpyruvate by the prephenate dehydratase, to 4-hydroxyphenylpyruvate by the prephenate dehydrogenase and to arogenate by the prephenate amino transferase. Aminotransferases convert phenylpyruvate to phenylalanine and 4-hydroxy-phenylpyruvate to tyrosine. Arogenate can be either dehydrated or decarboxylized by the arogenate dehydratase resulting in phenylalanine or oxidatively decarboxylized by the arogenate dehydrogenase to tyrosine. The arogenate pathway is characteristic for higher plants. Some microorganisms are also able to build arogenate from prephenate (i.e. *cyanobacteria*, *Pseudomonas aeruginosa*). Prephenate formation of *S. cerevisiae* and subsequently the prephenate dehydrogenase and dehydratase are described in detail in the chapters 1.1.2.2. and 1.1.2.4.

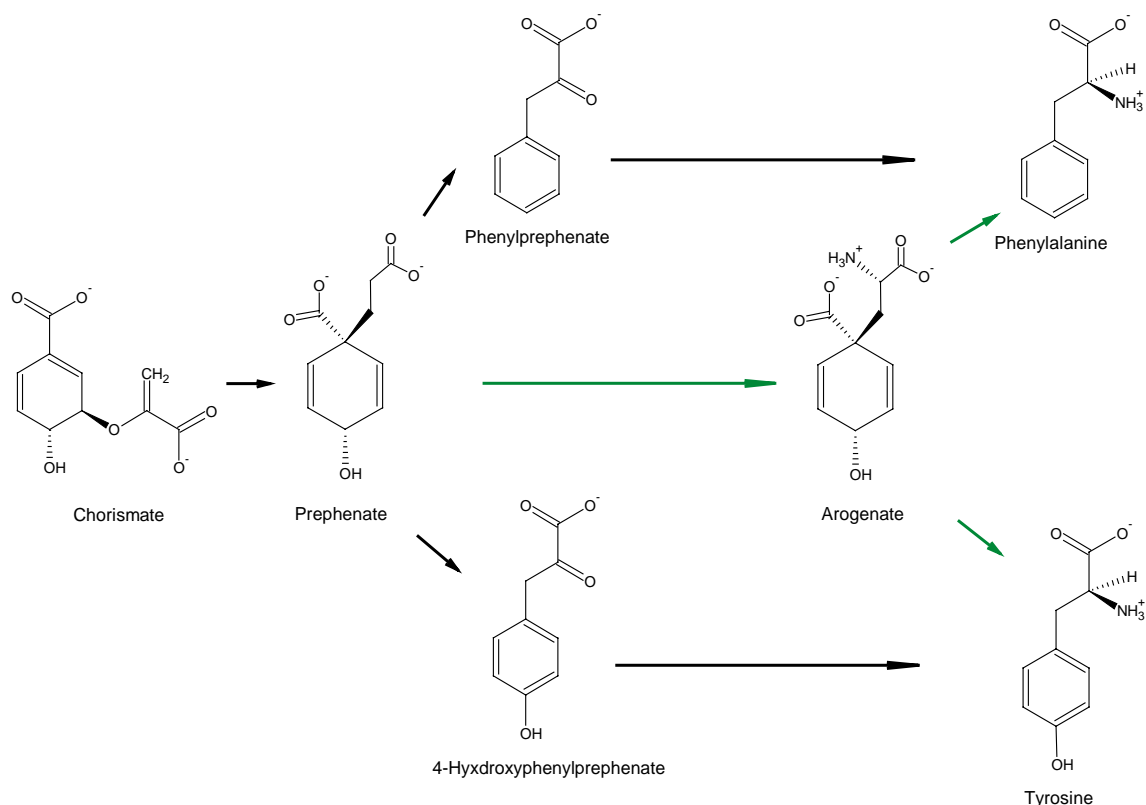


**Figure 11: Two pathways from prephenate to phenylalanine and tyrosine, respectively.** In *S. cerevisiae* prephenate is converted to phenylpyruvate by the prephenate dehydratase, which leads to phenylalanine, or to 4-hydroxyphenylpyruvate by the prephenate dehydrogenase, leading to tyrosine. In higher plants and some microorganisms (i.e. *cyanobacteria*, *Pseudomonas aeruginosa*) arogenate is built by the prephenate amino transferase, which can be either dehydrated or decarboxylized. The first pathway is indicated with black and the second with green arrows.

### 1.1.2.1. The chorismate mutase (EC 5.4.99.5)

The branch point enzyme chorismate mutase (EC 5.4.99.5) catalyzes the Claisen rearrangement from chorismate to prephenate (Andrews *et al.*, 1973). In prokaryotes chorismate mutase is often found to be part of a bifunctional enzyme, where a prephenate dehydratase (P-protein), a prephenate dehydrogenase (T-protein) or a DAHP synthase moiety is fused to the chorismate mutase (Romero *et al.*, 1995). In the bifunctional chorismate mutases both domains of the T-protein can be regulated by tyrosine, while the two domains of the bifunctional P-protein can be feedback regulated by phenylalanine. The monofunctional bacterial chorismate mutases are not regulated. Eukaryotic chorismate mutases generally are monofunctional enzymes and target to feedback regulation.

Crystal structures of several chorismate mutases were determined (Chook *et al.*, 1993; Xue *et al.*, 1994; Lee *et al.*, 1995). The two differently evolved folds of chorismate mutases can be grouped into different classes: AroH, a homotrimeric fold with  $\alpha$ -helices and  $\beta$ -sheets builds a pseudo- $\beta/\alpha$  barrel (i.e. chorismate mutases of *Bacillus subtilis* (Figure 12) and *Thermus thermophilus* (Chook *et al.*, 1993; Helmstaedt *et al.*, 2004)). AroQ, which has only  $\alpha$ -helices, is the fold of the bifunctional enzymes and most monofunctional chorismate mutases of prokaryotes (i.e. *E. coli* (Lee *et al.*, 1995)) and eukaryotes (i.e. *S. cerevisiae* (Xue *et al.*, 1994)) (Xia *et al.*, 1993). The latter class is divided into subclasses (Gu *et al.*, 1997): AroQ<sub>t</sub> (monofunctional), AroQ<sub>p</sub> (part of the bifunctional enzyme fused to the prephenate dehydratase domain), AroQ<sub>t</sub> (part of the bifunctional enzyme fused to the prephenate dehydrogenase domain) and AroQ<sub>d</sub> (part of the bifunctional enzyme fused to the DAHP synthase domain).

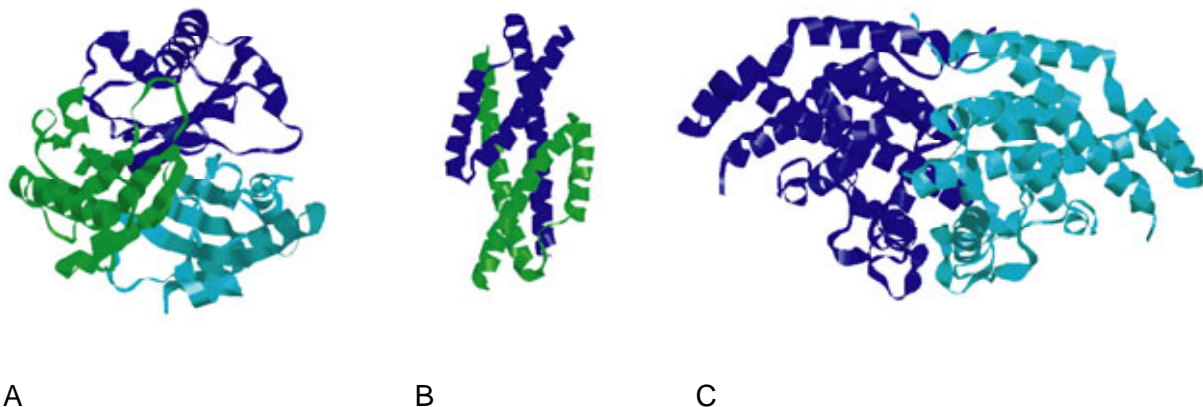


**Figure 12: Ribbon Crystal structures of chorismate mutase molecules of *Bacillus subtilis* (A), *E. coli* (B), *S. cerevisiae* (C).** The *B. subtilis* enzyme is displayed as a trimer and the enzymes of *E. coli* and *S. cerevisiae* are shown as dimers. The different chains are colored differently.

### 1.1.2.2. The prephenate dehydrogenase (EC 1.3.1.12)

Prephenate dehydrogenase (PDH; EC 1.3.1.12) catalyzes the formation of 4-hydroxyphenylpyruvate and NADH + H<sup>+</sup> from prephenate and NAD<sup>+</sup>. This enzyme can exist as monofunctional and as bifunctional enzyme (T-protein). While PDHs from the yeasts *Pichia guilliermondii* (Koll *et al.*, 1988), *Candida maltosa* (Bode and Birnbaum, 1991) and *S. cerevisiae* (Jones and Fink, 1982) are inhibited by tyrosine, the enzymes from *C. maltosa* and *N. crassa* are activated by tryptophan (Bode *et al.*, 1984) or phenylalanine, respectively (Catcheside, 1969). The *TYR1* gene is coding for the PDH of *S. cerevisiae*. In the putative gene product, a binding site for NAD<sup>+</sup> was found and it was shown that the expression of the *TYR1* mRNA is not affected by the final transcriptional activator of the general control, the transcription activator Gcn4p (Mannhaupt *et al.*, 1989). Recently the 373 amino acid containing homodimeric T-protein of *E. coli* was mapped (Chen *et al.*, 2003). While the functional chorismate mutase domain is constituted by the first 88 residues, the PDH activity and feedback-inhibition were found to be located in the residues 94-373.

### 1.1.2.3. The prephenate dehydratase (EC 4.2.1.51) and a regulatory domain

The prephenate dehydratase (PDT; EC 4.2.1.51) catalyzes the formation of prephenate to phenylprephenate. This enzyme can exist as monofunctional and as bifunctional enzyme (P-protein). Phenylalanine and tryptophan act as feedback inhibitors to the PDTs of *Corynebacterium glutamicum* and *Brevibacterium flavum*, while tyrosine acts as activator (Fazel and Jensen, 1980). The *PHA2* gene is coding for PDT of *S. cerevisiae*. There is no crystal structure of any PDT determined till now and there is no kinetic information about the yeast prephenate dehydratase. It was shown, that the P-protein of *E. coli* can be divided into three domains: the chorismate mutase domain, the prephenate dehydratase domain and a regulatory domain (Zhang *et al.*, 1998). There is a conserved motif (ESRP-motif = Glu-Ser-Arg-Pro-motif), which is also found in the ACT-domain of phenylalanine hydroxylases, was shown to participate in the binding of phenylalanine (Pohnert *et al.*, 1999) and plays a role as target for regulation in prephenate dehydratases (Gerlt and Babbitt, 2001; Hsu *et al.*, 2004). "ACT" are the initials of the three first named enzymes harboring this domain. The ACT domain is a ligand binding domain found in several proteins like aspartokinases, chorismate mutases, prephenate dehydrogenases (TyrA), prephenate dehydratases and many more (Aravind and Koonin, 1999). The archetypical ACT domain is the C-terminal regulatory domain of 3-phosphoglycerate dehydrogenase (3PGDH), which is folded ferredoxin-like ( $\beta\alpha\beta\beta\alpha\beta$ ) (Al Rabiee *et al.*, 1996; Grant *et al.*, 1996). Phenylalanine hydroxylases of the rat include a regulatory domain with similar fold but different ligand-binding mode (Chipman and Shaanan, 2001).

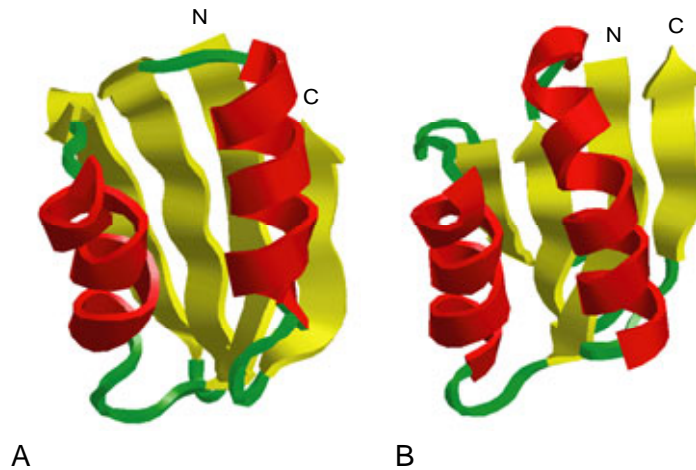


**Figure 13: ACT domains of 3-phosphoglycerate dehydrogenase (3PGDH) of *E. coli* (A; PDB code: 1PSD) and phenylalanine hydroxylase of rat (B; PDB code: 1PHZ).**

The crystal structures of the ACT domain or similar domains of other enzymes (i.e. phenylalanine hydroxylase) are important tools for *in silico* analysis of the not yet crystallized prephenate dehydratase, in order to postulate important residues for regulation, which can be tested by experiments including amino acid substitution variants of the enzymes.

### 1.1.3. The tryptophan branch

Chorismate is converted in five steps to tryptophan with seven participating enzymes (Weiss and Edwards, 1980). The first step of the tryptophan branch is the conversion from chorismate to anthranilate by the anthranilate synthase complex. The anthranilate phosphoribosyltransferase (EC 2.4.2.18), encoded by the gene *TRP4* in *S. cerevisiae*, transfers the 5-phosphoribosyl moiety from 5-phosphoribosylpyrophosphate to the amino group of anthranilate. The resulting phosphoribosylanthranilate (PRA) is converted to carboxyphenylamino-1-deoxy-ribulose 5-phosphate (CDRP). This essentially irreversible Amadori rearrangement is catalyzed by the PRA isomerase (EC 5.3.1.24), which is encoded by *TRP1*. Indole-3-glycerol-phosphate (IGP) is the product of the decarboxylation of CDRP, which is catalyzed by IGP synthase (*TRP3*; EC 4.1.1.48). The final step is the condensation of indole with serine catalyzed by the tryptophan synthase (*TRP5*; EC 4.2.1.20).

There are three general routes of divergent enzyme evolution possible in which substrate specificity, reaction mechanism or active site architecture of the progenitor enzyme is conserved and serves as template for evolution of new enzyme function (Gerlt and Babbitt, 2001). In the case of the TIM barrel enzymes of the tryptophan biosynthetic pathway substrate specificity serves as template for divergent evolution. Although the progenitor

enzyme and the newly evolved enzyme catalyze different reactions with different mechanisms, both enzymes bind a common substrate. Catalyzing subsequent reactions the PRA isomerase, IGP synthase and the tryptophan synthase are TIM barrel enzymes that are homologous and share about 15% to 20% sequence identity (Wilmanns *et al.*, 1991). The product of the PRA isomerase is the substrate for the IGP synthase and the product of the IGP synthase is the substrate for the tryptophan synthase. These common intermediates bind in a similar manner in each active site and evolved from a progenitor enzyme with the same substrate specificity (Wise and Rayment, 2004).

#### **1.1.3.1. The anthranilate synthase complex (EC 4.1.3.27)**

The initial conversion from chorismate to anthranilate is a two-step process catalyzed by the anthranilate synthase (EC 4.1.3.27), a heterodimeric enzyme complex of the gene products of *TRP2* and of *TRP3*. The latter encodes not only the glutamine-aminotransferase, but also an indole-3-glycerol phosphate (IGP) synthase, which catalyzes the fourth step (the decarboxylation of CDRP to IGP) of the tryptophan branch of the biosynthetic pathway of aromatic amino acids. In the first step the amino group of a glutamine residue is reversibly linked to chorismate catalyzed by the glutamin amidotransferase domain of the bifunctional Trp3p and in the second step pyruvate is irreversibly eliminated. The promoters of both the *S. cerevisiae TRP2* gene is target of the transcription activator Gcn4p of the general control, in contrast to the counterpart of the branch point *ARO7* (further information are given in chapter 1.1.4.2.).

#### **1.1.4. Regulation of the aromatic amino acid biosynthesis of *S. cerevisiae***

The enzymatic steps in the biosynthesis of aromatic amino acids are similar in various species, but there are differences in their genetic organization. In contrast to the situation in many prokaryotes, the genes, encoding the enzymatic activities in *S. cerevisiae*, are spread over the genome (Braus, 1991). Biosynthesis of aromatic amino acid is regulated by two mechanisms: 1) regulation of enzyme activities and 2) regulation of the gene expression with Gcn4p as part of the general control.

This complex regulatory network, links different pathways and is named “cross pathway control” in filamentous fungi, where it was first found, and “general control” in yeast (Piotrowska, 1980; Hinnebusch, 1988; Bode *et al.*, 1990).

##### **1.1.4.1. Regulation of enzyme activities of aromatic amino acid biosynthesis**

The main checkpoints for regulating the enzyme activity are the DAHP synthases at the beginning of the biosynthetic pathway and at the first branch point the chorismate mutase

leading to the synthesis of phenylalanine and tyrosine and the anthranilate synthase leading to the synthesis of tryptophan. These steps are critical for regulating the flux of intermediates. In *S. cerevisiae* two isoenzymes of the DAHP synthase are present. Aro3p is regulated by phenylalanine and Aro4p is feedback inhibited by tyrosine (Paravicini *et al.*, 1989; Schnappauf *et al.*, 1998). Chorismate mutase, encoded by *ARO7*, binds chorismate as positive allosteric ligand ( $[S]_{0.5} = 4 \text{ mM}$ ). Chorismate mutase is activated by tryptophan with the simultaneous loss of the positive cooperativeness. Tyrosine inhibits Aro7p, while the enzyme shows cooperativity with respect to the substrate (Schnappauf *et al.*, 1998).

The counterpart of the chorismate mutase at the first branch point, the anthranilate synthase, is feedback-inhibited by tryptophan (Prantl *et al.*, 1985). The transcription activator Gcn4p regulates the level of transcribed *TRP2*, leading to tryptophan, in contrast to the counterpart of the branch point *ARO7*, leading to phenylalanine and tyrosine. The expression of the unregulated chorismate mutase *ARO7<sup>C</sup>* allele and the loss of the transcription regulator Gcn4p of the general control of the biosynthetic pathways of amino acids is lethal, when yeast cells are starved for tryptophan. Growth can be restored, with the transcriptional induction of *TRP2* (Krappmann *et al.*, 2000).

#### **1.1.4.2. General control of amino acid biosynthetic pathway in fungi**

The general control of amino acid biosynthesis with the central regulation factor Gcn4p is a complex regulatory network, connecting different biosynthetic pathways (Hinnebusch and Natarajan, 2002). Fungi generally maintain high levels of amino acid biosynthetic proteins. Due to the high basal level of transcription yeast *S. cerevisiae* and other fungi possess a large pool of intracellular amino acids (Fantes *et al.*, 1976; Jones and Fink, 1982).

Amino acid imbalance or the starvation for one amino acids leads to a derepression of about 500 target genes of different biosynthetic pathways (Natarajan *et al.*, 2001). Besides the lack of amino acids, a lack of purines, tRNA synthases and glucose leads to activation of the general control system, as well as UV-radiation, treatment with rapamycin and high concentrations of salt (Meussdoerffer and Fink, 1983; Moesch *et al.*, 1991; Engelberg *et al.*, 1994; Yang *et al.*, 2000; Goosens *et al.*, 2001; Valenzuela *et al.*, 2001).

The extracellular signal (i.e. the absence of amino acids) is leading to an intracellular accumulation of unloaded tRNAs, which is noticed by the sensor kinase Gcn2p. Via a signal transduction cascade the translation of the central transcription activator Gcn4p is derepressed. Gcn4p is the transcription regulator of the target genes of the general amino acid control (Natarajan *et al.*, 2001; Hinnebusch and Natarajan, 2002). This derepression of translation of *GCN4* mRNA is controlled by four short upstream-located open reading frames (uORFs), which are like a barrier for the translation in the presence of amino acids. At amino acid starvation conditions, the sensor kinase Gcn2p phosphorylates the eukaryotic initiation

factor eIF2. As a result the concentration of ternary complexes of eIF2, initiator tRNA and GTP sinks, which leads to re-initiation of translation at the *GCN4* start codon and not at the uORF4 in the case of the presence of amino acids (Hinnebusch, 2000).

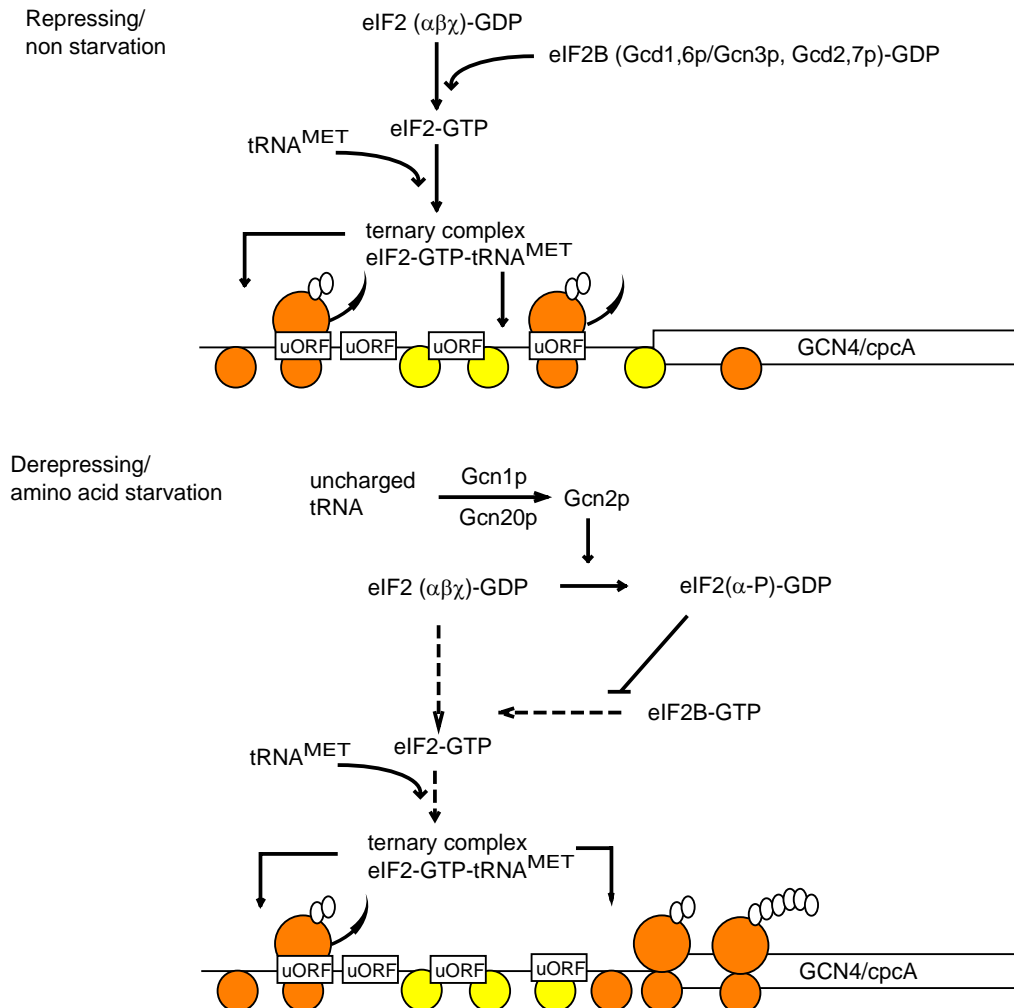


**Figure 14: Translational control of *S. cerevisiae* Gcn4p under non-starvation and starvation conditions.** Under conditions of amino acid limitation uncharged tRNA molecules are recognized by Gcn2p, which in turn phosphorylates the  $\alpha$  subunit of the eukaryotic elongation factor eIF2 on Ser51. The guanine nucleotide exchange factor eIF2B is inhibited and GDP can not be exchanged with GTP. This results in a downregulation of cellular translation efficiency caused by lower amounts of ternary complexes (eIF2, Met-tRNA and GTP). This leads to an affected ribosome reinitiation, which occurs at the start-codon of *GCN4* instead of the fourth uORF.

Furthermore transcription is controlled by the regulation of stability of the transcription activator Gcn4p itself (Irniger and Braus, 2003). The amount of Gcn4p is regulated within the cell. Therefore Gcn4p is rapidly degraded by specific protein degradation mechanism in the

nucleus. In the presence of amino acids the destabilization of Gcn4p is triggered by phosphorylation of the residue Thr165 by the cyclin dependent kinase complex Pho85p/Pcl5p. This serves as marker for ubiquitination of the protein by the SCF<sup>Cdc4</sup> ubiquitin ligase complex. Ubiquitinated Gcn4p is then degraded by the 26S proteasome (Figure 15).

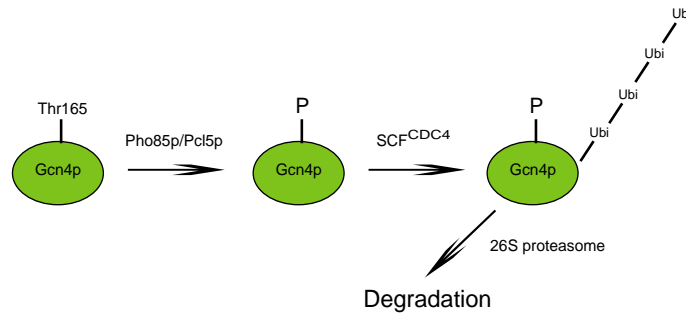


**Figure 15: Proposed model of the Gcn4p degradation pathway (Meimoun *et al.*, 2000).** Gcn4p is phosphorylated by the Pho85p/Pcl5p cyclin dependent kinase complex at Thr165, which results in the ubiquitination of Gcn4p by the SCF<sup>Cdc4</sup> ubiquitin ligase complex and leads subsequently to degradation in the 26S proteasome.

Most genes of biosynthetic pathways are subject to the general control and they are derepressed under amino acid starvation condition (Miozzari *et al.*, 1978; Teshiba *et al.*, 1986; Duncan *et al.*, 1987; Jones *et al.*, 1991). The only exceptions are *ARO7* encoding chorismate mutase, *TYR1* encoding prephenate dehydrogenase and *TRP1* encoding PRA isomerase. These are not controlled by the general control (Braus *et al.*, 1988; Mannhaupt *et al.*, 1989; Schmidheini *et al.*, 1990).

### 1.1.4.3. Networks of regulatory pathways

At the first branching point of aromatic amino acid biosynthesis, the different values of  $K_M$ -values of chorismate mutase and anthranilate synthase channels the chorismate into the tryptophan branch. The generated tryptophan inhibits anthranilate synthase by feedback inhibition and simultaneously activates chorismate mutase. As a result the chorismate is now channeled into the phenylalanine/tyrosine branch. The production of phenylalanine and tyrosine leads to the inhibition of Aro3p, Aro4p and Aro7p. There is evidence to the favored synthesis of phenylalanine because of the different sensitivities to the feedback inhibitors of the phenylalanine regulated DAHP synthase Aro3p ( $K_i = 75 \mu\text{M}$ ; (Paravicini *et al.*, 1989)) and the tyrosine regulated DAHP synthase Aro4p ( $K_i = 0,9 \mu\text{M}$ ; (Schnappauf *et al.*, 1998)). Furthermore the general control affects nearly all genes of the aromatic amino acid pathway. Under amino acid starvation condition the tryptophan synthesis is favored, because *ARO7* is

not a target of the general control system, but the gene product is strictly regulated by feedback activation and inhibition (Krappmann *et al.*, 2000).

## 1.2. Aim of this work

The first aim of this work was the identification of amino acid residues of the catalytic center of the tyrosine regulated DAHP synthase of *S. cerevisiae* which are important for catalysis. Crystal structures are not able to give insight in the dynamic situation of enzymes in an aqueous system. Therefore the crystal structure should be taken as hypothesis and for verification or falsification amino acid substitutions were inserted at the predicted catalytic center by site specific mutations in the *ARO4* gene.

The second aim was the identification of the intramolecular signal transduction pathway between the allosteric tyrosine binding site and the catalytic center of the DAHP synthase of *S. cerevisiae*. The crystal structures of different yeast Aro4p complexes were the basis which was used to approach this problem by introducing different codons into *ARO4* which result in amino acid substitution in the postulated intramolecular signal transduction pathway. The third aim was to find a solution for the so-called “phenylalanine-effect”. The “phe-effect” is the effect of starvation for tryptophan of mutant yeast cells, which contain the constitutively derepressed and unregulated chorismate mutase (Aro7<sup>c</sup>p) and lack the transcription factor Gcn4p as final effector of the general control, in the presence of an exogenous phenylalanine source described. The three possible ways of action for phenylalanine should be proofed – repression of the tryptophan biosynthetic branch, activation of the phenylalanine and tyrosine biosynthetic branch or repression of the whole aromatic amino acid pathway.

## 2. Materials and Methods

### 2.1. Materials

#### 2.1.1. Chemicals

Chemicals for the production of buffers, solutions and media were obtained of the firms Carl Roth GmbH & Co KG (Karlsruhe, Germany), Fluka (Neu-Ulm, Germany), Sigma-Aldrich Chemie GmbH (Steinheim, Germany), Invitrogen GmbH (Karlsruhe, Germany), Merck (Darmstadt, Germany), Roche GmbH (Mannheim, Germany) Gibco-BRL (Eggenstein, Germany) und IBA GmbH (Göttingen, Germany).

$\alpha$ -<sup>32</sup>P-dATP was obtained from Hartmann Analytic GmbH (Braunschweig, Germany).

Restriction enzymes, DNA-modifying enzymes and polymerases were delivered from MBI Fermentas GmbH (St. Leon-Rot, Germany), Promega (Madison, USA) and Novagen (San Diego, USA). As DNA-standard the 1kb DNA ladder Plus of MBI-Fermentas was used. Agarose was supplied from Carl Roth GmbH & Co KG. DNA-sequencing reagents were delivered from Applied Biosystems GmbH (Foster City, USA); synthetic oligonucleotids were delivered from Invitrogen GmbH. Chemicals for plasmid-DNA preparation and DNA gel-extraction were supplied by Qiagen (Hilden, Germany).

#### 2.1.2. Strains and plasmids

For cloning *E. coli* DH5 $\alpha$  [F',  $\phi$ 80d*lacZ* $\Delta$ M15,  $\Delta$ (*lacZYA-argF*), U169, *deoR*, *recA1*, *endA1*, *hsdR17*, (*r<sub>K</sub><sup>-</sup>*, *m<sub>K</sub><sup>+</sup>*), *supE44*,  $\lambda$ -, *thi-1*, *gyrA96*, *relA1*] (Hannahan, 1983) was taken.

The *S. cerevisiae* strains are listed in Table 1.

**Table 1: Used *S. cerevisiae* strains**

Strain	Genotype	Reference
RH770	<i>Mat<math>\alpha</math></i> , <i>gcd2</i> , <i>leu2-2</i> , <i>met8-1</i>	(Aebi, 1983).
YNL316c (Acc. No)	<i>MAT<math>\alpha</math></i> , <i>his3<math>\Delta</math>1</i> , <i>leu2<math>\Delta</math>0</i> , <i>met15<math>\Delta</math>0</i> , <i>ura3<math>\Delta</math>0</i> , <i>pha2<math>\Delta</math>::kanMX4</i>	Euroscarf, (Winzeler <i>et al.</i> , 1999).
RH1077a	<i>MAT<math>\alpha</math></i> , <i>ura3</i>	(Prantl <i>et al.</i> , 1985).
RH1408	<i>MAT<math>\alpha</math></i> , <i>ura3-52</i> , <i>gcn4-103</i>	(Hinnebusch, 1985).
RH2980	like RH1077a + <i>pha2<math>\Delta</math>::kanMX4</i>	This study.
RH2463	<i>MAT<math>\alpha</math></i> , <i>ura3-52</i> , <i>gcn4-103</i> , <i>ARO7<sup>c</sup></i>	(Krappmann, 2000).

Strain	Genotype	Reference
RH2475	<i>MATa</i> , <i>ura3</i> , <i>gcn4-103</i> , <i>aro3::kanMX4</i>	(Krappmann, 2000).
RH2476	<i>MATa</i> , <i>ura3</i> , <i>gcn4-103</i> , <i>ARO7<sup>c</sup></i> , <i>aro3::kanMX4</i>	(Krappmann, 2000).
RH3244	like RH2463 + <i>PHA2<sup>ESRP</sup></i>	This study.
RH3245	derivative of RH2476 <i>MATa</i> , <i>ura3</i> , <i>gcn4-103</i> , <i>ARO7<sup>c</sup></i> , <i>aro3</i> , <i>aro4::kanMX4</i> , <i>ARO4<sup>T162L</sup></i>	This study.

The plasmids listed in Table 2.

**Table 2: Used plasmids**

Plasmids	Description	Source
pME1513	pRS426MET25 (Mumberg <i>et al.</i> , 1994) with different Multi-cloning site	(Krappmann <i>et al.</i> , 1999).
pME2017	pME825 (Graf <i>et al.</i> , 1993) with <i>ARO4</i> promoter and terminator cloned into the MCS	(Hartmann, 2001).
pME2658	pME2017 (Hartmann, 2001) with the <i>ARO3</i> orf cloned between the <i>ARO4</i> promoter and terminator via <i>Bam</i> HI/ <i>Xho</i> I	This study.
pME1513	High copy plasmid with MET25 promoter and <i>URA3</i> as selective marker	(Krappmann <i>et al.</i> , 1999).
pME2659	Mutated 1.1 kb <i>ARO4</i> fragment inserted in pME1513 via <i>Bam</i> HI/ <i>Xho</i> I, exchanged codon GAG->GCG (331-333), mutation of the corresponding gene product: E111A	This study.
pME2542	Mutated 1.1 kb <i>ARO4</i> fragment inserted in pME1513 via <i>Bam</i> HI/ <i>Xho</i> I, exchanged codon AAG->GCG (334-336), mutation of the corresponding gene product: K112A	(König <i>et al.</i> , 2004).
pME2004	Mutated 1.1 kb <i>ARO4</i> fragment inserted in pME1513 via <i>Bam</i> HI/ <i>Xho</i> I, exchanged codon AGA->GCA (340-342), mutation of the corresponding gene product: R114A	(König <i>et al.</i> , 2004).

Plasmids	Description	Source
pME2660	Mutated 1.1 kb <i>ARO4</i> fragment inserted in pME1513 via <i>Bam</i> HI/ <i>Xho</i> I, exchanged codon AAA->GCA (358-360),mutation of the corresponding gene product: K120A	This study.
pME2661	Mutated 1.1 kb <i>ARO4</i> fragment inserted in pME1513 via <i>Bam</i> HI/ <i>Xho</i> I, exchanged codon AAA->GAA (358-360),mutation of the corresponding gene product: K120E	This study.
pME2662	Mutated 1.1 kb <i>ARO4</i> fragment inserted in pME1513 via <i>Bam</i> HI/ <i>Xho</i> I, exchanged codon CTT->GCT (478-480), mutation of the corresponding gene product: L160A	This study.
pME2663	Mutated 1.1 kb <i>ARO4</i> fragment inserted in pME1513 via <i>Bam</i> HI/ <i>Xho</i> I, exchanged codons GAG->GCG (331-333) + CTT->GCT (478-480), mutation of the corresponding gene product:E111A + L160A	This study.
pME2543	Mutated 1.1 kb <i>ARO4</i> fragment inserted in pME1513 via <i>Bam</i> HI/ <i>Xho</i> I, exchanged codon AGA->GCA (538-540), mutation of the corresponding gene product: R180A	(König <i>et al.</i> , 2004).
pME2664	Mutated 1.1 kb <i>ARO4</i> fragment inserted in pME1513 via <i>Bam</i> HI/ <i>Xho</i> I, exchanged codon CAA->GCA (553-555), mutation of the corresponding gene product: Q185A	This study.
pME2665	Mutated 1.1 kb <i>ARO4</i> fragment inserted in pME1513 via <i>Bam</i> HI/ <i>Xho</i> I, exchanged codon CAC->TTC (559-561),mutation of the corresponding gene product: H187F	This study.
pME2666	Mutated 1.1 kb <i>ARO4</i> fragment inserted in pME1513 via <i>Bam</i> HI/ <i>Xho</i> I, exchanged codon CAC->CTC (559-561),mutation of the corresponding gene product: H187L	This study.

Plasmids	Description	Source
pME2667	Mutated 1.1 kb <i>ARO4</i> fragment inserted in pME1513 via <i>Bam</i> HI/ <i>Xho</i> I, exchanged codon AGA->GAA (562-564),mutation of the corresponding gene product: R188E	This study.
pME2668	Mutated 1.1 kb <i>ARO4</i> fragment inserted in pME1513 via <i>Bam</i> HI/ <i>Xho</i> I, exchanged codon GAA->AGA (565-567),mutation of the corresponding gene product: E189R	This study.
pME2669	Mutated 1.1 kb <i>ARO4</i> fragment inserted in pME1513 via <i>Bam</i> HI/ <i>Xho</i> I, exchanged codon GAA->AAA (565-567),mutation of the corresponding gene product: E189K	This study.
pME2670	Mutated 1.1 kb <i>ARO4</i> fragment inserted in pME1513 via <i>Bam</i> HI/ <i>Xho</i> I, exchanged codons AAA->GAA (358-360) + GAA->AAA (565-567),mutation of the corresponding gene product: K120E + E189K	This study.
p426MET26	<i>URA3</i> , 2 $\mu$ m, <i>Amp</i> <sup>R</sup> , <i>MET25</i> -Promotor, <i>CYC1</i> -Terminator	(Mumberg <i>et al.</i> , 1994).
pME2532	like p426MET25 + 1.1 kb <i>PHA2</i> - ORF ( <i>Bam</i> HI/ <i>Hind</i> III) and a C-terminal <i>Strep</i> -tags® ( <i>Hind</i> III/ <i>Xho</i> I)	This study.
pRS426	<i>URA3</i> , 2 $\mu$ m, <i>Amp</i> <sup>R</sup>	(Christianson <i>et al.</i> , 1992).
pME2869	like pRS426 + 1.9 kb <i>TRP2</i> fragment inserted via <i>Eco</i> RI/ <i>Bam</i> HI	This study.
pME2870	like pRS426 + 1.9 kb <i>TRP2</i> fbr (L76) fragment inserted via <i>Eco</i> RI/ <i>Bam</i> HI	This study.
pME2871	like pRS426 + 1.9 kb <i>TRP2</i> fragment inserted via <i>Eco</i> RI/ <i>Bam</i> HI and 2.6 kb <i>TRP3</i> fragment via <i>Bam</i> HI/ <i>Sac</i> I	This study.
pME2872	like pRS426 + 1.9 kb <i>TRP2</i> fbr (L76) fragment inserted via <i>Eco</i> RI/ <i>Bam</i> HI and 2.6 kb <i>TRP3</i> fragment via <i>Bam</i> HI/ <i>Sac</i> I	This study.
pME2873	like pRS426 + 1.9 kb <i>TRP2</i> fbr (R65) fragment inserted via <i>Eco</i> RI/ <i>Bam</i> HI	This study.

Plasmids	Description	Source
pME2874	like pRS426 + 1.9 kb <i>TRP2</i> fbr (R65) fragment inserted via <i>EcoRI/BamHI</i> and 2.6 kb <i>TRP3</i> fragment via <i>BamHI/SacI</i>	This study.
pME2875	like pRS426 + 1.9 kb <i>TRP2</i> fbr (R65 + L76) fragment inserted via <i>EcoRI/BamHI</i>	This study.
pME2876	like pRS426 + 1.9 kb <i>TRP2</i> fbr (R65 + L76) fragment inserted via <i>EcoRI/BamHI</i> and 2.6 kb <i>TRP3</i> fragment via <i>BamHI/SacI</i>	This study.

## 2.2. Methods

### 2.2.1. Cultivation of cells

#### 2.2.1.1. Cultivation of *E. coli*

*E. coli* cells were grown overnight at 37°C in Luria-Bertani (LB)-medium (1 % tryptone, 0.5 % yeast extract, 1 % NaCl) (Sambrook *et al.*, 1989). Solid medium contained 2 % agar. For the selection of corresponding *E. coli*-strains supplements, listed in Table 3, were added to the media.

**Table 3: Media supplements**

supplement	stock solution	end concentration
ampicilin	100 mg/ml in H <sub>2</sub> O bidest	100 µg/ml
IPTG	100 mg/ml in H <sub>2</sub> O bidest	40 µg/ml
X-Gal	40 mg/ml in N,N-Dimethylformamid	40 µg/ml

#### 2.2.1.2. Cultivation of *S. cerevisiae*

*S. cerevisiae* cells were grown at 30°C in YEPD (2 % peptone, 1 % yeast extract, 2 % glucose) or in minimal vitamin (MV) medium (0.15 % yeast nitrogen base, 0.52 % ammonium sulfate, 2 % glucose, 1 % succinic acid, 0.3 % KOH (pH = 4.0 for liquid medium) or 8.5 % KOH (pH = 5.5 for solid medium)). For selection yeast was grown in synthetic complex (SC) medium (0.15 % yeast nitrogen base, 0.5 % ammonium sulfate, 0.2 mM *myo*-inositole, 0.2 % amino acid mix).

Amino acid supplements (Guthrie and Fink, 1991) or genitacin (G418; endconcentration 200 µg/ml) were added where applicable. For solid media 2 % agar were added.

For the growth of yeast in 10 l fermenters 8 l MV medium was inoculated and incubated at 30°C, while culture was stirred and aerated with sterile filtered air.

### **2.2.1.3. Cell storage**

For longer periods yeast and *E. coli* cells were stored in 15 % glycerol at –80°C.

## **2.2.2. Nucleic Acid Methods**

### **2.2.2.1. Isolation of plasmid DNA of *E. coli***

Two methods were applied: for small amounts of DNA, the quick-prep of Holmes and Quigley (1981) was applied and for larger amounts the Qiagen plasmid-DNA-Midi-preparation.

#### **2.2.2.1.1. Quick-Prep**

For the DNA isolation with the quick-prep-method (Holmes and Quigley, 1981) 1.5 ml of an overnight culture of plasmid containing *E. coli* strain was spun down in an e-cup with 13000 rpm for 1 min. The pellet was resuspended in 350 µl STET-buffer (100 mM NaCl, 10 mM Tris-HCl (pH 8.0), 1 mM EDTA (pH 8.0), 5 % Triton X-100) and 35 µl lysozyme (10 mg/ml) and boiled for 50 sec. After centrifugation at top speed for 15 min, the pellet was taken off with a toothpick and 40 µl Na-acetate (2.5 M, pH 5.2) and 420 µl isopropanole were supplied to the plasmid-DNA containing supernatant. An incubation for about 5 min at room temperature followed. Precipitated DNA was sedimented by centrifugation (13000 rpm, 1 min), washed with ethanol (70 %), dried and suspended with 50 µl TE-buffer with RNase (10 mM Tris-HCl, 1 mM EDTA, pH 8.0, 20 µg/ml RNase). Plasmid-DNA was stored at –20°C.

#### **2.2.2.1.2. Qiagen plasmid-DNA-Midi-preparation**

*E. coli* strains were grown overnight in a 100 ml culture. Instructions of the manufacturer (Qiagen, Hilden, Germany) for plasmid preparation were adhered. Plasmid-DNA was suspended in 200 µl H<sub>2</sub>O or 10 mM Tris-HCl (pH 8.5) and stored at –20°C.

#### **2.2.2.2. Isolation of chromosomal DNA from *S. cerevisiae***

Yeast strains were grown in 10 ml overnight at 30°C. Cells were harvested by centrifugation, suspended in 500 µl H<sub>2</sub>O, transferred into e-cups and resuspended with “Smash ‘n’ Grab”-buffer (2 % Triton X-100, 1 % SDS, 100 mM NaCl, 10 mM Tris-HCl (pH 8.0), 1 mM EDTA (pH 8.0)). 200 µl glass beads (∅ 0.45-0.5 mm, Carl Roth GmbH & Co KG) and 200 µl of a

TE-buffer saturated solution of phenol/chloroform/isoamylalcohol (25:24:1) were added to the cells. The samples were shaken for 10 min at 4°C. The cells were sedimented by centrifugation for 10 min at 4°C. The DNA in the supernatants was precipitated by the addition of 1 ml ethanol (99.9 %), spun down and suspended with 400 µl TE. DNA was purified by precipitation with 1 ml ethanol (99.9 %) and 10 µl 4 M ammoniumacetate. After DNA has dried, DNA-pellets were suspended in 50 µl TE buffer (10 mM Tris-HCl, 1 mM EDTA, pH 8.0).

### **2.2.2.3. DNA gel extraction**

DNA bands were cut out of the gel and purified by following the instructions of the manual of the Qiaex II-Kit (Qiagen, Hilden, Germany).

### **2.2.2.4. Determination of concentration of nucleic acids and purity control**

Concentration of nucleic acid solutions were determined by photometric determination of the absorption at 260 nm in a quartz cuvette (1 cm thickness). Blank was measured with the same solvent without nucleic acid. For OD<sub>260</sub> of 1.0 following concentration are assumed :

double-stranded DNA	50 µg/ml
single-stranded DNA	40 µg/ml
RNA	40 µg/ml
oligonucleotides	31 µg/ml

The purity of the nucleic acid solutions were checked by determination the OD at 280 nm wavelength.

### **2.2.2.5. Agarose gel-electrophoresis**

DNA solution was added to 0.1 volumes of DNA loading dye (7 M urea, 50 % sucrose, 0.1 % bromine phenol blue, 0.1 % xylene cyanol, 1 mM EDTA) and separated in a horizontal 1 % agarose gel, containing 0.5 µg/ml ethidium bromide, in TAE buffer (40 mM Tris-acetate, 20 mM Na-acetate, 2 mM EDTA, pH 8.3). DNA-bands were detected with an UV-transilluminator at  $\lambda = 254$  nm.

### **2.2.2.6. Polymerase chain reaction (PCR)**

Polymerase chain reaction (PCR) was made with the thermostable *Taq*-polymerase (MBI Fermentas GmbH, St. Leon-Rot, Germany), *Pfu* polymerase (Promega, Mannheim, Germany) or KOD-HiFi-DNA polymerase (Novagen, San Diego, USA). Normally 5-50 pmol primer-DNA, 10-100 ng DNA as matrix, in 20-50 µl reaction buffer accordant to the protocol of the manufacturer. The character of duration and temperature profile of the reaction were chosen after the used oligonucleotides, the general information of the manufacturers and DNA matrix.

#### **2.2.2.6.1. Introduction of site-directed mutations**

*Pfu* polymerase and KOD-HiFi-DNA polymerase possess the ability of proof reading and were therefore taken for the introduction of site-directed mutations. For this kind of mutagenesis four oligonucleotides were needed. Two primers for the start- and endpoint of the DNA-target and two primers for the introduction of the mutated codon, of which one anneals at the Watson- and one at the Crick-strand. With the first two PCR products resulted from the amplifications from the target-start to the mutation-primer and from the mutation-primer to the target end. After the PCR products were controlled for the right size in an agarose-gel and purified, 0.5 µl of these products were taken as matrix-DNA for PCR with start- and end-primer. This PCR step lead to the product with the mutated codon. After digestion of the ends, ligation into a vector, replication in *E. coli* and purification of the plasmid containing the mutated codon, the DNA sequence was verified.

#### **2.2.2.7. Enzymatical modification of nucleic acids**

##### **2.2.2.7.1. Restriction of DNA**

For the analytical digestion about 0.5 µg DNA were incubated for 2-3 h at 37°C with 1-2 U restriction enzyme (MBI Fermentas GmbH, St. Leon-Rot, Germany) in 20 µl reaction volume. For the digestion of preparative amounts of DNA, accordant higher volumes and enzyme amounts were taken.

##### **2.2.2.7.2. Ligation of DNA fragments**

Linear DNA fragments were incubated with 4 U T4-DNA-ligase (MBI Fermentas GmbH, St. Leon-Rot, Germany) and 2 µl of a 10x ligase buffer in a 20 µl volume overnight at 16-18°C. Concentration of DNA was 1-10 µg/ml and the ratio of vector-DNA/insert-DNA was about 1:4. Afterwards ligation attempt was taken for transformation without further purification steps.

##### **2.2.2.7.3. DNA sequencing**

Sequencing of double-stranded plasmid-DNA were made with the “ABI Prism™ BigDye Ready Reaction Terminator Cycle Sequencing Kit” (Applied Biosystems GmbH, Foster City, USA). 0.5 µg plasmid DNA was mixed with 2.0 µl Premix (*Taq* polymerase, dNTPs, fluorescent-marked ddNTPs and reaction buffer) and 3-10 pmol of the sequencing primer in a volume of 10 µl. Afterwards 25 cycles of following temperature profile were run through in a thermocycler: 20 sec denaturation at 96°C, 15 sec annealing of the primer at the annealing temperature ( $T_{\text{annealing}} = T_{\text{melting}} - 5^{\circ}\text{C}$ ) of the primer and 4 min extension at 60°C. DNA-precipitation followed with adding 90 µl H<sub>2</sub>O, 10 µl Na-acetate (3 M, pH 4.6) and 250 µl ethanole (99.9 %). After centrifugation and discarding the supernatant the not visible DNA pellet was washed with ethanole (70 %), sedimented by centrifugation and dried. To the

purified DNA 25 µl TSR buffer was added and the whole attempt was denatured at 95°C for 2 min. The electrophoretical separation of the DNA followed with the “ABI 300-Sequencer” (Applied Biosystems GmbH, Foster City, USA).

### **2.2.2.8. Transfer of DNA to *E. coli***

#### **2.2.2.8.1. Production of competent cells**

In order to make competent *E. coli* cells (Inoue *et al.*, 1990), 250 ml SOB-medium (2 % tryptone, 0.5 % yeast extract, 10 mM NaCl, 2.5 mM KCl, 10 mM MgCl<sub>2</sub>, 10 mM MgSO<sub>4</sub>) was inoculated with *E. coli* DH5α. Cells were shaken for about 24 h at 20°C till an OD<sub>595</sub> of 0.6-0.8 was reached. The cells were cooled down on ice for 10 min and sedimented in GSA-buckets per centrifugation (5000 rpm, 4°C, 10 min, Sorvall centrifuge 5C-5B, Fa. Du Pont Instruments, Bad Homburg). The cell pellet were washed with 80 ml TB (10 mM HEPES, 15 mM CaCl<sub>2</sub>, 250 mM KCl, 55 mM MnCl<sub>2</sub>, pH 6.7), incubated on ice for 10 min and spun down again (5000 rpm, 4°C, 10 min). Sedimented cells were carefully resuspended in 20 ml TB, 1.5 ml DMSO (7 % [v/v] endconcentration) was added, cells were aliquoted in 200 µl portions and immediately frozen within liquid nitrogen. The competent cells were stored at -80°C.

#### **2.2.2.8.2. Transformation of *E. coli***

To transform the competent *E. coli* DH5α cells, a 200 µl portion was slowly defrosted on ice. The whole ligation attempt (chapter 2.2.5.2.) were added to the cells and an incubation for 30-60 min on ice followed. For 90 sec the cells were shocked by heat at 42°C, cooled down on ice for 90 sec, appended with 1 ml LB medium and shaken at 37°C for 1 h. Afterwards the cells were plated on selective medium and incubated at 37°C over night.

#### **2.2.2.9. Transfer of DNA to *S. cerevisiae***

For making *S. cerevisiae* cells competent in order to transfer DNA (Ito *et al.*, 1983), 10 ml YEPD were inoculated and incubated overnight at 30°C. 100 ml main culture was inoculated in a ratio of 1:20 and incubated at 30°C to an OD<sub>595</sub> of 0.5. Afterwards cells were sedimented by centrifugation (5 min, 3500 rpm). With 20 ml Li-acetate/TE-buffer (0.1 M Li-acetate, 10 mM Tris-HCl, 1 mM EDTA, pH 8.0) cells were washed, centrifugated again, suspended in 1 ml Li-acetate/TE-buffer and incubated at 30°C for 30 min.

100 µl of these competent yeast cells were appended to a mix of 5 µl of freshly denatured salmon-sperm-DNA and 5 µg target DNA and 500 µl PEG 4000/Li-acetate/TE (50 % PEG 4000, 2.5 mM Tris-HCl (pH 8.0), 0.25 mM EDTA, 0.1 M Li-acetate) were added. An incubation of 30 min at 30°C followed. Afterwards the cells were heat-shocked at 42°C for 20 min. Cells were sedimented by centrifugation (3000 rpm, 5 min), resuspended in 1 ml

YEPD and incubated for 1-2 h at 30°C. Finally cells were plated on selective medium and incubated for 2-3 days at 30°C.

### **2.2.2.10. Transfer of nucleic acids on membranes**

#### **2.2.2.10.1. Southern Blot**

After chromosomal DNA (10 µg) was restricted overnight at 37°C and treated with RNase (37°C, 15 min), the resulted fragments were electrophoretically separated in an agarose gel (70 V, 2 h). Afterwards this gel is successively treated with 0.25 M HCl, 1 M NaCl in 0.5 M NaOH and 1 M NH<sub>4</sub>Ac in 0.02 M NaOH for 20 min each. DNA was transferred on a nylon-membrane (Biodyne B Transfer Membrane, Pall GmbH, Dreieich, Germany) by capillary blotting overnight. DNA was cross-linked to the membrane by uv-exposure for 2 min.

#### **2.2.2.11. Radiolabeling of DNA-fragments with [ $\alpha$ -<sup>32</sup>P] dATP**

Sample-DNA was radiolabeled with the Hexa-Label™ DNA Kit (MBI Fermentas GmbH, St. Leon-Rot, Germany) accordant to the instructions of the manufacturer. The DNA used for labeling was amplified by PCR.

#### **2.2.2.12. Hybridisation of radioactive labeled probes**

In order to saturate unspecific binding sites of the membrane, it was pre-hybridized for 2 h at 65°C with Church-buffer (7 % SDS, 1 % BSA, 1 mM EDTA, 250 mM Na-phosphate, pH 7.2). Hybridization was carried out overnight at 65°C with fresh 50 ml Church-buffer and the radioactive labeled sample DNA. Afterwards the membrane was washed twice for 30 min at 65°C with Northern-Wash (15 mM NaCl, 1.5 mM sodiumcitrate, 0.1 % SDS) and a phospho-imaging-screen (Fuji Photo Film Co., LTD, Nakanuma, Japan) was exposed with the membrane.

### **2.2.3. Protein Methods**

#### **2.2.3.1. Production of crude extracts of yeast cells**

Yeast cells were grown in MV medium till OD<sub>546</sub> between 3-4 is reached. Cells were sedimented by centrifugation in 1 l-buckets (4°C, 4500 rpm, Sorvall centrifuge RC-3C PLUS, Fa. Du Pont Instruments, Bad Homburg) and washed twice with 50 mM potassium-phosphate buffer (pH 7.6; PPB). Cells were suspended in 1 ml/g 50 mM PPB, added with 0.1 mM PMSF and 1 mM DTT and stored at -20°C or directly used.

Defrosted cells were opened with 2 kbar with the One Shot Cell Disruption Model (Constant System Ltd. Warwick, UK) and the cell fragments were separated from the crude extract by

centrifugation (12000 rpm, 4°C, 30 min, Sorvall centrifuge 5C-5B, Fa. Du Pont Instruments, Bad Homburg). The crude extract was stored at –20°C or directly used.

#### **2.2.3.2. Purification of DAHP synthase**

Crude extract were precipitated by ammonium sulfate, followed by centrifugation and filtration through gauze. This enzyme solution was loaded on a ethylamino-sepharose column (equilibrated with with 0.5 M PPB (pH 7.6), saturated with 30 % ammonium sulfate). Elution was carried out with H<sub>2</sub>O. Afterwards the pool of the EAS-column was loaded onto the MonoQ HR16/60 (equilibrated with 10 mM Tris, pH 7.6) and eluted with NaCl gradient.

#### **2.2.3.3. Purification of prephenate dehydratase**

The prephenate dehydratase of *S. cerevisiae* (Pha2p fusionprotein with C-terminal *Strep-tag*®) was purified by *Strep-tag*®-affinity-chromatography. *Strep-Tactin*®-Superflow®-column (IBA GmbH, Göttingen, Germany) was equilibrated with two volumes buffer W (100 mM Tris-HCl, pH 8.0, 150 mM NaCl, 1 mM EDTA). Before crude extracts were supplied to the column, they were incubated with avidin (endconcentration 1.5 µg/ml) for 30 min at 4°C, to block biotinylated proteins. After centrifugation (12000 rpm, 4°C, 10 min, Sorvall centrifuge 5C-5B, Fa. Du Pont Instruments, Bad Homburg) and filtration through gauze, protein extract is loaded onto the column. The column was washed with five volumes of buffer W. Pha2p fusion protein was eluted with three volumes buffer E (buffer W + 2.5 mM desthiobiotin) in fractions of 5 ml. All fractions were portioned in small aliquots, shock frozen in liquid nitrogen and stored at –80°C. The column was regenerated with 15 volumes buffer R (buffer W + 1 mM HABA) and washed with 8 volumes buffer W.

#### **2.2.3.4. Gelfiltration**

Gelfiltration was carried out at FPLC with Superdex 200 prep grade. Bluedextran was taken to determine the exclusion volumen and following enzymes were taken as standard proteins: Thyroglobulin: 670 kDa,  $\gamma$ -Globulin: 158 kDa, Ovalbumin: 44 kDa, Myoglobin: 17 kDa and Vitamin B 12: 1,35 kDa

#### **2.2.3.5. Concentration of enzyme solutions**

In order to concentrate proteins in solution Centricon® YM-30 centrifugal filter units (Milipore, Billerica, USA) with a cut-off of 30 kDa were used. Higher protein concentrations were necessary for crystallization experiments.

#### **2.2.3.6. Determination of protein concentration**

To determine the protein concentration in solution (Bradford, 1976) different volumes (1-10 µl) of these protein solutions were filled with H<sub>2</sub>O to 800 µl and 200 µl of Bradford reagent

(Bio-Rad Laboratories, Hercules, USA) was added. After 5 min of incubation optical densities were measured at 595 nm. BSA-solutions with different concentrations were taken as reference and H<sub>2</sub>O instead of protein solution as blank.

### 2.2.3.7. Elektrophoretical methods

#### 2.2.3.7.1. Discontinuous SDS-PAGE

Electrophoretic separation of protein mixtures were performed on denaturing conditions in discontinuous SDS-polyacrylamide gels (Laemmli, 1970). These gels consist of a stacking gel (375 mM Tris (pH 6.8), 3 % acrylamide, 0.08 % bisacrylamide, 0.1 % SDS) and a separating gel (375 mM Tris (pH 8.8), 10 % acrylamide, 0.4 % bisacrylamide, 0.1 % SDS). The anionic detergent destroys the quaternary structure of proteins and accumulates with the hydrophobic regions of the protein. The charge of the protein is covered and proteins are separated by mass and not by charge. Before the protein samples were loaded on a gel, the samples were denatured at 95°C in the presence of β-mercaptoethanol. Electrophoresis were driven in running buffer (0.25 M Tris, 2.5 M glycine, 1 % SDS, 0.34 % EDTA).

#### 2.2.3.7.2. Blue-Native PAGE

Blue native PAGE experiments is performed essentially as described (Schagger and von Jagow, 1991). An acrylamide gradient of 6 %-16.5 % were taken for the separation gel. Therefore 1.9 ml of each gel solution 6 % acrylamide/bisacrylamide and 16.5 % acrylamide/bisacrylamide were mixed in a gradient mixer and simultaneously poured for hardening. H<sub>2</sub>O was poured on top. When the gel was hard H<sub>2</sub>O was discarded and stacking gel was poured on top. Sample buffer (5 % Coomassie blue G, 500 mM ε-aminocaproic acid in 100 mM bistris, pH 7.0) was added to the samples (30 –50 µg protein) and they were loaded on the gel. The blue cathode buffer (50 mM trocine, 15 mM bistris, 0.02 % Coomassie blue G, pH 7.0) was poured into the middle tank and the colorless anode buffer (50 mM bistris, pH 7.0) into the outer. The gel was run at 4°C first for 30 min at 100 V, then 300 V till the blue front is at the bottom of the gel plus 30 minutes extra.

For the separation gel solutions a 3x gel-buffer (200 mM ε-aminocaproic acid, 150 mM bistris, pH 7.0) and an acrylamide/bisacrylamide-solution (AA/BA = 16:1; 51 % T, 0.62 % C) is required.

%	6 %	16.5 %	Stacking gel
3x gel-buffer	1.5 ml	1.5 ml	1.25 ml
acrylamide/bisacrylamide	0.535 ml	1.525 ml	0.3 ml
Glycerol	-	0.9 ml	-
H <sub>2</sub> O	2.444 ml	0.5585 ml	2.1835

per 1.9 ml for separation gel and for the whole stacking gel attempt:

10 % APS	8 µl	6 µl	15 µl
TEMED	0.8 µl	0.6 µl	1.5 µl

### 2.2.3.8. Transfer of proteins to membranes

Proteins were transferred overnight from SDS-PAGE with a wet-blot onto a nitrocellulose membrane (Protran; Schleicher & Schuell, Dassel, Germany) in transfer buffer (25 mM Tris Base, 192 mM glycine, 15 % methanol) at 30 V.

After the transfer the membrane was blocked with PBS-T (4 mM KH<sub>2</sub>PO<sub>4</sub>, 16 mM Na<sub>2</sub>HPO<sub>4</sub>, 115 mM NaCl, 0.1 % Tween 20) with 33.3 % milkpowder (or 3 % BSA for the *Strep-tag*<sup>®</sup> fusionproteins) for 1 h at room temperature. The blocking steps saturates unspecific binding of the antibodies to the membrane. Membrane was washed 3 times for 5 min with PBS-T. The primary antibody (Rabbit anti Aro4p 1:3000, Rabbit anti Cdc42p 1:200, Mouse anti *Strep-tag*<sup>®</sup> 1:200) was appended to PBS-T/milk or PBS-T (accordant to the manufacturers instruction) and the membrane was incubated within one of these antibody-solutions for 45 min. The membrane was washed three times for 5 min with PBS-T. The incubation with the second antibody (goat anti rabbit POD coupled 1:2000; goat anti mouse POD coupled 1:5000) in PBS-T/milk or PBS-T followed for 1 h. Afterwards the membrane was washed twice with PBS-T and protein bands were detected after ECL method. Therefore luminol solution (2.5 mM luminol, 400 µM paracoumaric acid, 100 mM Tris-HCl, pH 8.5) and a H<sub>2</sub>O<sub>2</sub> solution ( 5.4 mM H<sub>2</sub>O<sub>2</sub>, 100 mM Tris-HCl, pH 8.5) were given on the membrane and incubated for 2 min. The detection was carried out by exposure to a hyperfilm<sup>™</sup>-ECL<sup>™</sup> (Amersham Pharmacia Biotech, Buckinghamshire, GB) in the dark room. Exposure time was dependent on the signal density.

### 2.2.3.9. Staining proteins

#### 2.2.3.9.1. Coomassie staining

For unspecific protein staining (Weber and Osborn, 1969) with gels were stained with Coomassie stain (50 % methanol, 10 % acetic acid, 0.2 % Coomassie Brilliant Blue R250) for a few minutes at 60°C. The destaining of the background were done with Coomassie destain (20 % methanol, 5 % acetic acid) till single bands were visible.

#### 2.2.3.9.2. Silver staining

Silver staining (Blum *et al.*, 1987) is a more sensitive method for staining proteins than Coomassie staining. For the fixation of the proteins, the gel was incubated at least for 1 h in the fixation-solution (50 % methanol, 12 % acetic acid, 1.85 % formaldehyde) and washed 3

times for 1 min with 50 % ethanol. After that the gel was incubated for 1 min in thiosulfate solution (0.2 g  $\text{Na}_2\text{S}_2\text{O}_3 \times 5 \text{H}_2\text{O}$  in 1 l  $\text{H}_2\text{O}$ ) and washed three times in  $\text{H}_2\text{O}$  for 10 sec. A 20 min incubation in impregnation solution (0.2 %  $\text{AgNO}_3$ , 2.775 % formaldehyde) followed by a double washing step in  $\text{H}_2\text{O}$  for 10 sec. The protein bands become visible by the treatment with developer solution (6 %  $\text{NaCO}_3$ , 1.85 % formaldehyde, 4 mg  $\text{Na}_2\text{S}_2\text{O}_3 \times 5 \text{H}_2\text{O}$  in 1 l  $\text{H}_2\text{O}$ ). When the protein bands were clearly visible, the gel was quickly washed twice with  $\text{H}_2\text{O}$  and incubated in stop solution (1.86 % EDTA, pH 7-8) till clouding was visible. Finally gels were washed in  $\text{H}_2\text{O}$  for 15 min.

#### **2.2.3.10. Determination of the molecular masses of proteins**

To determine the molecular weight of proteins within SDS-PAGEs or Western blots, standard molecular weight marker had to be separated in the same gel. The migration distance of the proteins were compared with that of the standard proteins. The logarithm of the molecular masses is plotted against the  $R_f$  value of the standard proteins. The logarithm of the unknown molecular masses of the proteins can be deduced from this curve:

$$R_f = \frac{\text{migration distance of the protein}}{\text{migration distance of the dye}}$$

#### **2.2.3.11. DAHP synthase assay**

DAHP synthase assay was carried out as described (Takahashi and Chan, 1971) with following modifications: pH of the enzymatic reaction was adjusted to pH 6.8 instead of pH 6.5 and sodium periodate was dissolved in 0.25 instead of 0.125 M  $\text{H}_2\text{SO}_4$ .

#### **2.2.3.12. Prephenate dehydratase assay**

To determine the specific enzyme activities of the prephenate dehydratase (Fischer and Jensen, 1987) test tubes were preheated in the water bath at 30°C. 320  $\mu\text{l}$  Tris HCl (1 M, pH 7.9), 50  $\mu\text{l}$   $\text{H}_2\text{O}$  or effector (5 mM) and 30  $\mu\text{l}$  of protein solution (crude extract or purified) were given into the test tube. The enzymatic reaction was started with 100  $\mu\text{l}$  prephenate (5 mM). After an incubation of 10 min at 30°C the reaction was stopped with 2 ml 2.5 N NaOH. Reference values were stopped by 2 ml 2.5 N NaOH before starting the reaction with the enzyme solution. The end concentration of the substrate prephenate was 1 mM and of the effector was 0.1 mM in 500  $\mu\text{l}$  reaction volume. The absorption of the resulting product phenylpyruvate was measured at 320 nm in preheated (30°C) quartz cuvettes against the blank.

For the determination of the initial velocities  $v_i$ , 62.5  $\mu\text{l}$  prephenate solution were given into the 30°C preheated test tube and incubated for 30 sec. The reaction was started with 187.5  $\mu\text{l}$  of a mixture of enzyme/Tris-HCl (1 M, pH 7.9) and stopped with 2 ml NaOH (2.5 N) after an incubation of 1 min at 30°C. The endconcentrations of prephenate ranged between

0.015 mM and 2.5 mM in the reaction volume of and the enzyme-concentration in the reaction volume was about 1 ng/μl. The absorption of the resulting product phenylpyruvate was measured at 320 nm in preheated (30°C) quartz cuvettes against the blank.

#### **2.2.3.13. Evaluation of kinetic data**

The parameters from Michaelis-Menten equation were determined by non-linear curve fitting of the measured values to this equation. Therefore the Levenburg-Marquard-algorithm was taken. For statistical weighting the squared error was divided by the variance of the measurands. The program Microcal Origin 7.0 was used for the evaluation.

#### **2.2.3.14. Sample preparation for mass spectrometry by tryptical restriction**

In order to prepare samples for mass spectrometry by tryptical restriction (Shevchenko *et al.*, 1996), target bands were cut out of the silver stained SDS-PAGE and were transferred into an Eppendorf-cup without any additional liquid. In order to dehumidify the the piece of gel, it was covered with 25-35 μl acetonitrile and incubated for 10 min at room temperature. After that acetonitrile was discarded and the piece of gel was dried in the speed-vac-centrifuge for 10 min. The gel particle was moisture expanded for 1 h at 56°C with 150 μl 100 mM NH<sub>4</sub>HCO<sub>3</sub>/10 mM DTT. After the samples have cooled down, the solution was changed against 150 μl 100 mM NH<sub>4</sub>HCO<sub>3</sub>/50 mM iodoacetamide and the samples were incubated at room temperature for 45 min and sometimes shaken. Afterwards the gel pieces were incubated in 150 μl 100 mM NH<sub>4</sub>HCO<sub>3</sub> for 10 min, followed by a 10 min incubation in 150 μl acetonitrile, to dehydrate the gel again. The washing step with 150 μl 100 mM NH<sub>4</sub>HCO<sub>3</sub> for 10 min and the dehydratization with 150 μl acetonitrile were repeated. The gel particles were dried in the speed-vac-centrifuge for 10 min. To the dried samples 25-35 μl restriction buffer (12.5 ng/μl trypsin in 50 mM NH<sub>4</sub>HCO<sub>3</sub>) were added and incubated for 45 min in an ice water bath. Afterwards the trypsin containing solution was discarded and 5-10 μl 50 mM NH<sub>4</sub>HCO<sub>3</sub> was appended, to leave the gel pieces wet at the incubation at 37°C overnight. After centrifugation for 1 min at top speed, the supernatants were appended into a new Eppendorf-cup, the gel pieces were newly covered with 20 μl 50 mM NH<sub>4</sub>HCO<sub>3</sub>, incubated for 10 min at room temperature, spun down and the supernatants were united with the other supernatants. 25 μl of 5 % formic acid/50 % acetonitrile were added to the gel pieces and incubated at room temperature for 20 min. After centrifugation the supernatants were collected as well and appended to the others. This extraction with formic acid/acetonitrile was repeated twice. The united supernatants were dried in the speed-vac-centrifuge and stored at -20°C.

#### **2.2.3.15. Mass spectrometry**

The trypsin restricted samples were analyzed by Dr. Oliver Valerius (Department for Molecular Microbiology and Genetic) with Ultimate Nanao-HPLC (Dionex GmbH, Idstein) and

mass spectrometer LCQ Deca XP plus (Thermo Finnigan, Ringoes, USA). The selected raw data were evaluated with the software Turbo Sequest (Thermo Finnigan, Ringoes, USA).

### 3. Results

#### 3.1. The tyrosine-regulated DAHP synthase of *S. cerevisiae*

##### 3.1.1. Catalysis and regulation

##### 3.1.1.1. The substrate binding site of yeast Aro4p

The X-ray structures of crystals of the phenylalanine inhibitable DAHP synthase (AroG) of *E. coli* (Shumilin *et al.*, 1999; Shumilin *et al.*, 2002) and of the tyrosine-regulated isoenzyme (Aro4p) of *S. cerevisiae* (König, 2002; Hartmann *et al.*, 2003) were recently determined. In the crystal, the metal binding sites in the phenylalanine inhibitable DAHP synthase of *E. coli* are formed by Cys61, His268, Glu302, Asp326 (Shumilin *et al.*, 1999). The comparison of the crystals revealed that these residues correspond to the amino acids Cys76 of loop L1, His282 of loop L7, Glu316 of the  $\beta$ -sheet  $\beta$ 8 and Asp342 of loop L8 in the Aro4p enzyme of *S. cerevisiae* (König, 2002; König *et al.*, 2004).

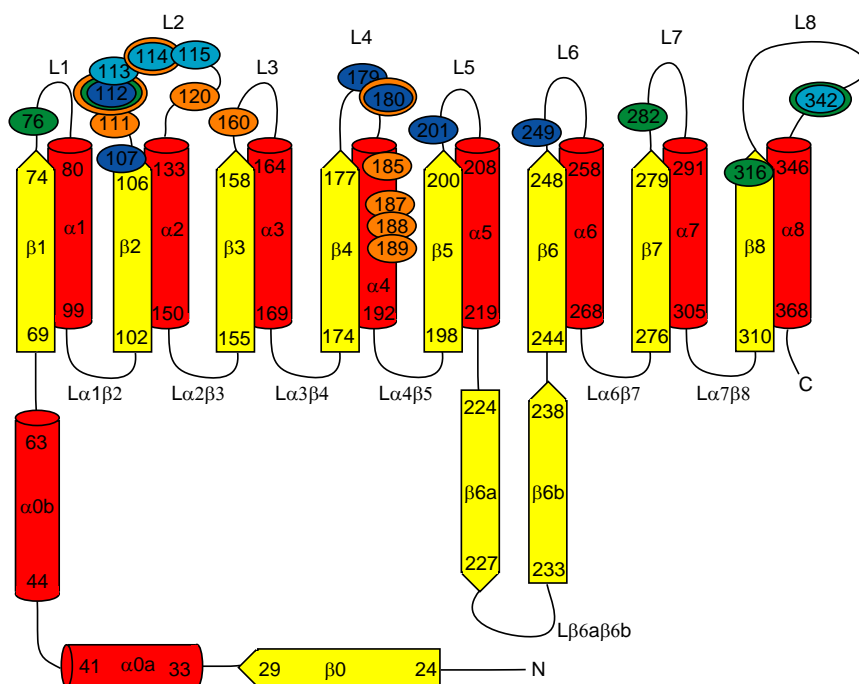


**Figure 16: Topology plot of tyrosine regulated DAHP synthase of *S. cerevisiae*.**  $\beta$ -sheets are displayed as yellow arrows and  $\alpha$ -helices as red cylinders. The binding sites of the divalent metal ion, PEP and E4P are marked in green, dark and light blue, respectively. Those amino acid residues, which have been substituted, are colored in orange.

Besides these four protein ligands, the metal cation is coordinated by the substrate PEP and an additional water bridge to Lys112 in Aro4p, which equals Lys97 in AroG (König, 2002; König *et al.*, 2004). The amino acid residues Arg107, Lys112, Ala179, Arg180, Lys201 and Arg249 coordinate the substrate PEP with hydrogen bonds in the crystal (König, 2002). Furthermore, König reported in 2002, that the E4P-analogue glycerol-3-phosphate (G3P) is bound in the crystal structure with its phosphate moiety to Arg114 and Thr115, whereas both of the hydroxyl groups of G3P build hydrogen bonds to Pro113 and Asp342 (Figure 17).

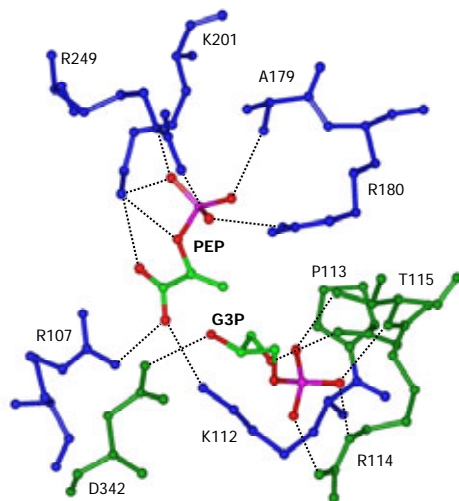


**Figure 17: Coordination of phosphoenolpyruvate (PEP) and glycerol-3-phosphate (G3P), the structural analogue of erythrose-4-phosphate (E4P).** The amino acids, which coordinate PEP, are given in blue, the G3P binding residues are colored in green.

We wanted to examine whether amino acid residues, which are located at critical positions in the crystal are essential *in vivo*. Therefore we focused on residues which coordinate one of the substrates or the divalent metal ion in the crystal structure. Amino acid substitutions were introduced into yeast Aro4p by mutagenising the corresponding codon in the *ARO4* open reading frame. The mutant alleles were expressed in yeast and the resulting enzyme variants were analyzed. K112 builds hydrogen bonds to the divalent metal ion as well as to PEP and is located in the loop L2 between sheet  $\beta 2$  and helix  $\alpha 2$  of Aro4p. A mutant gene was constructed, where the K112 codon was replaced by an alanine codon by PCR and the resulting *ARO4* allele was expressed from the plasmid pME2542 in the DAHP synthase deficient strain RH2424 (*MATa*, *can1-100*, *GAL*, *aro3::HIS3*, *aro4::LEU2*, *ura3-1*) (Hartmann *et al.*, 2003). Similarly the arginine residue at position 114, which is located in the same loop (L2) of Aro4p and which is required for E4P binding, was exchanged against an alanine residue resulting in plasmid pME2004. In addition, PEP coordinating Arg180, located in the loop L4 between sheet  $\beta 4$  and helix  $\alpha 4$ , was substituted by an alanine, leading to plasmid pME2543. All three mutant enzymes derived from high copy plasmids with the *MET25*

promoter driving the changed open reading frame of *ARO4*. Western hybridization experiments showed that the enzyme variants were stable (Figure 18).

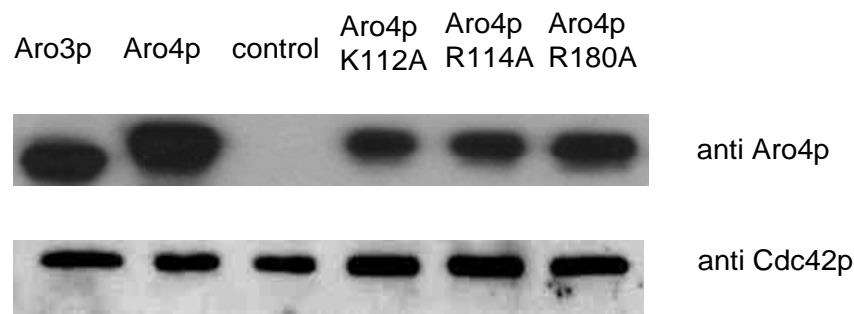


**Figure 18: Western hybridization experiment of Aro4p enzyme variants of *S. cerevisiae*.** The expression levels of Aro3p, Aro4p and variants of Aro4p, which have single amino acid exchanges at the catalytic center from high copy number plasmids are compared, in order to assure stable protein concentrations. Crude extracts of the plasmid containing yeast strains were prepared. 2 µg of protein were loaded onto each lane for visualization with anti Aro4p. Anti Cdc42p was taken to visualize the corresponding protein as loading control. For visualization the Cdc42 protein in the crude extracts 20 µg of protein were loaded per lane.

Specific activities of crude extracts of yeast strains containing Aro4p-Lys112A, Aro4p-Arg114A or Aro4p-Arg180A, respectively, in comparison to wildtype DAHP synthases were measured at least three times with three different transformants. All three mutant DAHP synthases did not show any detectable enzyme activity (data not shown). Growth tests were performed on media with and without aromatic amino acids. Corresponding to the lack of activity, these newly created DAHP synthase alleles did not allow growth of the yeast cells in a medium, which is not complemented by aromatic amino acids (Figure 19). Supplementing the medium with phenylalanine, tyrosine and tryptophan lead to growth of these yeast strains. These data suggest that Lys112, Arg114 and Arg180 are essential for functional *ARO4* encoded yeast DAHP synthase.

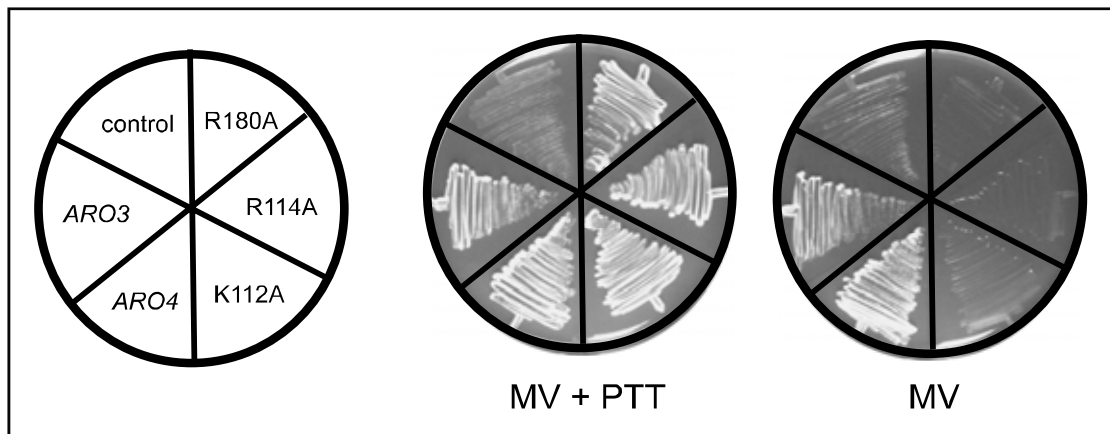


**Figure 19: Growth of *S. cerevisiae* strain RH2424 (*ura3-1*,  $\Delta$ *aro3*,  $\Delta$ *aro4*; control) carrying mutant alleles of *ARO4* was tested on MV medium with and without aromatic amino acids phenylalanine, tyrosine and tryptophan (PTT). Uracil auxotrophy was supplemented by the *URA3* marker of the high copy number plasmids containing *ARO4* chimeric alleles fused to the *MET25* promoter.**

These data corroborate the importance of each of the three exchanged amino acids Lys112, Arg114 and Arg180 of the crystal structure for the activity of the enzyme in solution. The residues, which were coordinating PEP, E4P or the divalent metal ion are each essential for catalytic features of DAHP synthase and alterations in any of these residues were not tolerated and completely abolish DAHP synthase activity.

### **3.1.1.2. Transmission of the inhibition signal within the tyrosine-regulated yeast DAHP synthase**

Amino acids located in the loops between the  $\beta$ -sheets and the  $\alpha$ -helices 1, 2, 4, 5, 6, 7 and 8 are important for the coordination of the divalent metal ion and the two substrates PEP and E4P (compare with Figure 16). These residues might be therefore required for catalysis. Loop L3 is the only loop of the  $\beta/\alpha$ -barrel, which does not take part in the condensation of PEP and E4P (Hartmann *et al.*, 2003; König *et al.*, 2004).

The crystal structure of the phenylalanine-regulated DAHP synthase AroG of *E. coli* in the presence of its inhibitor showed differences to the active form of this enzyme (Shumilin *et al.*, 2002). A comparison of the crystal structures of the active with the inhibited form of the tyrosine-regulated DAHP synthase of *S. cerevisiae* by superimpositions revealed differences. Similar differences can be observed by superimposition of the crystal structures of AroG of

*E. coli* of the active in comparison to the inactive state. In both DAHP synthases the start site for the transfer of the inhibition signal corresponds to the allosteric site. The N-terminus and loop L3 are drawn towards the inhibitor molecule. The major movement of loop L3 within the monomer leads to the break of the intradomain contact of the residues Leu160 (L3) and Glu111 (L2). As a result loop L2, which is required for catalysis, is destabilized (König, 2002). We characterized the change in inter- and intradomain contacts by constructing mutant forms of the tyrosine-regulated DAHP synthase of *S. cerevisiae*, by substituting amino acids in loops L2, L3 and L4, in order to examine the proposed inhibition-signal transmission. We exchanged the glutamate residue at position 111 within loop L2 and the leucine residue at position 160 of loop L3 against an alanine. Both substitutions resulted in DAHP synthase variants, which are reduced in specific enzyme activity. Although specific activity is lowered in crude extracts compared to wildtype enzyme, the activity can still be further reduced in the presence of the inhibitor tyrosine suggesting that feedback-inhibition is still at least partially functioning (Table 4).

**Table 4: Specific activities of crude extracts of different Aro4p mutant enzymes of *S. cerevisiae*.** Crude extracts of the plasmid containing strains were prepared and DAHP synthase stop assays were carried out for determination of specific activities. Aro4p wildtype specific activity without effector is set to 100 %. The residual-activity in the presence of 1 mM of the inhibitor tyrosine is compared to the specific activity without inhibitor. Those mutant enzymes, which are not able to restore growth of the yeast strain in the absence of aromatic amino acids and show enzyme activities below detection level, are indicated as inactive.

crude extract	location within Aro4p	w/o effector [%]	tyr [% rest-activity]
Aro4p WT		100	2
Aro4p E111A	loop L2	4	10
Aro4p K120A	loop L2	1	11
Aro4p K120E	loop L2	0,2	0
Aro4p L160A	loop L3	0,4	9
Aro4p R180A	loop L4	inactive	
Aro4p Q185A	helix $\alpha$ 4	13	0
Aro4p H187F	helix $\alpha$ 4	284	1
Aro4p H187L	helix $\alpha$ 4	inactive	
Aro4p R188E	helix $\alpha$ 4	inactive	
Aro4p E189R	helix $\alpha$ 4	0,7	43
Aro4p E189K	helix $\alpha$ 4	inactive	
Aro4p E111A +L160A	loops L2/L3	inactive	
Aro4p K120E + E189K	loop L2/helix $\alpha$ 4	inactive	

DAHP synthase deficient yeast strain carrying these *ARO4* alleles are able to grow in the presence of the three aromatic amino acids. However, in the absence of phenylalanine, tyrosine and tryptophan, growth of the cells is significantly reduced (Figure 20).

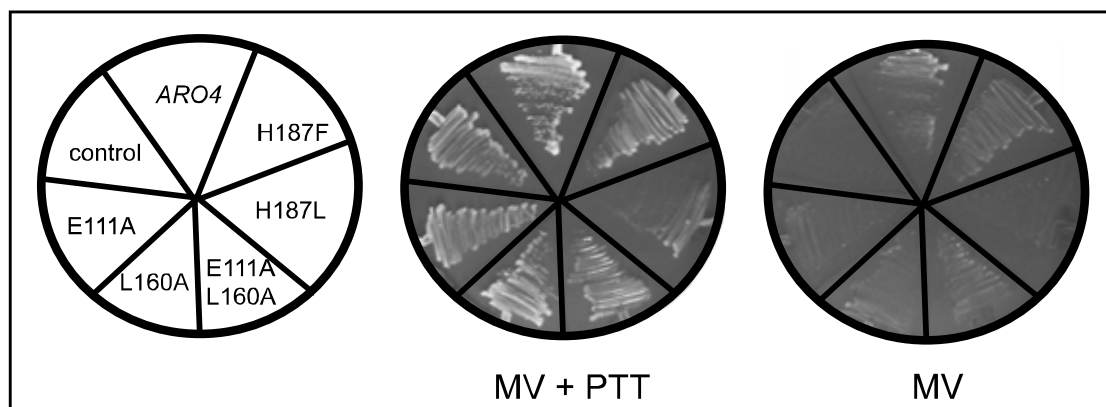


**Figure 20: Growth of *S. cerevisiae* strain RH2424 (*ura3-1*,  $\Delta$ *aro3*,  $\Delta$ *aro4*; control) carrying mutant alleles of *ARO4* was tested on MV medium with and without aromatic amino acids. Uracil auxotrophy was supplemented by the *URA3* marker of the high copy number plasmids containing the *ARO4* alleles downstream of the *MET25* promoter.**

The expression of these two DAHP synthase encoding alleles was controlled by western hybridization experiments and it was shown that the level is similar to the *ARO4* wildtype. The substitutions Glu111Ala and Leu160Ala both result in DAHP synthases, which are repressed in activity compared to the wildtype enzyme. However, this activity can still be further lowered by the presence of tyrosine (Table 4). Expression of these alleles did not result in significant differences. The combination of the substitution of the glutamate residue at position 111 by an alanine and the exchange of the leucine residue at position 160 against an alanine resulted in a mutant enzyme without any detectable activity (Table 4). In the absence of phenylalanine, tyrosine and tryptophan in the medium growth cannot be restored by the expression of double mutated *ARO4*, although the corresponding protein seems to be stable (Figure 21).

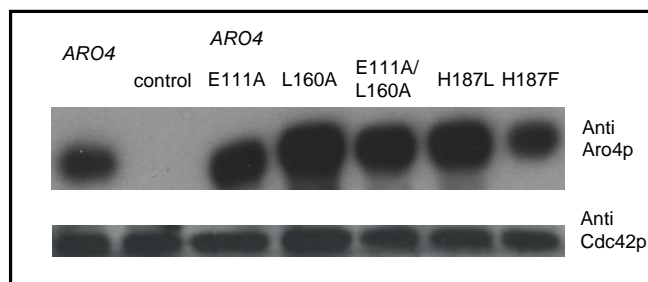


**Figure 21: Western blot hybridization of *S. cerevisiae* Aro4p variant enzymes.** The expression levels of *ARO4* and alleles of *ARO4* are compared, which have single codon exchanges for the amino acids between the catalytic center and the regulatory center from high copy number plasmids. Crude extracts of the plasmid containing strains were prepared. 2  $\mu$ g of proteins were loaded onto each lane for visualization with anti Aro4p and 20  $\mu$ g for visualization of the control-protein with anti Cdc42p.

The disruption of the intramolecular contact between Aro4p Glu111 (loop L2) and Aro4p L160 (loop L3), caused by genetic manipulation, leads to a loss of activity, that corresponds to a similar disruption induced by the integrated inhibitor molecule (Figure 22).

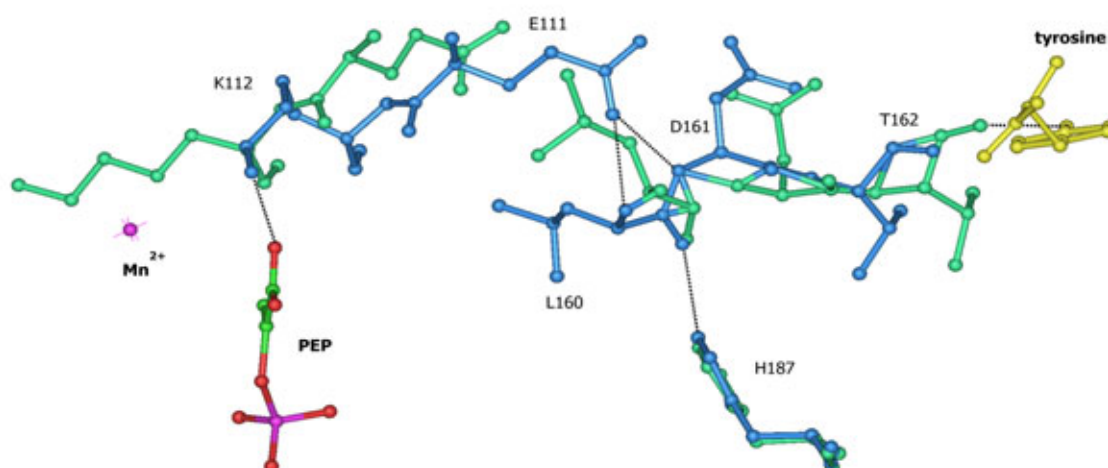


**Figure 22: Superimposition of Aro4p structures in the active and inactive state.** The blue structure was co-crystallized with PEP (colored) and  $Mn^{2+}$  (magenta) and the green was co-crystallized with tyrosine (yellow). Displayed is the intradomain contact between Glu111 of loop L2 and Leu160 of loop L3 in the active structure (blue) and the hydrogen bond between Leu160 (loop L2) and His187 (helix  $\alpha$ 4).

The remaining activity in the single and double mutant DAHP synthases can be further reduced by tyrosine. This suggests that there might be a second and/or supplementary pathway of signal transduction within the enzyme.

The histidine residue at position 187 is located in helix  $\alpha$ 4 and builds a hydrogen bond to Leu160, which is apparent in the active and inactive crystal structure (Figure 22). In order to

examine the importance of the hydrogen bond between His187 and Leu160 in the enzyme in solution, we exchanged the histidine against a phenylalanine and a leucine, respectively. We hypothesized that, in the Aro4p mutant enzyme the leucine residue at position 187 might no more be able to build this intradomain contact. We found that the exchange of this histidine residue against a leucine leads to an enzyme without detectable activity. If substituted against a phenylalanine residue the specific activity is increased to 284 % compared to Aro4p wildtype. By tyrosine this mutant enzyme can be inhibited to a residual activity of 1 % of its original activity (Table 4). Both mutant enzymes were analyzed for their competence to restore growth. Expression levels were compared to the wildtype enzyme. Growth can only be restored, when histidine is exchanged for phenylalanine (His187Phe) but not when exchanged by leucine. Protein levels derived from these two alleles are similar compared to wildtype *ARO4* derived protein levels (Figure 20, Figure 21).

Loop L2 is important for the binding of the substrates and the divalent metal ion, and therefore destabilizing loop L2 disturbs catalysis. Several hydrogen bonds in the active structure are located between helix  $\alpha 4$  and loop L2 of the two monomers of a dimer. These hydrogen bonds are not found in the inactive structure suggesting, that the break of these interdomain contacts might be an alternative path of transmission of the inhibition-signal within the tyrosine-regulated DAHP synthase.

We also analyzed those amino acid residues of helix  $\alpha 4$ , which had changed their inter- or intradomain contacts when comparing crystal structures of Aro4p in the active and inactive state (Figure 23). The residues Lys112 (König *et al.*, 2004), Arg114 (König *et al.*, 2004), Thr115 and Lys120 are part of loop L2. The exchange of lysine at position 120 against an alanine results in an enzyme, which is reduced in activity (1 % of wildtype activity; Table 4). Protein levels are similar and growth of RH2424 can be restored in the absence of phenylalanine, tyrosine and tryptophan (Figure 24, Figure 25). The substitution of R114 with an alanine residue leads to an inactive but stable protein (König *et al.*, 2004).

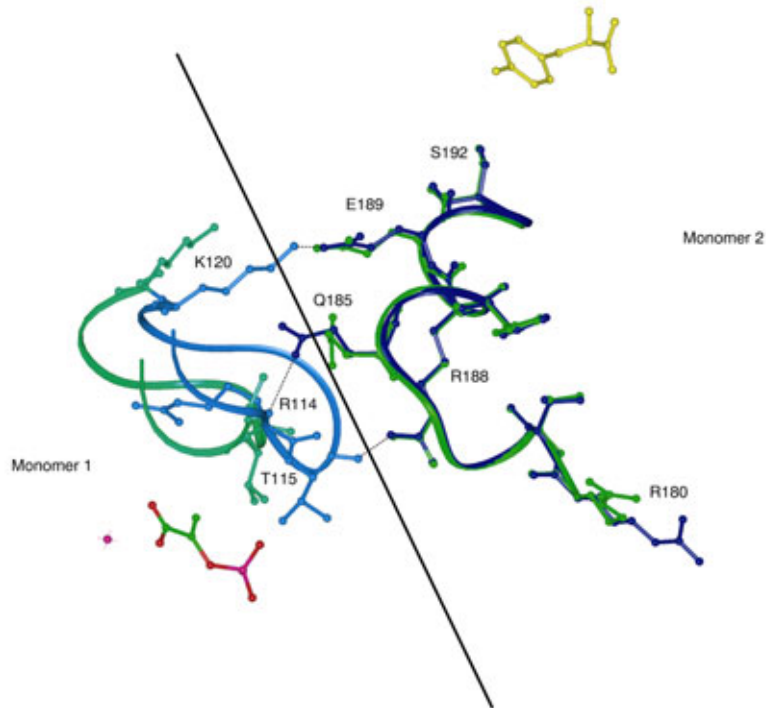


**Figure 23: Superimposition of Aro4p structures in the presence of substrate in comparison to the presence of inhibitor. Here, part of the dimeric interface in detail. (Blue: in the presence of PEP and  $Mn^{2+}$ ; green: in the presence of tyrosine).** The line illustrates the dimer interface with loop L2, next to PEP and the metal ion, on one side and helix  $\alpha_4$ , next to tyrosine, on the other side. The hydrogen bonds displayed as black dashed lines between Lys120 and Glu189, Arg114 and Gln185 and Thr115 and Arg188.

The exchange of glutamine at position 185 against an alanine leads to a DAHP synthase, with a reduced activity of approximately 13 % and regulation with tyrosine is still detectable. Arg188 was exchanged for a glutamate residue. The resulting enzyme has no detectable activity and is not able to restore growth of a yeast strain lacking the two wildtype DAHP synthases in the absence of aromatic amino acids in the medium (Figure 24, Table 4).

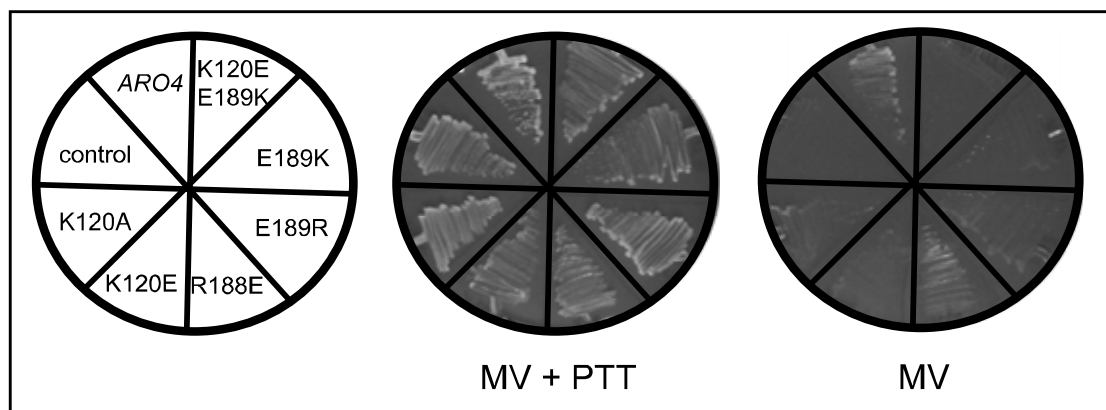


**Figure 24: Growth of *S. cerevisiae* strain RH2424 (*ura3-1*,  $\Delta$ *aro3*,  $\Delta$ *aro4*; control) carrying mutant alleles of *ARO4* was tested on MV medium with and without aromatic amino acids. Uracil auxotrophy was supplemented by the *URA3* marker of the high copy number plasmids containing the *ARO4* alleles downstream of the *MET25* promoter.**

Exchanging the adjacent residue Aro4p-Glu189 by an arginine residue leads to a reduced activity of 0.7 % compared to wildtype activity. In the presence of tyrosine, this low activity can be further reduced. In Aro4p, the connection between Glu189 and Lys120 in the active state seems to be important for activity, because substitutions at both positions lead to enzymes with a reduced activity. The exchange of only one of these two amino acids, so that two lysines or two arginines are located vis-à-vis, leads in both cases to specific activities, which are lower than 1 % of the wildtype specific activity. The inhibitor tyrosine is able to reduce even this small activity of Lys120Glu and Glu189Lys. A combination of these two amino acid substitutions results in an inactive DAHP synthase, which cannot restore growth of this yeast strain in the absence of any aromatic amino acid. Both residues (Lys120 and Glu189) are highly conserved in the protein sequence of DAHP synthases, which implicates that the simultaneous exchange leads to other catalysis disturbing effects within the enzyme.

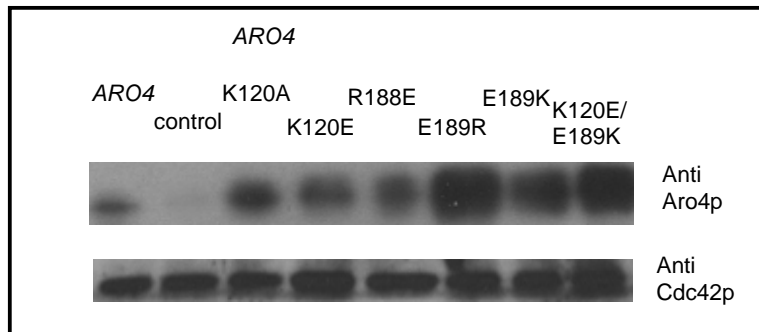


**Figure 25: Western blot hybridization of *S. cerevisiae* Aro4p variant enzymes.** The expression levels of *ARO4* wildtype in comparison to various *ARO4* alleles of *S. cerevisiae*, which have single codon exchanges for amino acids between the catalytic center and the regulatory center from high copy number plasmids. Crude extracts of the plasmid containing strains were prepared. 2 µg of proteins were loaded onto each lane for visualization with anti Aro4p; 20 µg of protein for visualization of Cdc42p as control with anti Cdc42p.

In summary, our results suggest that two parallel pathways of signal transduction within Aro4p result in inhibition of the catalytic site when tyrosine binds to the allosteric site (Figure 26). The first pathway is located within a monomer, where insertion of tyrosine causes movement of the catalytic site towards the inhibitor molecule. As a consequence the intradomain contacts between loop L3 (Leu160) and loop L2 (Glu111) are lost. The second pathway includes the interaction between the two monomers of the dimer where one monomer impairs the function of the second monomer. The interdomain contacts which are important for this second pathway are amino acid residues of helix  $\alpha 4$  (Gln185, Arg188 and Glu189) of one monomer which interact with loop 2 which is also involved in the first pathway of the other monomer including the crucial residues Arg114, Thr115 and Lys120. Tyrosine binding results in the loss of the hydrogen bonds and enhances the effect that the catalytic site is drawn towards the inhibitor site.

This dual pathway consisting of a monomeric and a dimeric part results in a destabilization of the catalytic site which make it less available for substrate binding.

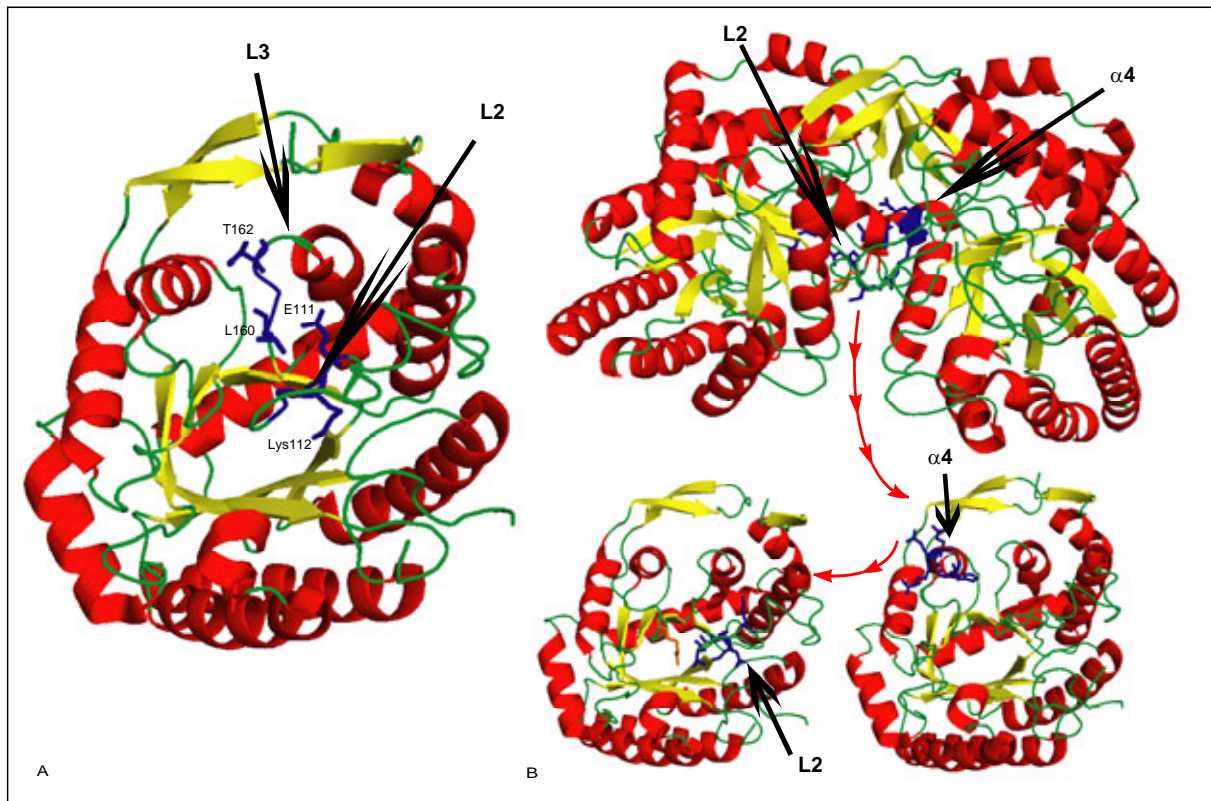


**Figure 26: Intramolecular (within the monomer, A) and intermolecular (between the two monomers of the dimer, B) transmission of the inhibition signal of yeast Aro4p. A** Ribbon presentation of an Aro4p monomer, with the transmission participating residues displayed in blue,  $\alpha$ -helices in red, loops in green and  $\beta$ -sheets as yellow arrows. **B** Inhibition signal transmission within the Aro4p dimer. The blue colored residues of helix  $\alpha 4$  display the first part of the second pathway of transmitting the inhibition signal starting at the allosteric site of one monomer and ultimately arriving at the catalytic site of the second monomer of a dimer via the blue colored residues of loop L2. L2 is located at the catalytic center. The red arrows indicate the second part which is in the intermolecular transmission pathway between the two monomers of a dimer. The black arrows point at helix  $\alpha 4$  and the loops L2 and L3 in the region of the catalytic site.

### 3.1.2. Tyrosine regulated DAHP synthase of *S. cerevisiae* is a dimer

#### 3.1.2.1. Oligomeric status of Aro4p

Yeast Aro3p has a molecular weight of 41.07 kDa and yeast Aro4p of 39.749 kDa, deduced from the primary amino acid sequence of the corresponding genes. The molecular mass of the phenylalanine inhibitable DAHP synthase monomer of *S. cerevisiae* was determined before as 42 kDa by SDS-PAGE (Paravicini *et al.*, 1989). The oligomeric organization of

DAHP synthases of the phenylalanine and tyrosine regulated DAHP synthases of *E. coli* have also been determined. *E. coli* AroG is preferentially described as a tetramer with a molecular weight of 110 kDa (33 kDa per monomer) and *E. coli* AroF is a dimer with 66 kDa (39 kDa per monomer) (Schoner and Herrmann, 1976; Simpson and Davidson, 1976). While the oligomeric status of tyrosine inhibited DAHP synthase of *S. cerevisiae* is not known, the molecular mass of native *S. cerevisiae* Aro3p was estimated by gel filtration as 53 kDa and proposed to be preferentially a monomer (42 kDa per monomer determined with SDS-PAGE) (Paravicini *et al.*, 1989). The molecular weight of the tyrosine inhibitable DAHP synthase Aro4p monomer of *S. cerevisiae* was determined as 42 kDa by SDS-PAGE (Schnappauf *et al.*, 1998). The oligomeric behavior of the tyrosine inhibitable DAHP synthase was estimated by gel filtration on a Superdex™ 200 prep grade column. Aro4p was eluted in a single peak with a volume of 94,02 ml, corresponding to a molecular weight of 63 kDa (Figure 27).

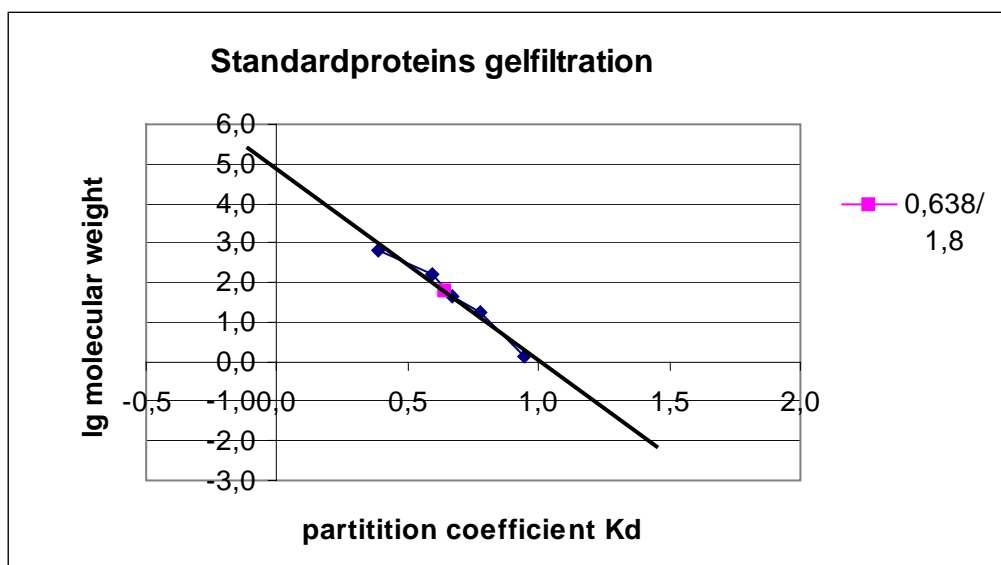


**Figure 27: Calibration curve of standard proteins (Thyroglobulin: 670 kDa,  $\gamma$ -Globulin: 158 kDa, Ovalbumin: 44 kDa, Myoglobin: 17 kDa and Vitamin B 12: 1,35 kDa) for determination of the molecular weight of Aro4p.** Exclusion volume of the gelfiltration column Superdex 200 prep grade was determined with 300  $\mu$ l of a solution of blue dextran (60  $\mu$ g/ $\mu$ l). 20 mM BPP was taken as running buffer. The elution volume of Aro4p was 94 ml, which corresponds to a molecular weight of 63 kDa of the tyrosine-regulated DAHP synthase.

The molecular mass of the native Aro4p estimated by gel filtration is one and a half times higher than the molecular weight of 40 kDa per Aro4p monomer determined with SDS-PAGE. As it is not clear whether Aro4p is a monomer or a dimer after gel filtration, a second approach to determinate the oligomeric status of the DAHP synthases of *S. cerevisiae* was applied which is the separation of purified Aro3p and Aro4p by blue native PAGE (Figure 28).

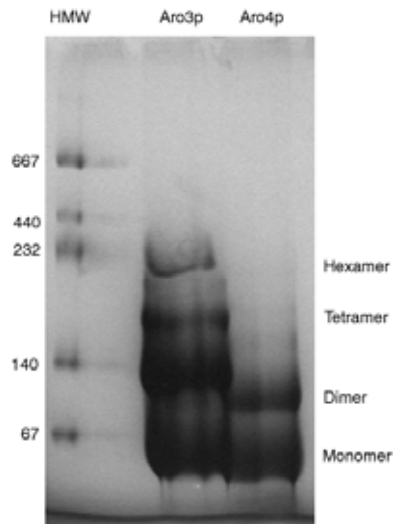


**Figure 28: Blue Native PAGE of wildtype DAHP synthases Aro3p and Aro4p of *S. cerevisiae*.** Aro3p and Aro4p were purified as described (Paravicini *et al.*, 1989; Schnappauf *et al.*, 1998). 30 µg of each were loaded per lane. This experiment was repeated at least four times with enzymes from two independent purifications.

The phenylalanine regulated Aro3p wildtype enzyme is separated in 4 bands with the molecular weights 54 kDa, 124 kDa, 172 kDa and 266 kDa, which correspond approximately the molecular weights of a monomer, dimer, tetramer and hexamer, regarding to the molecular weight of 42 kDa of one subunit of Aro3p (Paravicini *et al.*, 1989). The Aro4p isoenzyme is separated into two distinct bands with the molecular weights of 50 kDa and 83 kDa, which correspond approximately to monomer and dimer, regarding to the molecular weight of 40 kDa of one subunit of Aro4p.

These data suggest that both DAHP synthases can be organized as oligomers. In contrast to Aro3p Aro4p does not show any tendency to form tetramers or hexamers suggesting that the dimer might be the preferred state of oligomerization.

### 3.1.2.2. The dimeric interface of tyrosine regulated DAHP synthase

As described in chapter 3.1.2. binding of the inhibitor tyrosine results in the loss of several interdomain contacts which are present in the absence of the inhibitor. We tested the oligomeric status of the tyrosine regulated DAHP synthase of *S. cerevisiae* Aro4p-Lys120Ala mutant enzyme, which is poorly active but can still be regulated by tyrosine the wildtype Aro4p as control and the mutant enzyme were purified and blue native PAGE was applied (Figure 29).

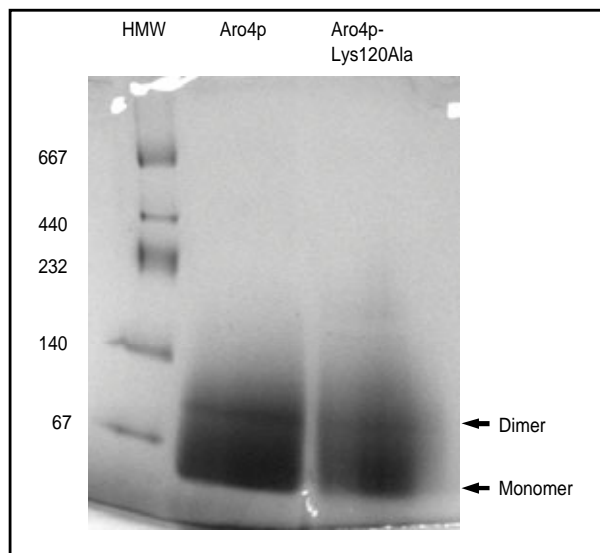


**Figure 29: BN-PAGE of wildtype Aro4p and Aro4p-K120A mutant.** Aro4p and Aro4p-K120A were purified as described (Paravicini *et al.*, 1989; Schnappauf *et al.*, 1998). 30  $\mu$ g of each were loaded per lane. This experiment was repeated at least four times.

The active wildtype and the hardly active mutant enzyme are not distinguishable in the blue native-PAGE. Both enzymes separate into two similar bands, which correspond to a monomer with a molecular weight of 50 kDa and a dimer with a molecular weight of 83 kDa, regarding to the estimated molecular weight of one molecule Aro4p with 40 kDa. These data suggest that the mutant enzyme is not impaired in dimerization. Therefore the dimer seems to be stabilized by multiple interaction in addition to this loop L2 and helix  $\alpha$ 4 interaction which is presumably irreversibly disturbed in this enzyme variant.

### **3.2. The role of phenylalanine in the regulation of the biosynthetic pathway of aromatic amino acids**

The end products phenylalanine, tyrosine and tryptophan of the aromatic amino acid biosynthetic pathway feedback regulate keyenzymes of their own synthesis. Important targets for feedback regulation in the baker's yeast *Saccharomyces cerevisiae* are the two DAHP synthases at the initial step of the pathway and the two enzymes at the first branching point, the chorismate mutase and the anthranilate synthase. Both enzymes compete for the substrate chorismate and direct the metabolic flux to tyrosine/phenylalanine and tryptophan, respectively. In several organisms additional enzymes of the branched pathway, like e.g. a third DAHP synthase or prephenate dehydratase or prephenate dehydrogenase at the second branch point are regulated as well. In yeast, the general control plays an additional important role for the fine-tuning of the expression rates of the enzymes of biosynthetic pathways. An interesting phenomenon, one which has not been explained yet, is the so-called "phenylalanine-effect" or "phe-effect". This reflects the following observations: In the absence of the general control transcription factor Gcn4p, and in the presence of the unregulated and constitutively activated chorismate mutase Aro7<sup>c</sup>p the addition of phenylalanine to the cultivation medium leads to tryptophan starvation (Krappmann, 2000; Krappmann *et al.*, 2000). The addition of tyrosine instead of phenylalanine to the medium does not cause this effect, but if phenylalanine and tyrosine are added both these yeast strains are not able to grow.

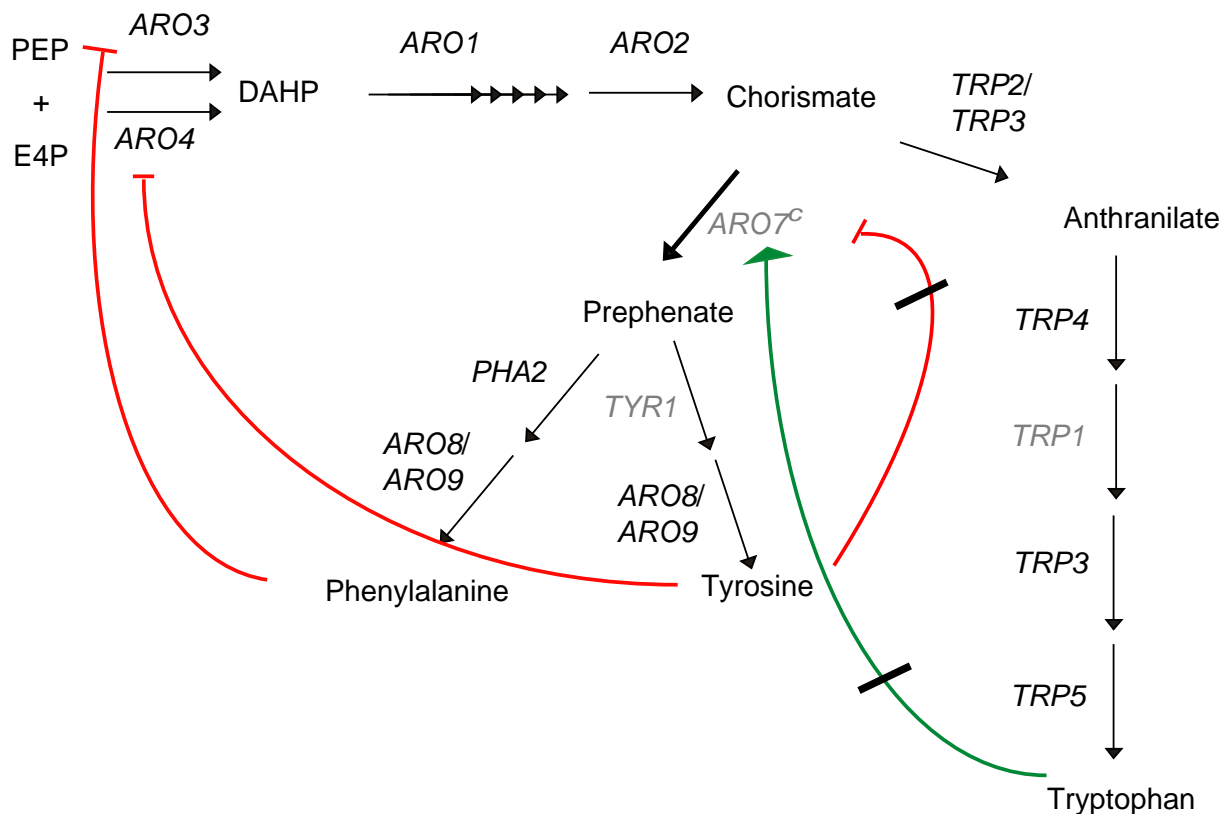


**Figure 30: Regulation modes of the aromatic amino acid biosynthetic pathway in *S. cerevisiae* *ARO7<sup>c</sup>* mutant strain which possesses a chorismate mutase insensitive towards the feedback-inhibitor tyrosine and the crosspathway activation tryptophan.** The pathway starts with the condensation of phosphoenolpyruvate (PEP) and erythrose-4-phosphate (E4P) to 3-deoxy-D-arabino-heptulosonate-7-phosphate (DAHP) catalyzed by the DAHP synthase. DAHP is converted via six enzymatically catalyzed steps to chorismate. This last common metabolite of the shikimate pathway is the initial intermediate of the two branches leading to tryptophan on one side and to phenylalanine and tyrosine on the other side. In the scheme above the corresponding genes of the enzymes are given. Genes, which are not derepressed under amino acid starvation conditions are colored in gray. While activation is indicated by a green arrow, inhibition is indicated by red lines. The black lines indicate a block of inhibition or activation.

Growth of *aro7<sup>c</sup> gcn4* strains in the presence of phenylalanine could be restored by either the expression of *GCN4* or by the addition of anthranilic acid into the medium. There are several possible reasons how phenylalanine might trigger in the tryptophan starvation effect: the activation of specific enzymes of the phenylalanine and tyrosine biosynthetic branch might channel all substrate towards phenylalanine and tyrosine, the specific inhibition of enzymes of the tryptophan branch by phenylalanine, the specific inhibition of the shikimate pathway by phenylalanine, resulting in less chorismate which is preferentially channeled towards the phenylalanine/tyrosine branch due to the constitutively activated chorismate mutase. In addition, a combination of several of these mechanisms might be possible.

### 3.2.1. The phenylalanine branch

Phenylalanine is only known to regulate one of the two DAHP synthases (Aro3p) and no additional effects of this end-product have been described in yeast. Therefore we were interested whether the phenylalanine specific branch of the aromatic amino acid biosynthesis is sensitive to phenylalanine. The initial step of the phenylalanine-specific branch is exhibited by the prephenate dehydratase (EC 4.2.1.51) which we aimed to purify and to characterize.

#### 3.2.1.1. The prephenate dehydratase

As prephenate dehydratases of several organisms (e.g. *E. coli*, *Bacillus subtilis*, *Kluyveromyces marxianus*) are feedback-regulated by phenylalanine, we wanted to know if the prephenate dehydratase activity of *S. cerevisiae*, encoded by *PHA2*, can be inhibited or activated by the end-products phenylalanine or tyrosine of this branch. We also speculated that even crosspathway activation of the prephenate dehydratase by tyrosine as and/or crosspathway activation of the prephenate dehydrogenase, encoded by *TYR1*, by phenylalanine might be possible effects, that could result in tryptophan starvation in *aro7<sup>o</sup> gcn4* strains in the presence of phenylalanine.

We amplified the *PHA2* gene with attached *Bam*HI and *Hind*III restriction sites, ligated into the vector p426MET25 in front of the *Strep*-tag®-DNA-sequence. After transformation of yeast  $\Delta$ *pha2*-strain RH2980, which was constructed by insertion of a kanMX4-cassette of the Euroscarf deletion strain BY4741 into the *PHA2* gene, with the resulting plasmid pME2532, cells were selected on SC medium without uracil. Growth restoration on MV medium in the absence of aromatic amino acids was tested. Cells were grown in 10 l MV, crude extracts were prepared with the One Shot Cell Disruption Model (Constant System Ltd. Warwick, UK) and the resulting gene product was purified by *Strep*-tag®-technology (Skerra and Schmidt, 2000; Terpe, 2003) with a 10 ml *Strep*-Tactin® Superflow® column with the FPLC. The purified Pha2p fusion protein was separated by SDS-PAGE into three bands with molecular weights of 45 kDa, 40 kDa and 38 kDa. All three bands could be identified by Western-hybridization analysis through the detectable *Strep*-tag® as enzyme with a fused *Strep*-tag®.



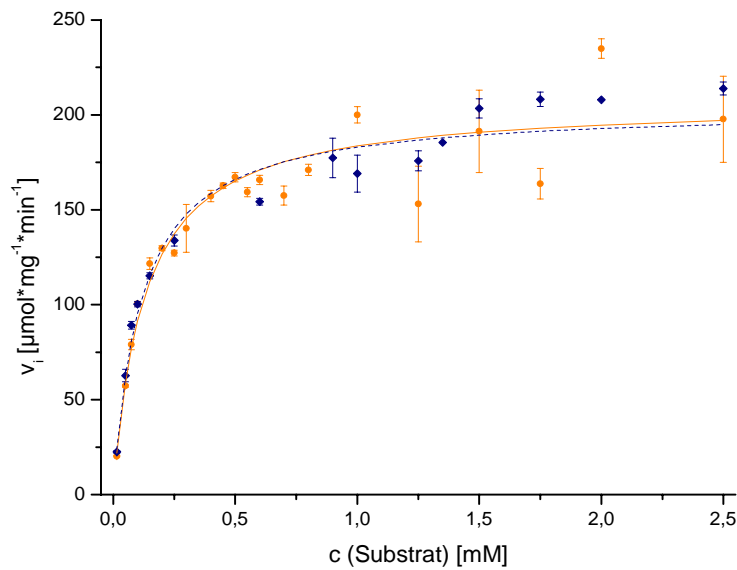


**Figure 32: Michaelis-Menten kinetic of Pha2p fusion protein with C-terminal *Strep*-tag®.** A substrate saturation curve of Michaelis-Menten-type is given. Initial velocities are averaged out of 4 independent measurements. Standard deviation is given as error bars in vertical direction. Initial velocities  $v_i$  were determined by its catalytic reaction of the substrate prephenic acid (1 mM) within 1 min at 30°C. The blue and the yellow color represent two different measurements of the substrate saturation curve with independently purified Pha2p.

Out of the fitted substrate saturation curves  $V_{max}$  and  $K_m$  could be determined:  $V_{max} = 206 \mu\text{mol} \cdot \text{min}^{-1} \cdot \text{mg}^{-1}$ ,  $K_m = 0,121 \text{ mM}$  and  $k_{cat} = 16 \text{ s}^{-1}$ .

**Table 5: Kinetic data of the fusion protein Pha2p with C-terminal *Strep*-tag®.** Values for  $V_{max}$ ,  $K_m$ ,  $k_{cat}$  and  $k_{cat}/K_m$  were determined by fitting initial velocity data of 4 independent measurements to equations describing hyperbolic saturation.

$V_{max} [\mu\text{mol} \cdot \text{min}^{-1} \cdot \text{mg}^{-1}]$	$206 \pm 2,1$
$K_M [10^{-3} \cdot \text{M}]$	$0,121 \pm 0,009$
$k_{cat} [\text{s}^{-1}]$	$(16,1 \pm 0,12)$
$k_{cat}/K_M [\text{M}^{-1} \cdot \text{min}^{-1}]$	$(0,125 \pm 0,007) \cdot 10^{-3}$

Prephenate dehydratases of several organisms (*Bacillus subtilis*, *Amycolatopsis methanolica*, *Neisseria gonorrhoeae*) are inhibitable by phenylalanine (Davidson, 1987; Fischer and Jensen, 1987; Euverink *et al.*, 1995).

Therefore the influence of phenylalanine and tyrosine was tested on the specific activity of the fusion protein Pha2p with the C-terminal *Strep*-tag® of *S. cerevisiae*. In the presence of

the two endproducts phenylalanine and tyrosine of the common branch no significant regulation could be detected (Table 6).

**Table 6: Specific activities of the fusion protein Pha2p with C-terminal *Strep*-tag® in the crude extract and as purified protein.** The phenylalanine concentration in the reaction volume was 0.5 mM. Specific activities have been determined three times.

	Crude extract Pha2p-fusion protein with C-terminal <i>Strep</i> -tag®		Pha2p-fusion protein with C-terminal <i>Strep</i> -tag®	
	Specific activity		Specific activity	
	10 <sup>-3</sup> * [U/mg]	[%]	[U/mg]	[%]
H <sub>2</sub> O	415 ± 100	100 ± 24	132 ± 2,8	100 ± 6
Phenylalanine	396 ± 31	95 ± 8	118 ± 9,4	89 ± 8
Tyrosine	524 ± 30	126 ± 6	127 ± 16	96 ± 12

### 3.2.1.2. The regulatory domain of the prephenate dehydratase of *S. cerevisiae*

In order to find putative regulatory domains in the prephenate dehydratase of *S. cerevisiae* the amino acid sequence was compared with other corresponding enzymes of other organisms by protein sequence alignments. The protein sequences of prephenate dehydratases of *S. cerevisiae* (YEAST), *E. coli* (ECOLI), *N. gonorrhoeae* (NEIGO), *B. subtilis* (BACSU), *Lactococcus lactis* (LACLA) and *Amycolatopsis methanolica* (AMYME) have been taken for this alignment. The enzymes of *E. coli* and *N. gonorrhoeae* are bifunctional enzymes and have chorismate mutase activities besides their prephenate dehydratase activity. The other proteins represent monofunctional prephenate dehydratases.



Three different domains are described for the bifunctional prephenate dehydratase of *E. coli*: 1) a chorismate mutase domain, 2) a prephenate dehydratase domain and 3) a regulatory domain, also known as ACT-domain (the name results of three enzymes inter alia, where this domain is found: aspartokinases, chorismate mutases and prephenate dehydrogenases (TyrA) (Zhang *et al.*, 1998; Liberles *et al.*, 2005)). Furthermore different conserved regions can be identified in the alignment. The TRF-motif (Thr, Arg, Phe), which is located in the prephenate dehydratase domain, is involved in the catalytic activity (Zhang *et al.*, 2000). The ESRP-site (Glu, Ser, Arg, Pro) is part of the regulatory domain and binds phenylalanine (Pohnert *et al.*, 1999). In the prephenate dehydratase of the endosymbiont *Buchnera aphidicola* the residues ESRP correspond to the amino acids Thr, Ser, Gln and Lys (TSQK). This enzyme can not be inhibited by phenylalanine as a result of the differences at this site (Jimenez *et al.*, 2000). In the wildtype Pha2p of *S. cerevisiae* the acidic glutamate is exchanged by an uncharged asparagine residue.

The ACT-domain is found in several enzymes. The highly conserved ESRP-site is part of the ACT-domain and is proposed to be a conserved regulatory binding fold, linked to a wide range of metabolic regulatable enzymes. Therefore we made an *in silico* amino acid substitution in the ESRP-site of the phenylalanine hydroxylase of *Rattus norvegicus*, in order to compare the possibility of inhibitor-binding concerning the room-management and the behavior of building hydrogen bonds at this site. Figure 34 shows the comparison of the wildtype ESRP-site of the phenylalanine hydroxylase of *Rattus norvegicus* and the site, where the glutamine residue was changed *in silico* against an asparagine in order to imitate the NSRP-site in the prephenate dehydratase of *S. cerevisiae*.

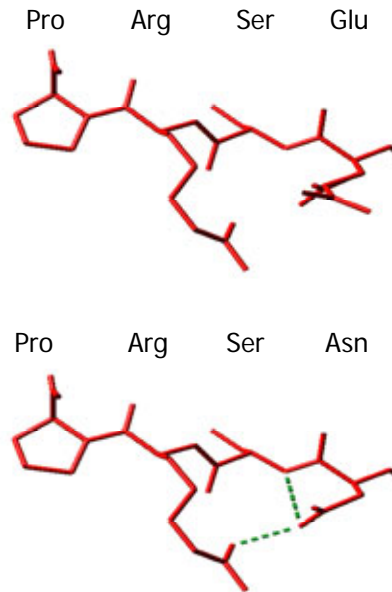


**Figure 34: ESRP (Glu, Ser, Arg, Pro)-site of phenylalanine hydroxylase of *R. norvegicus* at the top and the deduced NSRP (Asn, Ser, Arg, Pro)-site at the bottom.** *In silico* substitution of the acidic glutamate residue against an uncharged asparagine at the ESRP-site of phenylalanine hydroxylase of *R. norvegicus* leads to a possible situation in the unregulated prephenate dehydratase of yeast. The green dashed lines in the bottom figure are calculated H-bondings, which are possibly the reason for circumvention of the integration of phenylalanine at this site.

The deduced NSRP-site with the calculated H-bonds between the amino acid residues of this site shows, that the insertion and binding of phenylalanine into the NSRP-site of the yeast Pha2p is presumably disturbed by the different architecture of the NSRP-site in comparison to the ESRP-site. These *in silico* idea lead to the idea, that an exchange of asparagine against glutamine at the NSRP-site of yeast Pha2p might lead to a regulated enzyme.

In order to test this hypothesis of the *in silico* examination the asparagine residue at position 308 in the NSRP-site of Pha2p of *S. cerevisiae* was substituted for a glutamate. The resulting Pha2p-ESRP *Strep-tag*<sup>®</sup> fusion protein could not be purified because of weak expression. Therefore the specific activity of crude extract was measured in the absence and presence of phenylalanine (Table 7). We found that the asparagine in the NSRP-site of *S. cerevisiae*'s Pha2p is crucial for the inability for being regulated, which indicates that the Pha2 protein has a regulated ancestor which has lost the phenylalanine regulation during the course of evolution.

**Table 7: Specific activities of crude extracts with the *Strep-tag*<sup>®</sup>-fusion protein of wildtype Pha2p and Pha2p with an ESRP-site.** The concentration of the effector phenylalanine was 0.5 mM in the reaction volume. The specific activities have been determined three times.

	Yeast crude extract Pha2p-NSRP (WT) with C-terminal <i>Strep-tag</i> <sup>®</sup>		Yeast crude extract Pha2p-ESRP (= Asp308Glu) with C-terminal <i>Strep-tag</i> <sup>®</sup>	
	Specific activity		Specific activity	
	[U/mg]	[%]	[U/mg]	[%]
H <sub>2</sub> O	0.415 ± 0.1	100 ± 24	0.011 ± 0.001	100 ± 7
Phenylalanine	0.396 ± 0.031	95 ± 8	0.004 ± 0.0002	41 ± 2

### 3.2.2. Phenylalanine inhibition of *aro7<sup>c</sup> gcn4 S. cerevisiae* strains

In the presence of phenylalanine in the cultivation medium those *S. cerevisiae* strains, which are lacking the general control transcription factor Gcn4p and possess an unregulated and constitutively activated chorismate mutase Aro7<sup>c</sup> starve for tryptophan (Krappmann, 2000; Krappmann *et al.*, 2000). The next chapter deals with the question with the phe-effect is caused by the loss of the ability of regulating the prephenate dehydratase in *S. cerevisiae*.

#### 3.2.2.1. The regulated Pha2p-Asp308Glu mutant does not restore growth of an *aro7<sup>c</sup> gcn4* strain in the presence of phenylalanine

*S. cerevisiae* starves for tryptophan in the presence of phenylalanine in a strain carrying an unregulated chorismate mutase and deficient in the general control by the lack of the transcription factor Gcn4p (Krappmann *et al.*, 2000). The wildtype prephenate dehydratase is not inhibitable by the endproduct phenylalanine and the amino acid substitution in the NSRP-site of the ACT-domain from asparagine in wildtype at position 308 to glutamate leads to a regulated mutant variant of the prephenate dehydratase. In order to compensate the effect of starving for tryptophan under conditions described before, the wildtype *PHA2* allele in the strain RH2463 (*MATa*, *ura3-52*, *gcn4-103*, *ARO7<sup>c</sup>*) was exchanged against the *PHA2<sup>ESRP</sup>* allele, resulting in the strain RH3244 (*MATa*, *ura3-52*, *gcn4-103*, *ARO7<sup>c</sup>*, *PHA2<sup>ESRP</sup>*). The growth of this strain was tested in the presence or absence of phenylalanine (Figure 35).

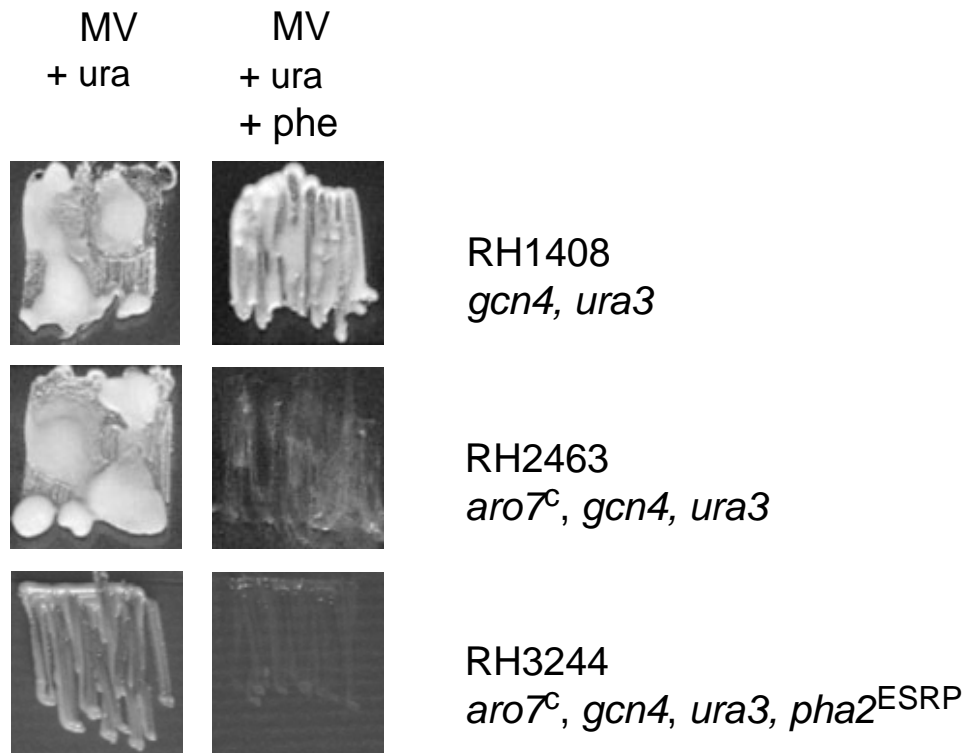


**Figure 35: Growth of RH3244 (*MATa, ura3-52, gcn4-103, ARO7<sup>c</sup>, PHA2<sup>ESRP</sup>*) in the absence (left) and presence (right) of phenylalanine (50 mg/l) in comparison to the control strains RH1408 (*MATa, ura3-52, gcn4-103*) and RH2463 (*MATa, ura3-52, gcn4-103, ARO7<sup>c</sup>*). *PHA2<sup>ESRP</sup>* was integrated at the original *PHA2* locus in the genome of RH2463 without *Strep-tag*®.**

The Pha2p<sup>ESRP</sup> mutant enzyme is not able to restore growth of Gcn4p lacking and Aro7<sup>c</sup>p containing yeast in the presence of exogenous phenylalanine. The unregulated Pha2p wildtype enzyme of *S. cerevisiae* is not the reason for the phe-effect, because starvation for tryptophan could not be abolished by feedback regulated prephenate dehydratase. In summary, the phe-effect is not originated in the phenylalanine branch and phenylalanine uses another target.

### **3.2.2.2. Overexpression of the *TRP2/TRP3* genes encoding the anthranilate synthase complex suppresses the growth inhibition by phenylalanine of the *aro7<sup>c</sup> gcn4* mutant strain**

The *S. cerevisiae* strains RH2463 (*MATa, ura3-52, gcn4-103, ARO7<sup>c</sup>*) and RH2476 (*MATa, ura3-52, gcn4-103, aro3::kanMX, ARO7<sup>c</sup>*) are not able to grow, when exogenous phenylalanine is supplemented to the medium. As Krappmann (2000) was able to show, growth could be restored at one hand by supplementation of anthranilate and on the other

hand by the expression of the transcription factor Gcn4p (Krappmann, 2000). Here we tested the effect of additionally expressed anthranilate synthase and two feedback resistant variants. Therefore *TRP2* and the *TRP2<sup>fbr</sup>*-alleles with amino acid substitutions in highly conserved LLESX<sub>10</sub>S-region (*TRP2<sup>fbr</sup>R65* and *TRP2<sup>fbr</sup>L76R65* (Graf *et al.*, 1993)) were cut out with *EcoRI* and *BamHI* and cloned into the high copy vector pRS426 (Christianson *et al.*, 1992). The LLESX<sub>10</sub>S-element is part of the variable N-terminal domain of feedback-regulated anthranilate synthases (Graf *et al.*, 1993). *TRP3* was amplified with attached *BamHI* and *SacI* restriction sites and ligated into pRS426 in the same direction downstream of *TRP2<sup>fbr</sup>*. RH2463 and RH2476 were transformed with the resulting plasmids and selected on SC-URA. Growth tests were performed by spotting yeast cell suspensions with 10, 50, 250 and 1250 cells on MV medium supplemented with phenylalanine, tyrosine and tryptophan in different combinations (Figure 36 and Figure 37).

The expression of *TRP2* or the feedback resistant variants in RH2463 or RH2476 were not able to restore growth in the presence of phenylalanine. This is presumably due to the fact that a functional anthranilate synthase complex requires two genes, *TRP2* and *TRP3*. The simultaneous expression of *TRP3* and *TRP2* leads to growth restoration and therefore suppresses the phe-effect. With the additional expression from the high copy vector pRS426 the level of anthranilate synthase complexes in the yeast cells is raised. Growth can be restored with the additional expression of wildtype anthranilic synthase. In yeast wildtype cells the metabolic flux is directed into the tryptophan branch until the tryptophan concentration is high enough for the supply which is needed for translation and other cellular processes. Subsequently the chorismate mutase is crosspathway activated by tryptophan and chorismate is primarily re-directed towards the phenylalanine/tyrosine branch. In mutant strains containing unregulated Aro7<sup>c</sup>p but no Gcn4p, the generated chorismate molecules are converted to prephenic acid by the constitutively expressed unregulated chorismate mutase. With the higher amount of anthranilate synthase the cell is now able to convert chorismate into anthranilic acid. The phe-effect is suppressed with the elevation of the anthranilate synthase complex level in the cell. So far, these data do not suggest a specific and pronounced role of phenylalanine in neither the tryptophan nor the phenylalanine/tyrosine branch of the aromatic amino acid pathway. Alternatively, phenylalanine might play an additional role in the stem of the aromatic amino acid biosynthesis which is the shikimate pathway.

RH2463 (*MAT<sub>a</sub>*, *ura3-52*, *gcn4-103*, *ARO7<sup>c</sup>*)

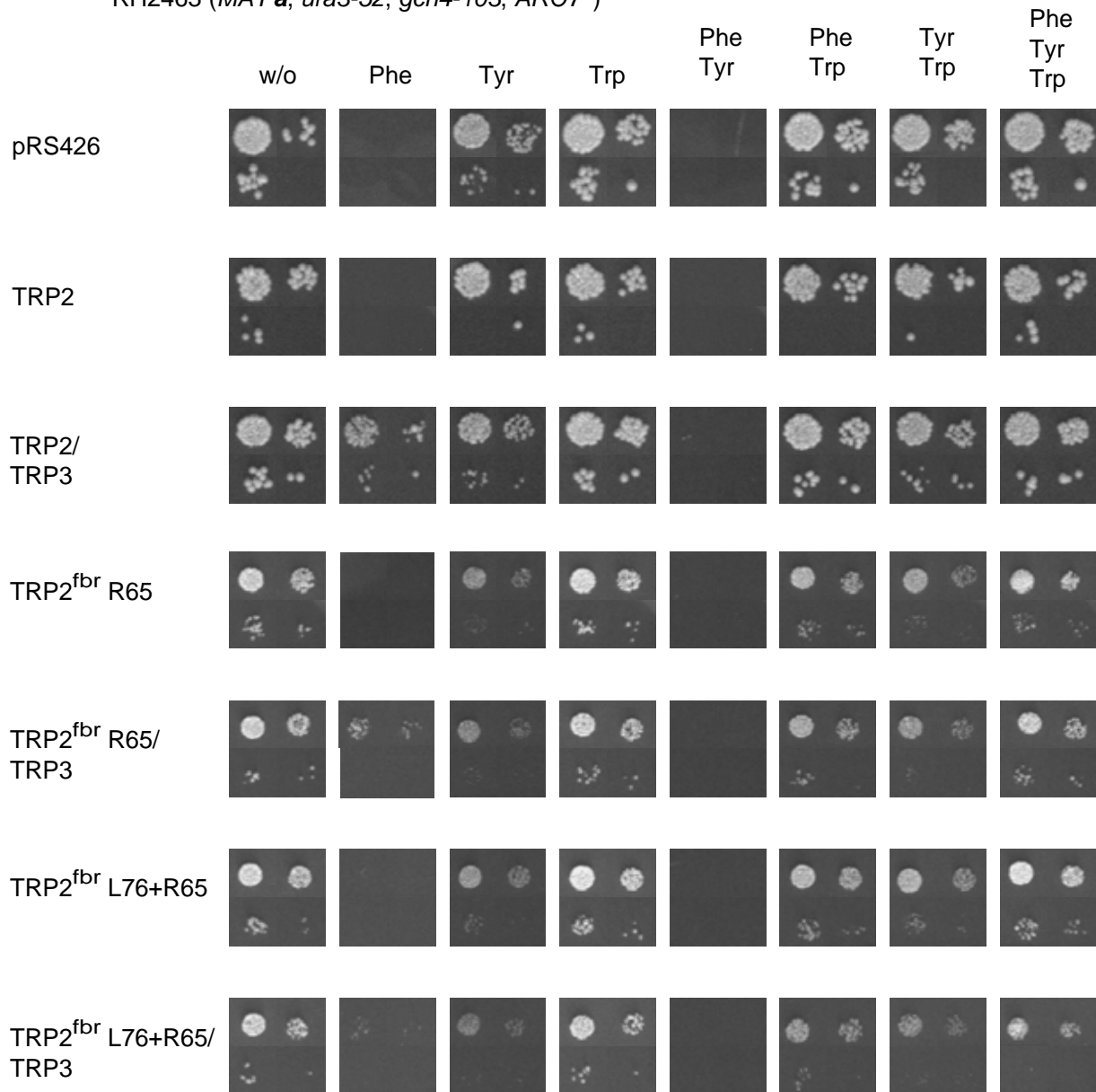


**Figure 36: Growth test of RH2463 (*MAT<sub>a</sub>*, *ura3-52*, *gcn4-103*, *ARO7<sup>c</sup>*) with additionally expressed *TRP2* wildtype or mutant alleles with or without *TRP3* from the high-copy vector pRS426 on MV (minimal vitamins) supplemented with phenylalanine, tyrosine and tryptophan, respectively. 1250, 250, 50 and 10 cells of each strain were spotted on the media. Strains with the empty vector pRS426 serves as control. Growth tests was performed three times.**

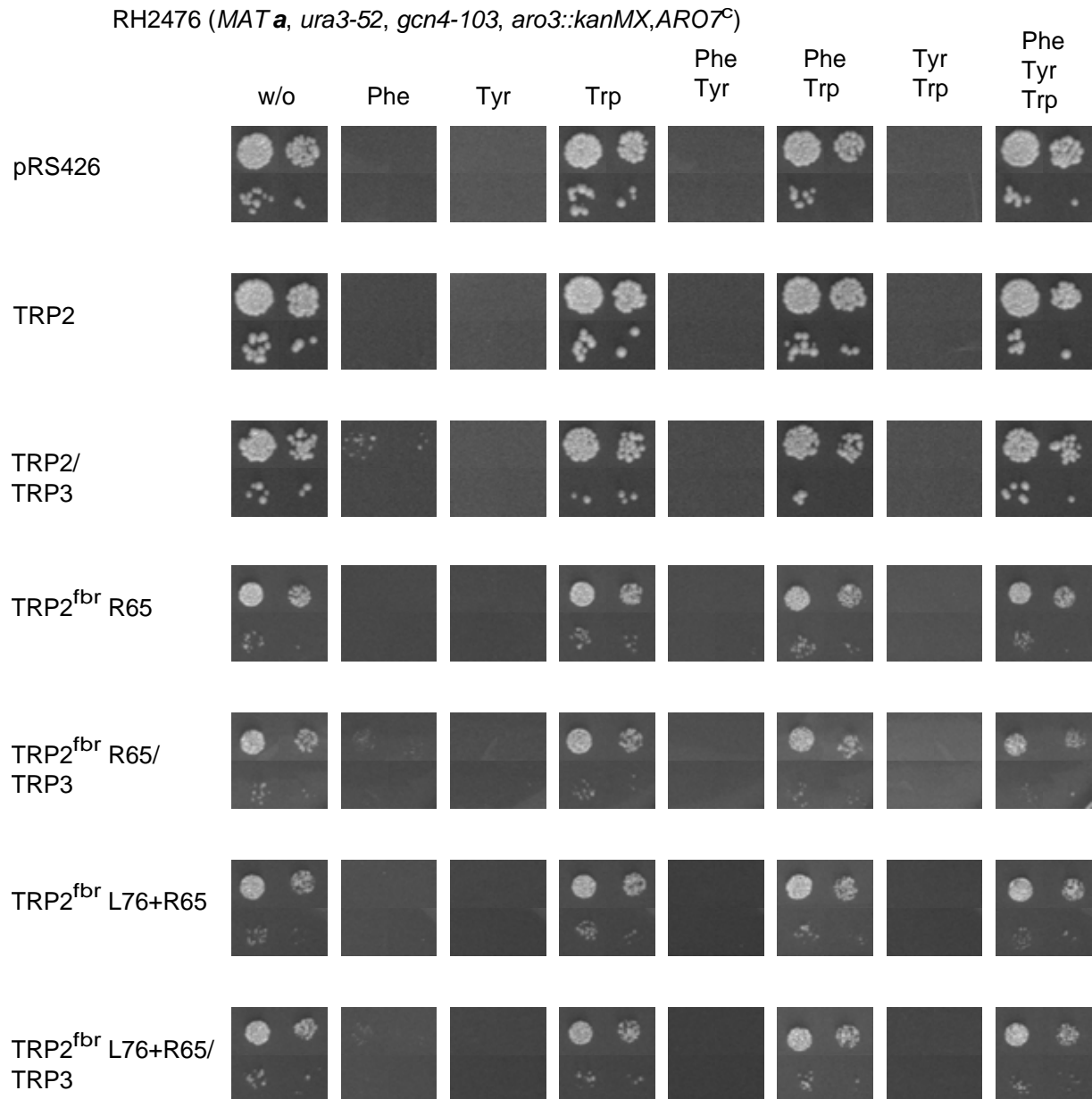


**Figure 37: Growth test of RH2476 (*MATa*, *ura3-52*, *gcn4-103*, *aro3::kanMX*, *ARO7<sup>c</sup>*) with additionally expressed *TRP2* wildtype or mutant alleles with or without *TRP3* from the high-copy vector pRS426 on MV (minimal vitamins) supplemented with phenylalanine, tyrosine and tryptophan, respectively. 1250, 250, 50 and 10 cells of each strain were spotted on the media. Strains with the empty vector pRS426 serves as control. Growth tests was performed three times.**

### 3.2.2.3. The tyrosine regulated DAHP synthase and the effect of phenylalanine

The third proposed mode of action of phenylalanine is the inhibition of a key step of the shikimate pathway besides the phenylalanine inhibitable DAHP synthase. Aro3p is the only known point of regulation for phenylalanine and is one of the DAHP synthases at the

beginning of the biosynthetic pathway for aromatic amino acids. The two yeast DAHP synthases Aro3p and Aro4p are not only regulated by phenylalanine and tyrosine, respectively, the third aromatic amino acid tryptophan acts as additional effector, which is required for the fine tuning of the feedback control (Helmstaedt *et al.*, 2005).

Phenylalanine is a competitive inhibitor with erythrose 4-phosphate (E4P) and non-competitive to phospho*enol*phosphate (PEP) for Aro3p with a  $K_i$  of 10  $\mu$ M (Paravicini *et al.*, 1989). Furthermore tyrosine is a competitive inhibitor to PEP and non-competitive to E4P for Aro4p with a  $K_i$  of 270  $\mu$ M (Schnappauf *et al.*, 1998). Although the concentration of phenylalanine has to be about more than 10 times higher for the inhibition of Aro4p than of Aro3p, the standard concentration of 50 mg/l (= 303  $\mu$ M) of phenylalanine in the medium is higher than the  $K_i$  of Aro4p for this effector.

Lowering the phenylalanine concentration in the medium leads as well to a growth restoration (Figure 38). This suggests, that the additional phenylalanine regulation of the tyrosine regulated DAHP synthase Aro4p might be crucial for viability in the absence of Gcn4p and the presence of the constitutively active and unregulated chorismate mutase with an exogenous phenylalanine source.

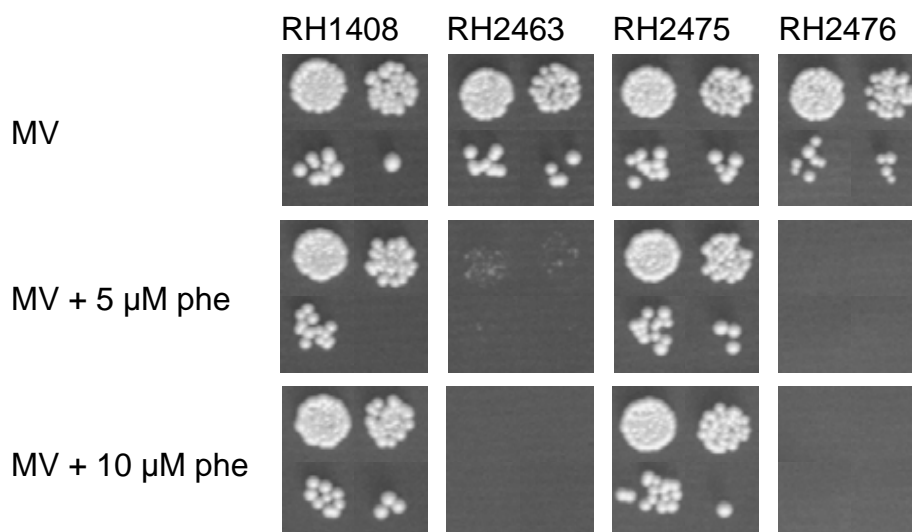


**Figure 38: Growth of yeast strains RH1408 (*MATa*, *ura3-52*, *gcn4-103*), RH2463 (*MATa*, *ura3-52*, *gcn4-103*, *ARO7<sup>o</sup>*), RH2475 (*MATa*, *ura3-52*, *gcn4-103*, *aro3::kanMX*) and RH2476 (*MATa*, *ura3-52*, *gcn4-103*, *aro3::kanMX*, *ARO7<sup>o</sup>*) can be restored by the reduction of the phenylalanine concentration. Yeast strains were dropped on MV with different end-concentrations (5  $\mu$ M and 10  $\mu$ M) of phenylalanine in the medium.**

The susceptibility to phenylalanine of the yeast strains RH2463 (*MATa*, *ura3-52*, *gcn4-103*, *ARO7<sup>o</sup>*) and RH2476 (*MATa*, *ura3-52*, *gcn4-103*, *aro3::kanMX*, *ARO7<sup>o</sup>*), lacking the transcription factor Gcn4p and containing the constitutively expressed and unregulated chorismate mutase implicates an additional regulation target of phenylalanine besides Aro3p.

A possible candidate protein is the tyrosine inhibitable Aro4p which has recently been shown to be in addition regulated by phenylalanine *in vivo* (Helmstaedt *et al.*, 2005). In order to test the hypothesis, that the additional regulation by phenylalanine of the tyrosine regulated DAHP synthase of *S. cerevisiae* is responsible for this “phe-effect”, we exchanged the wildtype *ARO4* gene against the *ARO4*<sup>T162L</sup> allele. The resulting mutant enzyme can just be inhibited by tyrosine to 71 % of its specific activity without effector and can not be regulated by phenylalanine in contrast to the specific activity of Aro4p wildtype, that can be reduced to 2 % rest-activity in the presence of tyrosine and 54 % by phenylalanine. To exchange the wildtype Aro4p against the unregulated mutant, the *kanMX*-cassette, which was integrated into the *ARO3*-locus, was removed with the simultaneous expression of the Cre recombinase from the plasmid pSH47 (Güldener *et al.*, 1996) and the *ARO4* gene was knocked out by insertion of a *kanMX4*-cassette of the Euroscarf deletion strain BY4741 into the *ARO4* gene. After that the *kanMX*-cassette was substituted with the *ARO4*<sup>T162L</sup> allele (Hartmann *et al.*, 2003) by homologous recombination with 5´and 3´ untranslated regions of the *ARO4*-locus, which results in the strain RH3245 with the unregulated DAHP synthase Aro4p-T162L as the only DAHP synthase. The exchange leads to restoration of growth in the presence of exogenous phenylalanine (Figure 39).

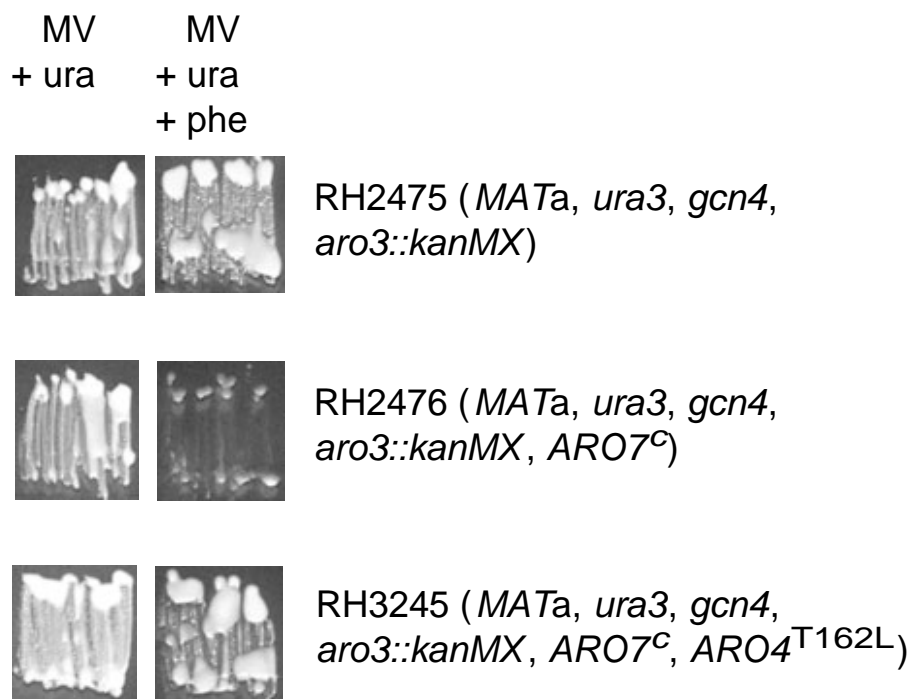


**Figure 39: Growth of RH3245 (*MATa*, *ura3-52*, *gcn4-103*, *aro3::kanMX*, *ARO7<sup>c</sup>*, *ARO4*<sup>T162L</sup>) in the absence (left) and presence (right) of phenylalanine (50 mg/l) in comparison to the control strains RH2475 (*MATa*, *ura3-52*, *gcn4-103*, *aro3::kanMX*) and RH2476 (*MATa*, *ura3-52*, *gcn4-103*, *aro3::kanMX*, *ARO7<sup>c</sup>*). *ARO4*<sup>T162L</sup> was integrated at the original *ARO4* locus.**

The initial enzymes of the biosynthetic pathway of the aromatic amino acids are strictly regulated and responsible for the shut off, when all endproducts are synthesized. Gcn4p is required for the up regulation of transcription of several enzymes of this pathway and important to equalize the imbalance given through the constitutively expressed and unregulated chorismate mutase in the presence of phenylalanine. The cell is not able to produce enough chorismate when both DAHP synthases are down regulated by phenylalanine. The unregulated Aro4p-T162L mutant enzyme is able to restore growth of yeast cells containing the unregulated Aro7<sup>c</sup>p and lacking Gcn4p in the presence of exogenous phenylalanine (Figure 40).

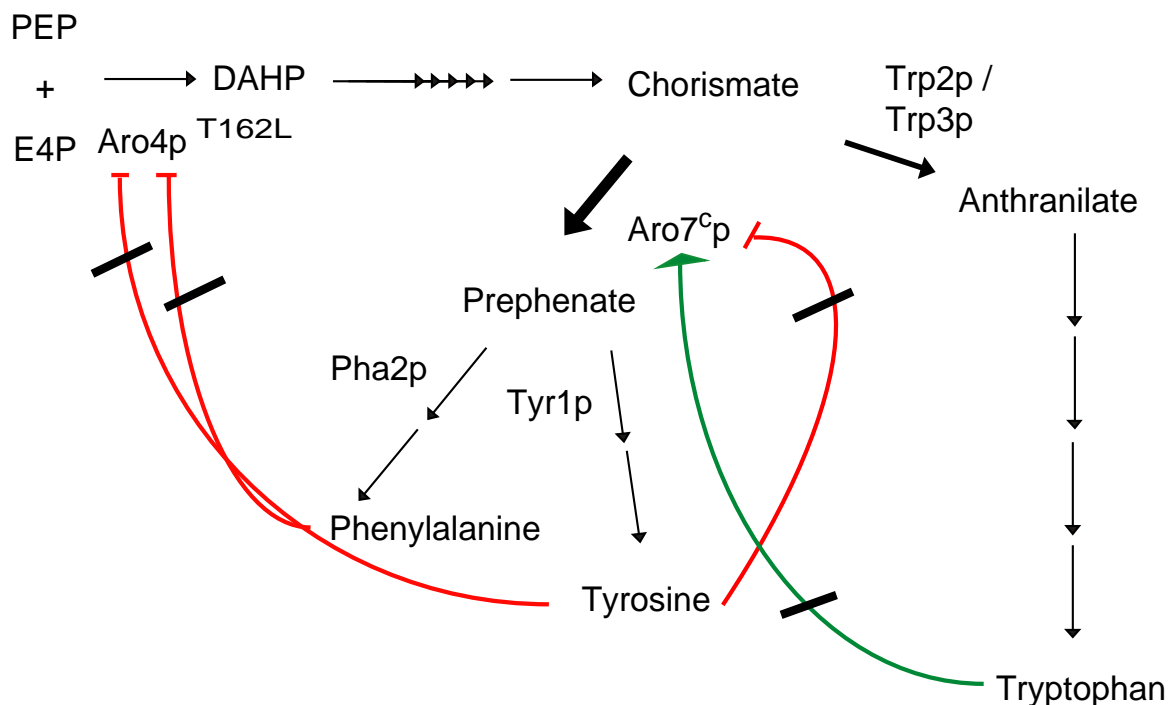


**Figure 40: Aromatic amino acid biosynthetic pathway of *Saccharomyces cerevisiae*, here the situation in the mutant yeast strain RH3245 (*MATa*, *ura3*, *gcn4*, *aro3::kanMX*, *ARO7<sup>c</sup>*, *ARO4<sup>T162L</sup>*).** The pathway starts with the condensation of phosphoenolpyruvate (PEP) and erythrose-4-phosphate (E4P) to 3-deoxy-D-*arabino*-heptulosonate-7-phosphate (DAHP) catalyzed by the DAHP synthase. DAHP is converted via six enzymatically catalyzed steps to chorismate. This last common metabolite of the shikimate pathway is the initial intermediate of the two branches leading to tryptophan on one side and to phenylalanine and tyrosine on the other side. In the scheme above the enzyme names are deduced from the names of the encoding genes. While activation is indicated by a green arrow, inhibition is indicated by red lines. The black lines indicate a block of inhibition or activation.

The “phe-effect” can be abolished with an unregulated DAHP synthase in the beginning of the biosynthetic pathway, so that enough chorismic acid is produced and cells are able to produce tryptophan.

In summary the “phe-effect” is a consequence of the additional regulation by phenylalanine of the tyrosine regulated DAHP synthase Aro4p, that shuts off the shikimate pathway and the entire aromatic amino acid biosynthetic pathway, respectively. Consequently the production of chorismic acid is decreased and is predominantly channeled into the phenylalanine/tyrosine branch, which leads to starvation for tryptophan of the cell. The unregulated DAHP synthase mutant (Aro4p-T162L) prevents the reduction of the production of chorismic acid and the supply of chorismate for the tryptophan branch is even in *aro7<sup>o</sup> gcn4* yeast cells sufficient in the presence of phenylalanine.

## 4. Discussion

### 4.1. Catalysis of DAHP synthase

In the past numerous enzymes were biochemically and structurally analyzed in order to understand the mechanism of catalysis and regulation (Blow, 2000). Examples for well studied model enzymes are the ATCase, OTCCase, chorismate mutase and phosphoenolpyruvate carboxylase (Kai *et al.*, 2003; Helmstaedt *et al.*, 2004; Izui *et al.*, 2004; Massant and Glansdorff, 2004; Woycechowsky and Hilvert, 2004). The catalytic mechanism of DAHP synthase which includes the condensation of two substrates, PEP and E4P and also a divalent metal ion located close to the catalytic site has been proposed based on the crystal structure of the phenylalanine regulated enzyme of *E. coli* (Shumilin *et al.*, 1999). However, crystal structures neglect the dynamic situation of enzymes in an aqueous system. Catalysis of enzymes in general is a concerted action. This means that each amino acid residue in the catalytic center, taking part in the substrate binding, might be crucial. The residues, which bind the substrates are drawn towards the ligands, which in turn affects the whole architecture of the substrate-bound in comparison to the free enzyme.

In the first part of this work the importance of three residues of the catalytic center of the yeast DAHP synthase, coordinating the divalent metal ion and the substrates PEP and E4P, was demonstrated by substituting each of these amino acids against an alanine. The resulting three mutant enzymes of the tyrosine regulated DAHP synthase of *S. cerevisiae* showed, that the residues coordinating the substrates and the metal ion in the crystal are also required *in vivo* for catalysis. The crystal structure of this tyrosine-regulated isoenzyme bares the residues coordinating the divalent metal ion, PEP and the structure analogon of E4P (= glycerol-3-phosphate (G3P)). The amino acids Cys76, His282, Glu316 and Asp342 interact with the metal ion, the residues Arg107, Lys112, Ala179, Arg180, Lys201 and Arg249 coordinate PEP, and G3P is coordinated by Pro113, Arg114, Thr115 and Asp342 (Figure 41).

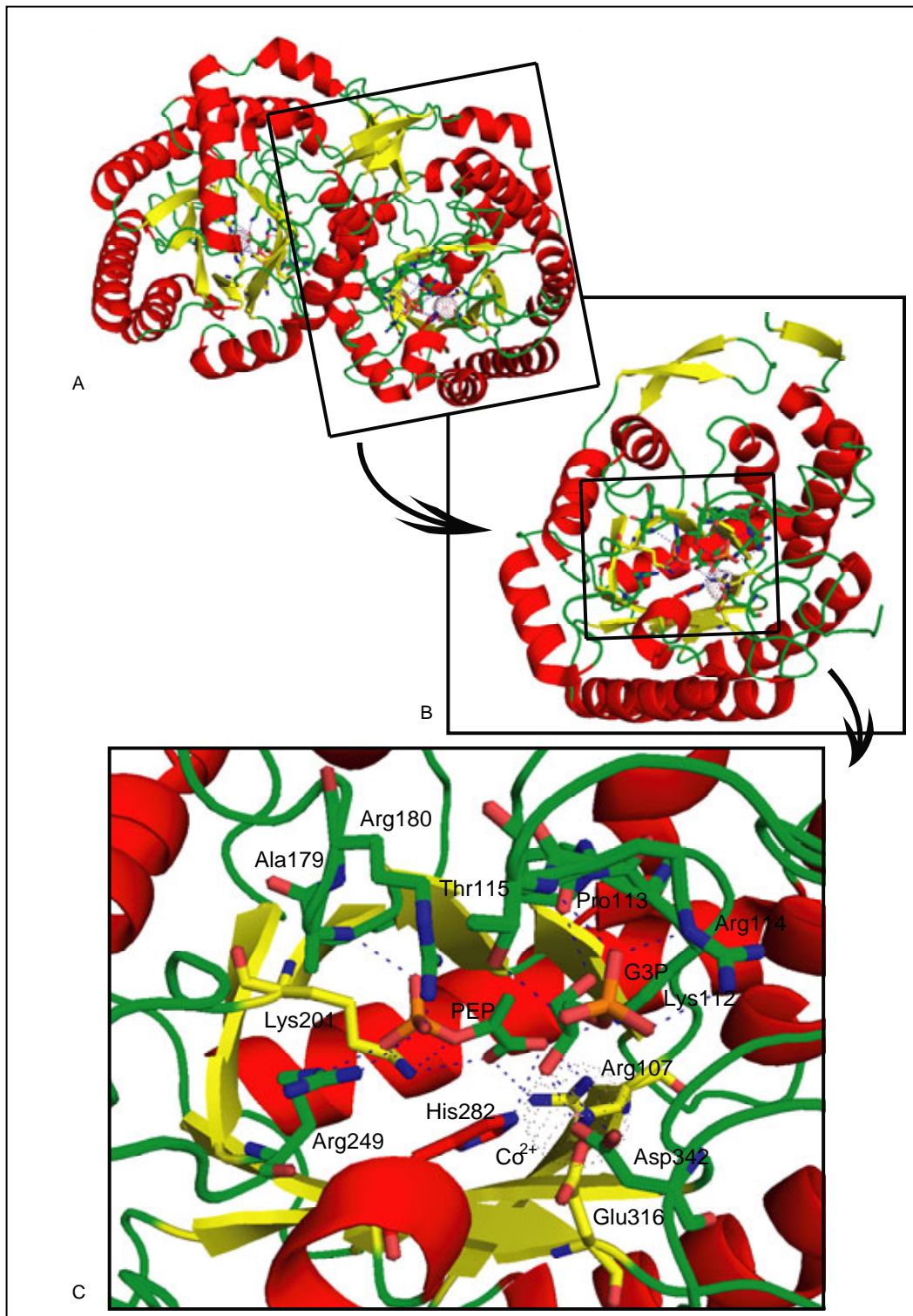


**Figure 41: Ribbon presentation of the tyrosine regulated DAHP synthase Aro4p of *S. cerevisiae*.** **A** Dimer of the Aro4 protein with the PEP, E4P and metal coordinating residues accentuated in the catalytic center. **B** Blown-up presentation of one monomer of the dimer of picture **A**. **C** Blown-up presentation of the catalytic center of a monomer of picture **B**. The metal and substrates coordinating amino acids are accentuated and designated.  $\alpha$ -helices are displayed as red helices,  $\beta$ -strands are given as yellow arrows and loops are colored in green. The divalent metal is displayed as dotted circle.

The lysine at position 112 builds a water bridge to the metal ion in the structure with the E4P-analogue G3P and is linked with the substrate PEP. Exchanging this residue leads to the loss of catalytic activity. Yeast containing the Aro4p-Lys112A mutant enzyme as the only DAHP synthase leads to an inactive enzyme and therefore to the inability in growth in the absence of aromatic amino acids. The residue AroG-Lys97 of the phenylalanine regulated DAHP synthase of *E. coli* corresponds to yeast Aro4p-Lys112 and is required for the coordination of PEP and E4P in AroG (Wagner *et al.*, 2000; Shumilin *et al.*, 2003). In the related metal-dependent as well as the metal independent KDOP synthases this highly conserved lysine can be found (Asojo *et al.*, 2001). The loss of activity caused by the exchange of this lysine at position 112 of Aro4p within the catalytic center confirmed that the waterbridge between the metal ion and E4P mediated by Lys112 is important for the catalysis of DAHP.

Furthermore the mutant Aro4 proteins with an amino acid substitution each by an alanine of the residue Arg180 and Arg114 result in inactive DAHP synthase variants. While the arginine residue at position 180 is required for PEP binding, Arg114 is required for the interaction of E4P. The residues AroG-Arg99 and AroG-Arg165, which are homologous residues to Aro4p-Arg114 and Aro4p-Arg180, have similar roles in both enzymes. KDOP synthase (EC 2.5.1.55; PDB-code i.e. 1D9E; Figure 42) and N-acetyl-neuramic acid (NeuAc) synthase (EC 2.5.1.56) belong to the same group of PEP-utilizing enzymes like DAHP synthase (EC 2.5.1.54; PDB-code i.e. 1HFB; Figure 42), which catalyze the formation of PEP with an aldehyde to a net aldol condensation product (Radaev *et al.*, 2000; Hartmann *et al.*, 2003). Only crystal structures of the KDOP synthase and of the DAHP synthase are solved to date. The PEP-utilizing enzymes of the other group, which catalyze the reaction of PEP with an alcohol under formation of an *enol* ether linkage, are EPSP synthase (EC 2.5.1.19; PDB-code i.e. 1G6T; Figure 42) and UDP-GlcNAc *enol*pyruvoyl transferase (EC 2.5.1.7; PDB-code i.e. 1DLG; Figure 42). Crystal structures of both enzymes were solved (Schönbrunn *et al.*, 2000; Schönbrunn *et al.*, 2001). Both types of PEP-utilizing enzymes can be classified into alpha-beta-enzymes, but the architecture of these two groups differ. The DAHP synthase and the KDOP synthase are classified as  $(\beta/\alpha)_8$ -barrel enzymes with the  $\beta$ -strands surrounded by the  $\alpha$ -helices and the EPSP synthase and UDP-GlcNAc *enol*pyruvoyl transferase are classified as  $\alpha/\beta$  prisms with the  $\alpha$ -helices surrounded by the  $\beta$ -strands. Striking differences to other PEP-utilizing enzymes and no crystal structure of the third enzyme of the PEP + aldehyde condensing group are the reasons for the comparison of the catalytic centers of KDOP synthase with DAHP synthase.

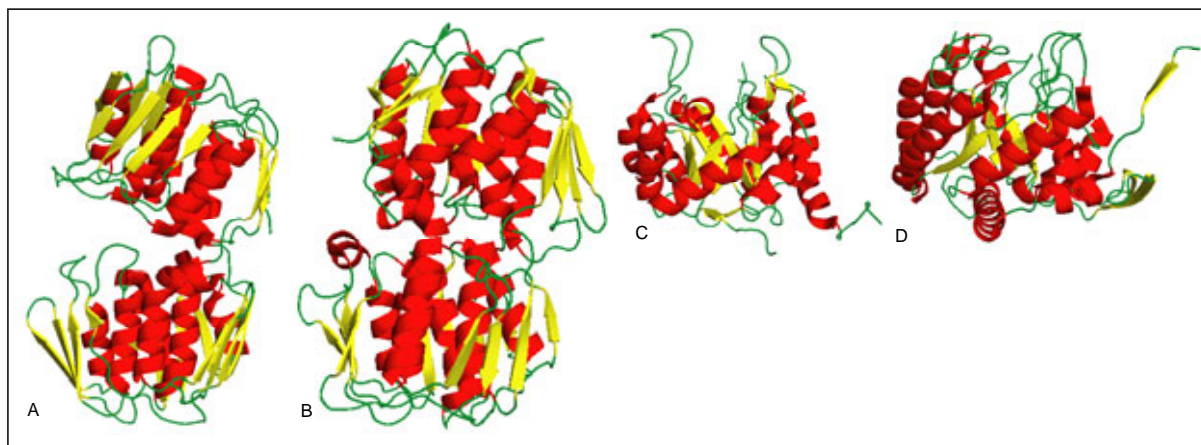


**Figure 42: Ribbon presentation of monomers of PEP-utilizing enzymes.** **A** UDP-*N*-Acetylglucosamine enolpyruvoyl transferase of *Enterobacter cloacae* (PDB-code: 1DLG). **B** EPSP synthase of *Enterobacter cloacae* (PDB-code 1G6T). **C** KDOP synthase of *E. coli* (PDB-code 1D9E). **D** DAHP synthase of *S. cerevisiae* (PDB-code 1HFB). The  $\beta$ -sheets are displayed as yellow arrows, the loops are colored in green and the  $\alpha$ -helices are given in red. The first two enzymes (A and B) are inside-out ( $\beta/\alpha$ )-barrels and catalyze the reaction of PEP and an alcohol. The other two enzymes (C and D) are classical ( $\beta/\alpha$ )<sub>8</sub>-barrels catalyzing the condensation of PEP with an aldehyde.

The Aro4p-Lys180, which is important for DAHP synthase activity and regulation is not found in the unregulated KDOP synthases (König, 2002). The substrate and metal coordination in KDOP synthases and DAHP synthases are similar and therefore the reaction of KDOP- and DAHP synthases are comparable. As proposed on the basis of the crystal structure the inactive mutant enzymes support that these amino acids are essential for enzyme function and catalysis.

Active sites of TIM barrel enzymes generate a positive electrostatic potential to attract the preferred negatively charged substrates (Raychaudhuri *et al.*, 1997). This is consistent with the situation in DAHP synthases, where the positively charged residues lysines (at positions 112 and 201 in the active site of Aro4p) and arginines (at positions 107, 114, 180, 249 in the active site of Aro4p) are crucial for the coordination of the phosphate moieties of the carbohydrate-substrates. An exchange of these positively charged amino acids lysine (at position 112) and arginine (at position 114 and 180) against the small hydrophobic alanine negatively affects the positive electrostatic potential of the catalytic center, resulting in inactive enzyme which presumably are incompetent to bind the phosphate groups of the substrates.

As Jensen and co-workers showed, the class I DAHP synthases are related to the KDOP synthases (Jensen *et al.*, 2002) and as well the structural conservation of the active site in these enzymes as the conserved reaction mechanism show divergent evolutionary development from a common ancestor. Enzymes can evolutionary diverge with a conserved

substrate specificity, reaction mechanism or active site architecture (Wise and Rayment, 2004). Our results which confirm the importance of these residues in DAHP synthase catalysis are further supported by the fact that these residues except Aro4p-Arg180, are conserved in class I DAHP synthases and KDOP synthases.

## **4.2. Transmission of the inhibition signal within the DAHP synthase**

When the inhibitor molecule tyrosine binds at the regulatory site of an allosterically inhibited enzyme, the residues of the active site become destabilized and therefore the enzyme becomes inactive (Luque and E., 2000). As a consequence the substrate is released. In the second part of this work the transmission signal of inhibition within the tyrosine regulated DAHP synthase was examined. Those amino acid residues which are relevant for the forwarding of the inhibition-information from the regulatory site to the catalytic center were identified.

By comparison of DAHP synthase structures in the active (PDB-code 1OF8) and inhibited (PDB-code 1OF6) state changes were observed which allow conclusions about the possible transmission mechanism of the inhibition signal. In addition, the regulatory mechanism of the phenylalanine regulated DAHP synthase AroG of *E. coli* allows further conclusion (Shumilin *et al.*, 2002). The data which are gathered in this thesis revealed that there is not a single simple intramolecular signal transduction pathway between the catalytic and the allosteric site. However, there is the interplay between two pathways: within the monomer the allosteric site affects its own catalytic site; within the dimer, one allosteric site affects the catalytic site of the other monomer of the dimer.

The first pathway to forward the inhibition signal within the monomer is described in detail in chapter 4.2.1. and had been described based on the crystal structure (König, 2002). The additional pathway which requires the communication between the two monomers of the dimeric DAHP synthase is here described. Within the tyrosine regulated DAHP synthase Aro4p of *S. cerevisiae* the transduction of both pathways starts at the allosteric site with the binding of the tyrosine molecule at Thr162, Gln166, Ser195, Phe224, Val227, Glu21\* and Asp22\*. (The asterisk indicates that the residue belongs to the other monomer of the dimer.) Substituting amino acid residues at these positions (Thr162Leu, Gln166Glu, Gly193Lys, Ser195Ala, Lys229Leu and Thr236Arg) result in unregulated mutant enzymes (Hartmann *et al.*, 2003), suggesting that these residues are relevant for inhibitor binding and subsequently for inhibition of the tyrosine regulated DAHP synthase Aro4p of yeast.

### 4.2.1. The intramolecular transmission of the inhibition signal

In the tyrosine regulated *S. cerevisiae* Aro4p and in the phenylalanine regulated *E. coli* AroG the inhibitor is bound in the hydrophobic cavity and attracts the N-terminus of the second monomer of the dimer to close the binding pocket. Through fixation of tyrosine in Aro4p the  $\beta$ -sheets  $\beta 0^*$ ,  $\beta 6a$  and  $\beta 6b$ , as well as the loop L3 are drawn towards the tyrosine molecule. Loop L2 consequently moves as well, which results in the drawing apart of the active center and the kick off of the second substrate, because E4P cannot be fixed anymore.

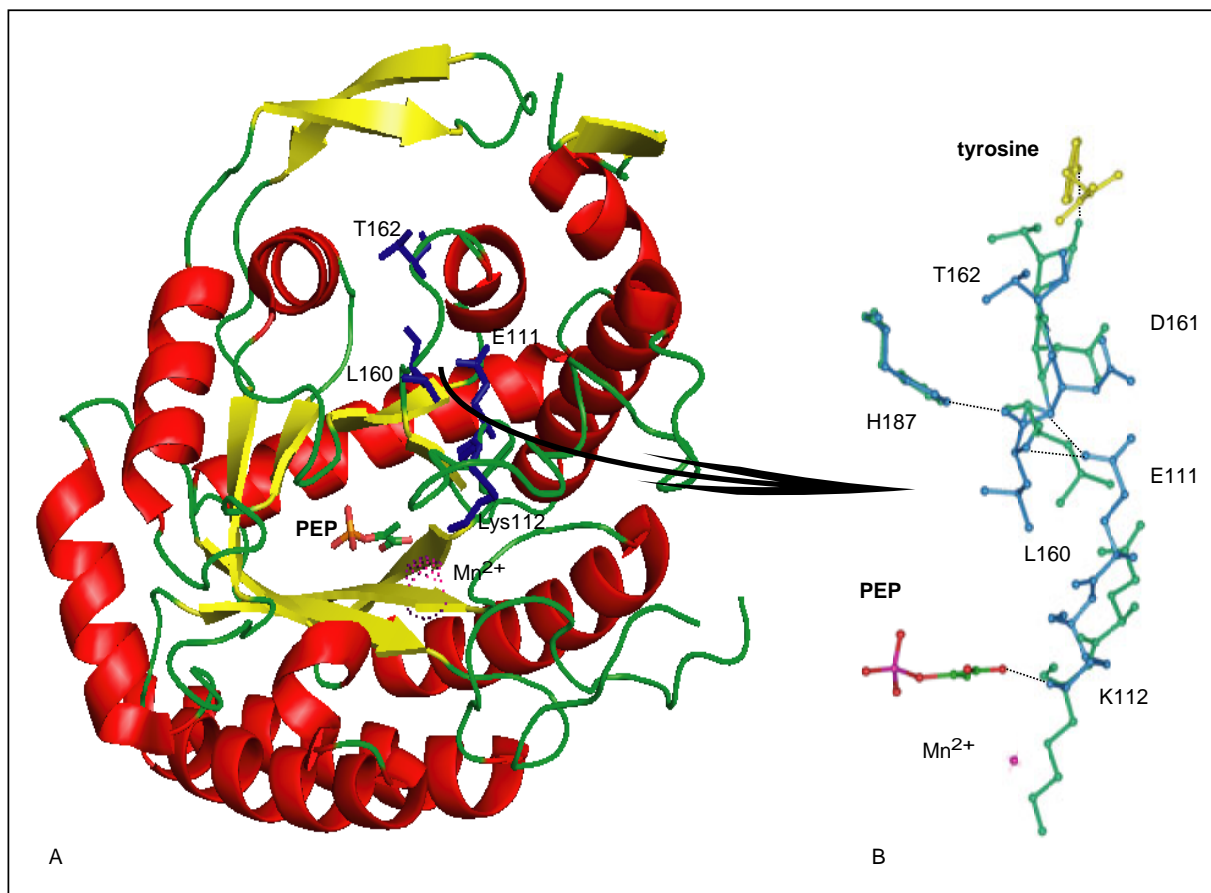


**Figure 43: Intramolecular transmission of the inhibition signal.** **A** Ribbon presentation of Aro4p monomer, with the transmission between the allosteric tyrosine binding site and the participating residues displayed in blue,  $\alpha$ -helices in red, loops in green and  $\beta$ -sheets as yellow arrows. PEP is displayed as colored stick-model and  $Mn^{2+}$  as dotted ball in magenta within the catalytic center. **B** Section from the allosteric to the catalytic site within a monomer with superimposed crystal structures of Aro4p in the presence of the substrate PEP and  $Mn^{2+}$  (blue structure) and in the presence of the inhibitor tyrosine (green structure). Hydrogen bonds are indicated as dashed lines.

The effector is bound in the phenylalanine regulated DAHP synthase of *E. coli* (AroG) by the amino acids Ser180, Gln151 and the two amino acids Asp6\* and Asp7\* from the N-terminus

of the other monomer (Shumilin *et al.*, 2002). These residues are conserved in many DAHP synthases and correspond to the residues Ser195, Gln166, Glu21\* and Asp22\*. Although a turning of AroG-Leu145 (=Aro4p-Leu160) in the phenylalanine sensitive DAHP synthase of *E. coli* is not observed, in both enzymes a movement of loop L3 results in a break of a hydrogen bond between loop L3 and Aro4p-Glu111 (AroG-Glu96) of loop L2. The changes in the active center are determined from the different rotamers, compared to the active structure, of the PEP coordinating amino acid residues AroG-Lys97 (= Aro4p-Lys112) and AroG-Arg164 (=Aro4p-Arg180). Crystal structures are rigid and are just able to display one situation per time. The comparison of structures in the active and inactive state gives an idea of the movement within the enzyme and to test the hypothesis amino acids between the regulatory and the catalytic center were exchanged.

Single amino acid substitutions in the DAHP synthase regions which are most flexible and which are significantly moved after binding of tyrosine as inhibitor (Glu111Ala, Leu160Ala, Glu111Ala+Leu160Ala) resulted in mutant enzymes, which are nearly inactive and completely inactive in case of Aro4p-Glu111Ala+Leu160Ala. Glu111 of loop L2 is fixed in the active conformation and this fixation is lost in the inactive state. Substituting this amino acid equals the unfixed state in the inhibited conformation. A similar situation is found for Leu160 which is coordinated with hydrogen bonds to Glu111 and His187. The substitution of Leu160 results in a mutant enzyme, which is reduced in activity, presumably because hydrogen bonds were broken. The substitution of histidine for leucine resulted in an inactive mutant enzyme. This might be caused by the loss of the hydrogen bond between this amino acid residue at position 187 to Leu160. Although the mutant enzymes Aro4p-Glu111 and Aro4p-Leu160 are reduced in specific activity, specific activity can further reduced by the inhibitor tyrosine (compare with Table 4 of chapter 3.1.1.2.). In summary, the intramolecular inhibition signal is transmitted from the allosteric site, via loops L3 and L2, to the catalytic center. This signal transduction pathway cannot reflect the only communication between allosteric and catalytic site. In addition, the communication between monomers, which bind the inhibitor is an additional way of controlling enzyme activity.

#### **4.2.2. The intermolecular transmission of the inhibition signal**

As the specific activities of mutant Aro4 proteins with substitutions of single amino acids between the allosteric and the catalytic center within a monomer indicate, there has to be an alternative intermolecular pathway of transmitting the inhibition signal. Through fixation of tyrosine the  $\beta$ -sheets  $\beta 0^*$ ,  $\beta 6a$  and  $\beta 6b$ , as well as the loop L3 are drawn towards the tyrosine molecule. As a consequence loop L3 and in turn loop L2 at one hand are drawn towards the fixed tyrosine. At the other hand small movements between the two monomers

of the dimer (between helix  $\alpha 4$  and loop L2\*) shows, that networking occurs and simultaneously indirect affection of the catalytic site takes place.

Changes at the dimer interface are observed as well in the phenylalanine-regulated AroG of *E. coli*. The connection between loop L2 of one monomer and helix  $\alpha 4^*$  and loop L4\* of the second monomer by hydrogen bonds is broken in the inactive state. The substrate coordinating residues AroG-Lys97 (= Aro4p-Lys112) and AroG-Arg99 (=Aro4p-Arg114) of loop L2 are involved in this breakage of hydrogen bonds.

The three hydrogen bonds at the dimeric interface between the two monomers are only present in the active conformation between the flexible loop L2 and helix  $\alpha 4$ . The insertion of tyrosine results in an interruption of these hydrogen bonds (Figure 44).

A mechanic break of single hydrogen bonds can be caused by single amino acid substitutions of corresponding amino acids of helix  $\alpha 4$  or loop L2. These exchanges of amino acid residues lead to nearly inactive and inactive, respectively, DAHP synthase mutant enzymes (compare with Table 4 of chapter 3.1.1.2.).

Furthermore different intermolecular hydrogen bonds at the dimeric interface are observed in crystal structures in the active and inhibited state, respectively, that display two end point states. From amino acids of loop L2, which is important for the coordination of the substrates (Shumilin *et al.*, 2003; König *et al.*, 2004) and therefore for catalysis, hydrogen bonds are built to amino acids of helix  $\alpha 4$  of the second monomer. These hydrogen bonds are absent, when tyrosine is bound at the inhibitor binding site.

The inhibition signal is transmitted via the loss of interdomain contacts between residues of helix  $\alpha 4$  of monomer 1 and loop L2 of monomer 2 (Figure 44). In the presence of tyrosine an interdomain contact between Aro4p-Gln185 of monomer 1 and Aro4p-Arg180 of the second monomer is observed, which is not found in the phenylalanine regulated DAHP synthase of *E. coli*. Shumilin *et al.* in 2003 proposed different conformations of AroG-Arg165 (which corresponds to Aro4p-Arg180) as a result of the flipping substrate PEP, while we propose for the tyrosine regulated DAHP synthase the loss of the PEP binding as a result of the interdomain contact between Aro4p-Gln185 and Aro4p-Arg180. This is consistent with the fact that tyrosine is a competitive inhibitor with PEP as substrate for Aro4p.

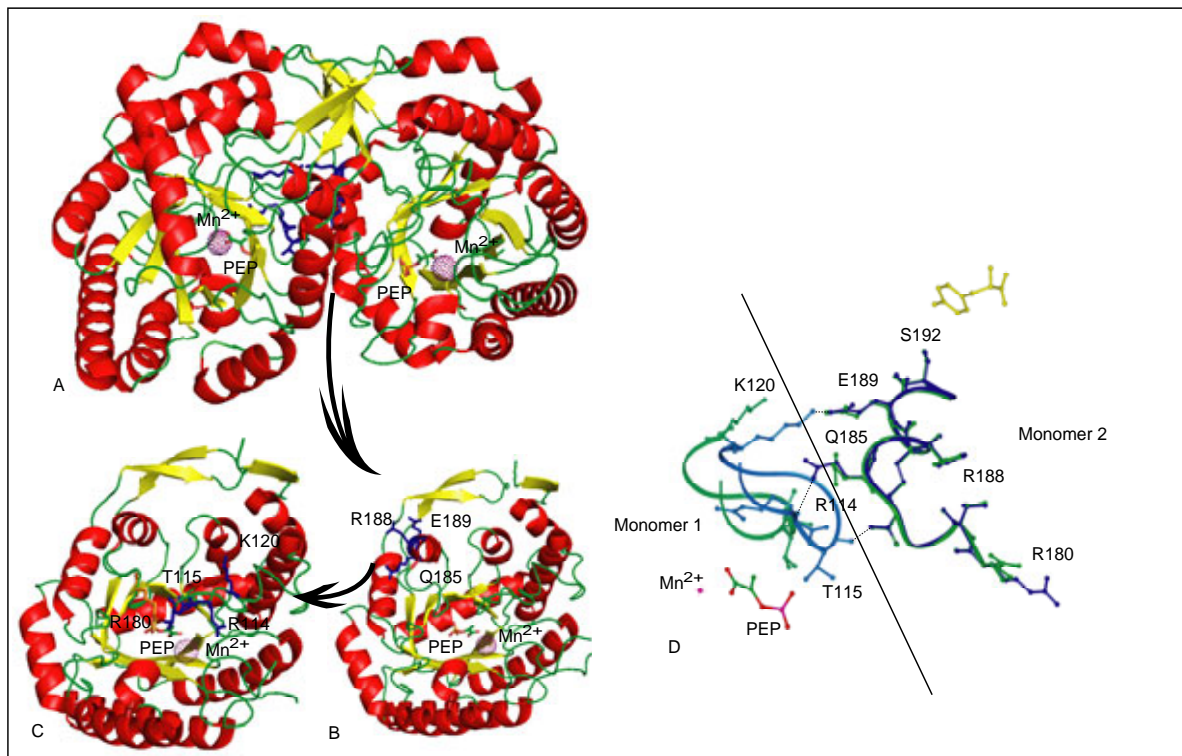


**Figure 44: Intermolecular transmission of the inhibition signal of tyrosine within *S. cerevisiae*'s Aro4p.** **A** Ribbon presentation of an Aro4p dimer, with the transmission participating residues displayed in blue,  $\alpha$ -helices in red, loops in green and  $\beta$ -sheets as yellow arrows. PEP is displayed as colored stick-model and  $Mn^{2+}$  as dotted ball in magenta within the catalytic center. The residue displayed in orange is Arg180. Tyrosine insertion results in the loss of contact of Arg180 to Glu185 of the other monomer. The signal is transmitted from the regulatory site via helix  $\alpha 4$  and loop L2 to the catalytic center. **B** Monomer of yeast Aro4p. The blue colored residues of helix  $\alpha 4$  display the first part of the second way of forwarding the inhibition signal. **C** The continuation of signal transmission in the second monomer of a dimer via the blue colored residues of loop L2 at the catalytic center. **D** Section from the allosteric to the catalytic site within a monomer with superimposed crystal structures of Aro4p in the presence of the substrate PEP and  $Mn^{2+}$  (blue structures) and in the presence of the inhibitor tyrosine (green structures). Hydrogen bonds are indicated as dashed lines. The black line marks the dimeric interface between the two monomers.

As shown, Aro4p exists as a dimer with a molecular weight of 83.8 kDa. Dimerisation is still possible when hydrogen bonds between Glu189 and Lys120 in the Aro4p-Lys120Ala mutant are broken. Although reduced in activity, regulation by tyrosine is still possible, because the other inter- and intradomain contacts are not interrupted and therefore sufficient for inhibition-signal transmission.

TIM barrel enzymes span hydrogen-bonding networks through the enzyme to connect the N-terminal end with the C-terminal end (Wierenga, 2001). With this hydrogen network the

active site of  $(\beta/\alpha)_8$ -barrels at the C-terminal site of the  $\beta$ -sheets, which is true for DAHP synthases, and the regulatory domains of the regulatable class I $\alpha$  DAHP synthases at the N-terminal end, the signal can be transmitted. The network of hydrogen bonds described here for Aro4p is the shuttle-service for the inhibition signal (Figure 45).

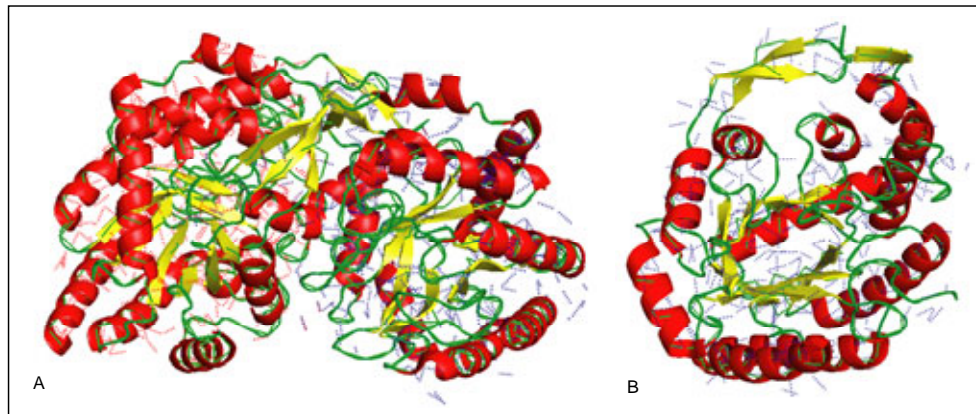


**Figure 45: Hydrogen network of the tyrosine regulated yeast DAHP synthase within a dimer (A) and a monomer (B).**  $\beta$ -sheets are displayed as yellow arrows,  $\alpha$ -helices are given in red, loops in green and hydrogen bonds as red or blue dashed lines.

The hydrogen network between secondary structure of the TIM barrel monomer and dimer seems to play an important role as well for catalysis as for regulation. The insertion of the inhibitor molecule causes a changeover of this network. Some hydrogen bonds, which are essential for stability in the active state break with the insertion of tyrosine. Therefore the intramolecular inhibition signal transmission within the monomer is the most obvious pathway deduced from the crystal structures. However, there is a second intermolecular communication pathway. Amino acid substitutions in this work support both signal transductions within the DAHP synthase. Learning from crystal structures and enzymes carrying substitutions, the inhibition signal is transmitted via both pathways simultaneously in a concerted action, but if one way is blocked for transmission, the second can be used as bypass. The nearly inactive mutant enzymes argue for the re-enactment of the insertion of the inhibitor molecule with the mechanical break of the hydrogen bonds.

3-deoxy-D-*manno*-octulosonate-8-phosphate (KDOP) synthases lack any structural extensions and are not regulated, although related to DAHP synthases in structure and reaction catalysis (Jensen *et al.*, 2002).

The recently solved crystal structure of the class I $\beta$  DAHP synthase of *Thermotoga maritima* shows striking differences to the known crystal structures of the class I $\alpha$  DAHP synthases in the regulatory domain. In both cases the  $(\beta/\alpha)_8$  barrel contains the catalytic center, but the I $\alpha$

enzymes have got two extra  $\beta$ -sheets and N-terminal extensions, which are important for regulation, while the ferredoxin-like domain is proposed to take part in regulation through interaction with loop L2 of the barrel of the second monomer of the dimer (Shumilin *et al.*, 2004). In the case of the DAHP synthases loop L2 is unavoidable for catalysis and target of the signal transmission from the regulatory site to the catalytic site.

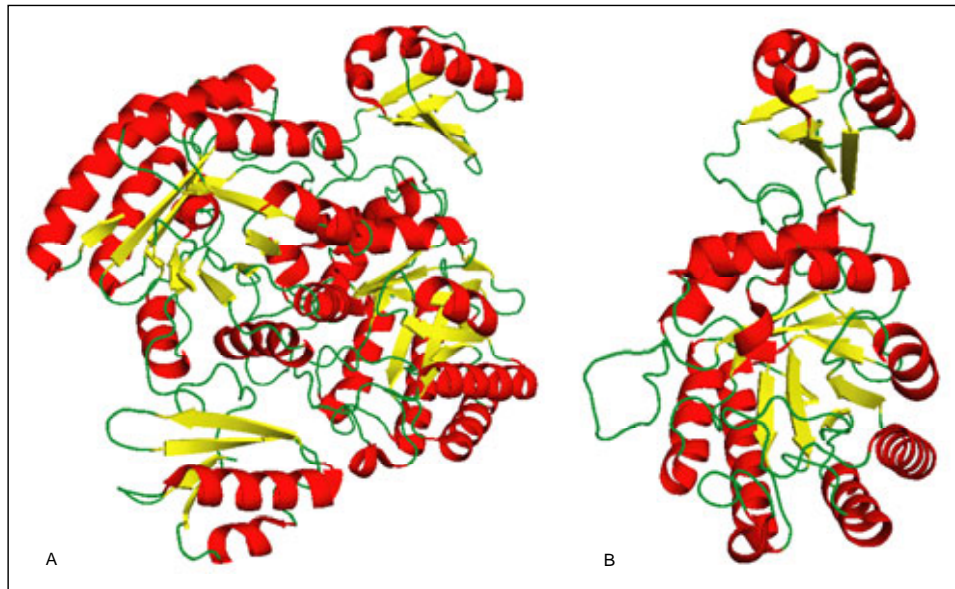


**Figure 46: Ribbon presentation of the DAHP synthase of *Thermotoga maritima* (PDB-code: 1RZM).**  $\beta$ -strands are displayed as yellow arrows,  $\alpha$ -helices in red and loops in green. **A** Dimer. **B** Monomer with the ferredoxin-like regulatory domain upside the  $(\beta/\alpha)_8$ -barrel.

However, for  $(\beta/\alpha)_8$  barrels the network of hydrogen bonds are important for stability and subsequently for catalysis. A change of the organization in H-bond network by the insertion of the inhibitor molecule or by specific amino acid substitutions drives the transmission of the inhibition signal, which in turn leads to the inability of catalysis. The inhibition mechanism of the tyrosine regulated DAHP synthase of yeast is mediated via two pathways within the enzyme: intramolecular within a monomer and intermolecular between the two monomers of the dimer. In both cases the amino acid residues of loop L2 play a key role, because these residues are important for the binding of the divalent metal ion and the substrates and therefore for catalysis.

## 4.3. Phenylalanine regulation of the aromatic amino acid pathway

### 4.3.1. The prephenate dehydratase of *S. cerevisiae*

In the third part of this work we investigated the prephenate dehydratase (PDT) of *S. cerevisiae*, encoded by the *PHA2* gene. After purification of Pha2p with a C-terminal fused *Strep-tag*<sup>®</sup> the kinetic parameters were determined. The fusion protein shows a substrate saturation curve of the Michaelis-Menten-type. The catalytic constant of Pha2p ( $k_{\text{cat}} = 16 \text{ s}^{-1}$ ) is two to three times higher than the  $k_{\text{cat}}$  of the tyrosine regulated DAHP synthase Aro4p with  $6 \text{ s}^{-1}$ , but 10 times lower than of the chorismate mutase Aro7p ( $k_{\text{cat}} = 176 \text{ s}^{-1}$ ). (The  $k_{\text{cat}}$  of the phenylalanine regulated DAHP synthase Aro3p is  $10 \text{ s}^{-1}$ .) The high catalytic constant of Aro7p indicates, that the chorismate mutase is strictly inhibited by tyrosine and activated by tryptophan. In contrast to Aro7p, the two DAHP synthases and the prephenate dehydratase possibly are not needed to be strictly regulated. Regulation of prephenate dehydratase by phenylalanine could not be observed. Although a C-terminal *Strep-tag*<sup>®</sup> is fused to Pha2p the tag is presumably not blocking the regulatory site, because it is a small tag consisting of only eight amino acids. Protein sequence alignment showed high similarities of the conserved ESRP region, responsible for phenylalanine binding (Pohnert *et al.*, 1999). Feedback-regulated prephenate dehydratases, mono- or bifunctional, of several organisms (*E. coli*, *N. gonorrhoeae*, *B. subtilis*, *A. methanolica*, and others) possess this ESRP-site. The yeast PDT carries an amino acid substitution in this motif, resulting in an NSRP site. *In silico* comparison of the ESRP- and the NSRP-motif displayed striking differences caused by the hydrogen bondings within the NSRP-site. Possibly these hydrogen bondings block this site, so that phenylalanine is not able to bind. In the phenylalanine-regulated prephenate dehydratase of *C. glutamicum* the arginine at position 236 within the ESRP-site was substituted by a leucine. The resulting mutant enzyme showed less inactivation by phenylalanine (Hsu *et al.*, 2004). The exchange of the asparagine within the NSRP site of yeast PDT against a glutamate resulted in a regulatable mutant enzyme. The expression rate of the ESRP-mutant enzyme was worse than bad wildtype expression. A reason for this low expression rate as well for the Pha2p wildtype enzyme might be the corrected transcription start point, which is about 102 nucleotides downstream of our start (Kellis *et al.*, 2003).

### 4.3.2. The “phe-effect” of *aro7<sup>c</sup> gcn4 S. cerevisiae* strains

The yeast strains, which contain unregulated and constitutively expressed chorismate mutase and no final effector Gcn4p of the general control, starve for tryptophan in the presence of exogenous phenylalanine. This effect of lethality under this conditions is called “phe-effect” and possible modes of feedback-control by phenylalanine are the inhibition of

the enzymes of the tryptophan branch, the activation of the enzymes of the phenylalanine/tyrosine branch or the inhibition of the enzymes of the shikimate pathway. The additional expression of *TRP2/TRP3* can suppress this effect, like the additional expression of *GCN4* (Krappmann, 2000) or the supplementation with anthranilate (Krappmann, 2000). As prephenate dehydratase of yeast is an unregulated enzyme there must be another target to phenylalanine and the decision where to channel the metabolic flux within the aromatic amino acid biosynthetic pathway is made earlier. Besides the regulation of Aro3p phenylalanine is able to inhibit Aro4p (Paravicini *et al.*, 1989; Schnappauf *et al.*, 1998). Integrating the mutant gene *ARO4*<sup>T162L</sup> (Hartmann *et al.*, 2003) at the *ARO4* locus of RH2476, leads to a yeast strain with an unregulated DAHP synthase as the only DAHP synthase in the cell. This unregulated Aro4p is able to suppress the effect caused by exogenous phenylalanine.

The aromatic amino acid biosynthetic pathway is completely shut off after phenylalanine and tyrosine are synthesized. This pathway is fine tuned in yeast wildtype strains and the manipulation at the first branch point leads to a redistribution of the metabolic flux and yeast is not able to compensate the inhibition by exogenous phenylalanine when the general control broke down. Besides the additional phenylalanine inhibition of the tyrosine regulated Aro4p both DAHP synthases of *S. cerevisiae* can be reduced in specific activity by the third aromatic amino acid tryptophan (Helmstaedt *et al.*, 2005).

The biosynthetic pathway of leucine, isoleucine and valine is another branched biosynthetic pathway for amino acids (Figure 47). This biosynthetic pathway consists of a common pathway from pyruvate and  $\alpha$ -ketobutyrate to valine and isoleucine. A branch from the direct precursor of valine,  $\alpha$ -ketoisovalerate, leads to leucine. In *S. cerevisiae* as well as in *N. crassa* the transcription of the genes encoding for the enzymes of this biosynthetic pathway (*ILV* and *LEU*) is individually controlled by the transcription factor Leu3p in complex with the leucine precursor  $\alpha$ -isopropylmalate and the general control (Kohlhaw, 2003). The first common step in isoleucine, leucine and valine biosynthesis is catalyzed by the acetolactate synthase consisting of the Ilv2p catalytic subunit and the Ilv6p regulatory subunit. The *ILV2* gene transcription is controlled by the Leu3p- $\alpha$ -isopropylmalate complex (Baichwal *et al.*, 1983; Friden and Schimmel, 1988; Brisco and Kohlhaw, 1990). The branch point isoenzymes  $\alpha$ -isopropylmalate synthase I and II, which catalyze the reaction from  $\alpha$ -ketoisovalerate to  $\alpha$ -isopropylmalate, are encoded by *LEU4* and *LEU9* (Voss *et al.*, 1997; Casalone *et al.*, 2000). The activities of the  $\alpha$ -isopropylmalate synthase I and II are subject to feedback inhibition by leucine and can be reversible inactivated by CoA and Zn<sup>2+</sup>. Besides, the transcription of *LEU4* is controlled by the transcription factors Leu3p and Gcn4p. The final effector of the general control Gcn4p acts twofold on this pathway: a) Gcn4p increases the level of Leu3p, which in turn can lead to the an increased expression of the Leu3p target

genes and b) Gcn4p acts directly on at least 4 genes of the extended leucine pathway (*ILV3*, *LEU4* and *BAT1-BAT2*), while the effect on three more genes (*ILV2*, *ILV5* and *LEU1*) may be indirect through Leu3p. The simultaneous stimulation of *LEU3* and *LEU4* ensures the building of both components of the Leu3p- $\alpha$ -isopropylmalate complex and consequently the production of leucine, isoleucine and valine.

Both biosynthetic pathways of the aromatic amino acids (phenylalanine, tyrosine and tryptophan) and the branched amino acids (leucine, isoleucine and valine) are regulated via feedback-inhibition. The common pathway of leucine, isoleucine and valine can be shut off by the feedback-inhibitor leucine. While leucine causes a stop of the  $\alpha$ -isopropylmalate production, which does not lead to transcriptional activation of the *ILV2* gene. The following indirect effect is the shut off of the pathway. Within the aromatic amino acid pathway tyrosine acts on chorismate mutase and tyrosine regulated DAHP synthase (Aro4p) as a feedback inhibitor and phenylalanine inhibits the second DAHP synthase (Aro3p) of yeast. As the Aro4p is not only inhibited by tyrosine and phenylalanine reduces its activity as well and both feedback-inhibitors can shut off the pathway directly (Figure 47).

Considering all facts, the aromatic amino acid biosynthetic pathway is strictly regulated with subtle regulation of the initial isoenzymes by all three end-products phenylalanine, tyrosine and tryptophan. Therefore the production succession is important. As tryptophan is the first produced aromatic amino acid, it is able to reduce the specific activities of the anthranilate synthase complex (to stop the metabolic flux into the tryptophan branch) and the two DAHP synthases with a simultaneous activation of the chorismate mutase. There are still enough DAHP synthases left to assure a high enough level of chorismate. Now phenylalanine and tyrosine can be produced. When the cellular pools of phenylalanine are filled the activity of Aro3p is nearly completely feedback inhibited and the specific activity of Aro4p is reduced. When tyrosine has been built this endproduct reduces the specific activities of the chorismate mutase at the beginning of the phenylalanine/tyrosine branch and the tyrosine regulated DAHP synthase Aro4p as initial isoenzyme of the whole pathway. The transcription factor Gcn4p of the general control system serves as an additional backup system of regulating the enzyme levels in the cell to balance the pool of aromatic amino acids.

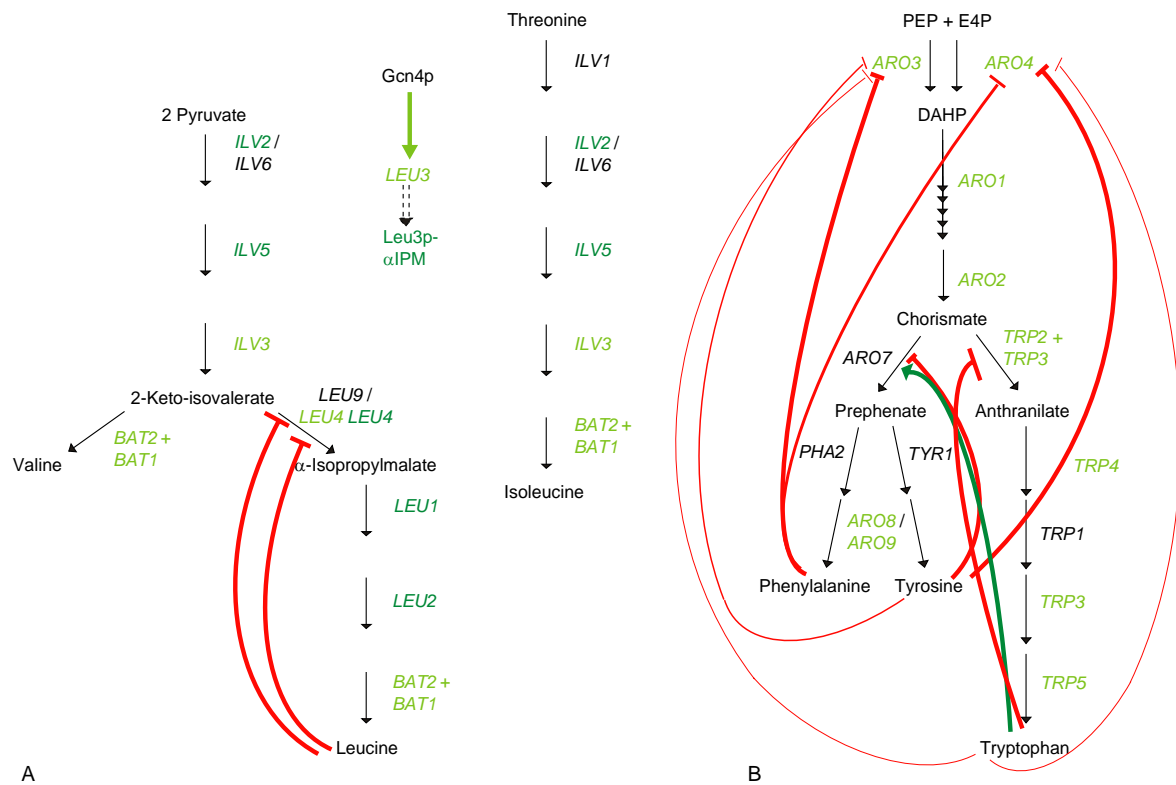


**Figure 47: Comparing overview of the branched biosynthetic pathways of branched-amino acids (leucine, isoleucine and valine) and aromatic amino acids (phenylalanine, tyrosine and tryptophan).** In the scheme above, the corresponding genes of the enzymes are given. Those, which are transcriptional activated by the Leu3p- $\alpha$ -isopropylmalate complex (Leu3p- $\alpha$ -IPM) in the pathway of leucine, isoleucine and valine, are given in dark green. Transcriptional activation by Gcn4p is displayed in light green gene names in both pathways. Red lines indicate feedback inhibition of the resulting enzyme activities and the thickness display the intensity of inhibition. The dark green arrow indicate activation of the resulting enzyme activity. The light green arrow (A) indicates the derepression of the *LEU3* gene by Gcn4p (Kohlhaw, 2003).

## 5. Conclusions

The biosynthetic pathway of aromatic amino acids is strictly regulated in different modes – transcriptional activation and the regulation of the enzyme specific activities by the endproducts. Most genes encoding for enzymes of this pathway are derepressed under amino acid starvation conditions by Gcn4p, so that the pools of phenylalanine, tyrosine and tryptophan can be filled if imbalanced. The down regulation of the pathway occurs one step after another by feedback regulating enzymes at the first branch point and at the beginning with built tryptophan, phenylalanine and tyrosine. If the feedback-regulation of chorismate mutase at the first branch point is deranged Gcn4p serves as backup system. If this backup system fails as well, the survival of the cell can be assured in the presence of an exogenous phenylalanine source by an unregulated DAHP synthase at the beginning of the biosynthetic pathway. This “phe”-effect is an artificial starvation for tryptophan in the presence of exogenous phenylalanine of yeast, which contain unregulated and constitutively expressed chorismate mutase and no final effector Gcn4p of the general control. While investigating in the inhibitory effect of phenylalanine we prompted us to ask if the prephenate dehydratase Pha2p is feedback inhibited by phenylalanine, like prephenate dehydratases of other organisms. A single amino acid substitution in the potentially regulatory ACT-domain of the enzyme transforms *S. cerevisiae*'s prephenate dehydratase in a phenylalanine-regulated enzyme. Presumably this regulation was abolished during evolution.

The regulation of a whole biosynthetic pathway is strictly organized and the tyrosine regulated DAHP synthase Aro4p is part of this complicated interplay. To understand the mode of action of this enzyme catalysis, which was further deduced from crystal structure as investigated. Therefore amino acid substitutions at the catalytic site (Lys112, Arg114 and Arg180) were introduced and the importance of especially these residues was confirmed. The mode of action of the inserted inhibitor molecule tyrosine within the allosteric site of Aro4p was also deduced from crystal structures in the presence of different ligands. Internal movement and changing of structural elements of the DAHP synthase caused by the fixation of tyrosine leads to a re-arrangement of the H-bond network, which displays signal transduction within one monomer from the regulatory to its catalytic site and between the two monomers of a dimer, from the allosteric site of monomer 1 to the catalytic site of monomer 2.

## 6. References

- Aebi, M.** (1983). *Die Struktur des TRP3-Gens von Saccharomyces cerevisiae*. Dissertation. Nr.7349, Eidgenössische Technische Hochschule, Zürich.
- Ahn, H. J., H. J. Yoon, B. n. Lee and S. W. Suh** (2004). Crystal structure of chorismate synthase: a novel FMN-binding protein fold and functional insights. *J. Mol. Biol.* **336**: 903-915.
- Al Rabiee, R., Y. Zhang and G. A. Grant** (1996). The mechanism of velocity modulated allosteric regulation in D-3-phosphoglycerate dehydrogenase: site-directed mutagenesis of effector binding site residues. *J. Biol. Chem.* **271**: 23235-23238.
- Anderson, K. S.** (1999). Fundamental mechanisms of substrate channeling. *Methods Enzymol.* **308**: 111-145.
- Anderson, K. S.** (2005). Detection of novel enzyme intermediates in PEP-utilizing enzymes. *Arch. Biochem. Biophys.* **433**: 47-58.
- Andrews, P. R., G. D. Smith and I. G. Young** (1973). Transition-state stabilization and enzymic catalysis. Kinetic and molecular orbital studies of the rearrangement of chorismate to prephenate. *Biochemistry* **12**: 3492-3498.
- Aravind, I. and E. V. Koonin** (1999). Gleaning non-trivial structural, functional and evolutionary information about proteins by iterative database searches. *J. Mol. Biol.* **287**: 1023-1040.
- Asojo, O., J. Friedman, N. Adir, V. Belakhov, Y. Shoham and T. Baasov** (2001). Crystal structures of KDOP synthase in its binary complexes with the substrate phosphoenolpyruvate and with a mechanism-based inhibitor. *Biochemistry* **40**: 6326-34.
- Atkinson, D. E.** (1977). *Cellular Energy Metabolism and its Regulation*. New York, Academic press.
- Babbitt, P. C., M. S. Hasson, J. E. Wedekind, D. R. Palmer, W. C. Barrett, G. H. Reed, I. Rayment, D. Ringe, G. L. Kenyon and J. A. Gerlt** (1996). The enolase superfamily: a general strategy for enzyme-catalyzed abstraction of the alpha-protons of carboxylic acids. *Biochemistry* **35**: 16489-16501.
- Baichwal, V. R., T. S. Cunningham, P. R. Gatzek and G. B. Kohlhaw** (1983). Leucine biosynthesis in yeast: Identification of two genes (*LEU4*, *LEU5*) that affect  $\alpha$ -isopropylmalate synthase activity and evidence that *LEU1* and *LEU2* gene expression is controlled by  $\alpha$ -isopropylmalate and the product of a regulatory gene. *Curr. Genet.* **7**: 369-377.

- Banner, D. W., A. Bloomer, G. A. Petsko, D. C. Phillips and I. A. Wilson** (1976). Atomic coordinates for triose isomerase from chicken muscle. *Biochem. Biophys. Res. Commun.* **72**: 146-155.
- Barea, J. L. and N. H. Giles** (1978). Purification and characterization of quinate (shikimate) dehydrogenase, an enzyme in the inducible quinic acid catabolic pathway of *Neurospora crassa*. *Biochim. Biophys. Acta* **524**: 1-14.
- Bentley, R.** (1990). The shikimate pathway - A metabolic tree with many branches. *Crit. Rev. Biochem. Mol. Biol.* **25**: 307-384.
- Blow, D.** (2000). So do we understand how enzymes work? *Structure* **8**: 77-81.
- Blum, H., H. Beier and H. J. Grossert** (1987). Improved silver staining of plant proteins, RNA and DNA in polyacrylamide gels. *Electrophoresis* **8**: 93-99.
- Bode, R. and D. Birnbaum** (1991). Regulation of chorismate mutase activity of various yeast species by aromatic amino acids. *Ant. van Leeuwenhoek Int. J. Gen. Microbiol.* **59**: 9-13.
- Bode, R., C. Melo and D. Birnbaum** (1984). Absolute dependence of phenylalanine and tyrosine biosynthetic enzyme on tryptophan in *Candida maltosa*. *Z. Physiol. Chem.* **365**: 790-803.
- Bode, R., K. Schüssler, H. Schmidt, T. Hammer and D. Birnbaum** (1990). Occurrence of the general control of amino acid biosynthesis in yeasts. *J. Basic Microbiol.* **30**: 31-35.
- Bradford, M. M.** (1976). A rapid and sensitive method for quantitation of microgram quantities of protein utilizing the principle of protein-dye binding. *Anal. Biochem.* **72**: 248-254.
- Braus, G. H.** (1991). Aromatic amino acid biosynthesis in the yeast *Saccharomyces cerevisiae*: a model system for the regulation of a eukaryotic biosynthetic pathway. *Microbiol. Rev.* **55**: 349-370.
- Braus, G. H., K. Luger, G. Paravicini, T. Schmidheini, K. Kirschner and R. Hütter** (1988). The role of the *TRP1* gene in yeast tryptophan biosynthesis. *J. Biol. Chem.* **263**: 7868-75.
- Brisco, P. R. G. and G. B. Kohlhaw** (1990). Regulation of yeast *LEU2*: total deletion of regulatory gene *LEU3* unmasks *GCN4*-dependent basal level expression of *LEU2*. *J. Biol. Chem.* **265**: 11667-11675.
- Cain, R. B.** (1981). *Regulation of aromatic and hydroaromatic catabolic pathways in nocardiaform actinomycetes*. New York, Gustav Fischer Verlag: 335-354.
- Carpenter, E. P., A. R. Hawkins, J. W. Frost and K. A. Brown** (1998). Structure of dehydroquinate synthase reveals an active site capable of multistep catalysis. *Nature* **394**: 299-302.

- Casalone, E., C. Barberio, D. Cavalieri and M. Polsinelli** (2000). Identification by functional analysis of the gene encoding  $\alpha$ -isopropylmalate synthase II (*LEU9*) in *Saccharomyces cerevisiae*. *Yeast* **16**: 539-545.
- Catcheside, D. E.** (1969). Prephenate dehydrogenase from *Neurospora*: feedback activation by phenylalanine. *Biochem. Biophys. Res. Commun.* **36**: 651-656.
- Chen, S., S. Vincent, D. B. Wilson and B. Ganem** (2003). Mapping of chorismate mutase and prephenate dehydrogenase domains in *Escherichia coli* T-protein. *Eur. J. Biochem.* **270**: 757-763.
- Chipman, D. M. and B. Shaanan** (2001). The ACT domain family. *Curr. Opin. Struct. Biol.* **11**: 694-700.
- Chook, Y. M., H. Ke and W. N. Lipscomb** (1993). Crystal structures of the monofunctional chorismate mutase from *Bacillus subtilis* and its complex with a transition state analog. *Proc. Natl. Acad. Sci. USA* **90**: 8600-8603.
- Christianson, T. W., R. S. Sikorski, M. Dante, J. H. Shero and P. Hieter** (1992). Multifunctional yeast high-copy-number shuttle vector. *Gene* **110**: 119-122.
- Coggins, J. R., C. Abell, L. B. Evans, M. Fredereickson, D. A. Robinson, A. W. Roszak and A. J. Laphorn** (2003). Experiences with the shikimate-pathway enzymes as targets for rational drug design. *Biochem. Soc. Trans.* **31**: 548-552.
- Coggins, J. R., M. R. Boocock, M. S. Campbell, S. Chaudhuri, J. M. Lambert, A. Lewendon, D. M. Mousdale and D. D. Smith** (1985). Functional domains involved in aromatic amino acid biosynthesis. *Biochem. Soc. Trans.* **13**: 299-303.
- Copley, R. R. and P. Bork** (2000). Homology among (betaalpha)(8) barrels: implications for the evolution of metabolic pathways. *J. Mol. Biol.* **303**: 627-641.
- Corpet, F.** (1988). Multiple sequence alignment with hierarchical clustering. *Nucl. Acids Res.* **16**: 10881-10890.
- Davidson, B. E.** (1987). Chorismate Mutase-Prephenate Dehydratase from *Escherichia coli*. *Methods Enzymol.* **142**: 432-439.
- Davis, B. D.** (1955). Intermediates in amino acid biosynthesis. *Adv. Enzymol.* **16**: 287-295.
- Dotson, G. D., P. Nanjappan, M. D. Reily and R. W. Woodard** (1993). Stereochemistry of 3-deoxyoctulosonate 8-phosphate synthase. *Biochemistry* **32**: 12392-12397.
- Duewel, H. S., S. Radaev, J. Wang, R. W. Woodard and D. L. Gatti** (2001). Substrate and metal complexes of 3-deoxy-D-manno-octulosonate-8-phosphate synthase from *Aquifex aeolicus* at 1.9-Å resolution. Implications for the condensation mechanism. *J. Biol. Chem.* **276**: 8393-402.
- Duncan, K., R. M. Edwards and J. R. Coggins** (1987). The pentafunctional arom enzyme of *Saccharomyces cerevisiae* is a mosaic of monofunctional domains. *Biochem. J.* **246**: 375-386.

- Elsemore, D. A. and L. N. Ornston** (1994). The *pca-pob* supraoperonic cluster of *Acinetobacter calcoaceticus* contains *quiA*, the structural gene for quinate-shikimate dehydrogenase. *J. Bacteriol.* **176**: 7659-7666.
- Engelberg, D., C. Klein, H. Martinetto, K. Struhl and M. Karin** (1994). The UV response involving the ras signaling pathway and AP-1 transcription factors is conserved between yeast and mammals. *Cell* **77**: 381-390.
- Euverink, G. J. W., D. J. Wolter and L. Dijkhuizen** (1995). Prephenate dehydratase of the actinomycete *Amycolatopsis methanolica*: purification and characterization of wild-type and deregulated mutant proteins. *Biochem. J.* **308**: 313-320.
- Eykmann, J. F.** (1891). Über die Shikimisäure. *Ber. Dtsch. Chem. Ges.* **24**: 1278.
- Fani, R., P. Lio, I. Chiarelli and M. Bazzicalupo** (1994). The evolution of the histidine biosynthetic genes in procaryotes: a common ancestor for the *hisA* and *hisF* genes. *J. Mol. Evol.* **38**: 489-495.
- Fantes, P. A., L. M. Roberts and R. Hütter** (1976). Free tryptophan pool and tryptophan biosynthetic enzymes in *Saccharomyces cerevisiae*. *Arch. Microbiol.* **107**: 207-214.
- Fazel, A. M. and R. A. Jensen** (1980). Regulation of prephenate dehydratase in Coryneform species of bacteria by L-phenylalanine and by remote effectors. *Arch. Biochem. Biophys.* **200**: 165-176.
- Fischer, R. and R. Jensen** (1987). Prephenate Dehydratase (Monofunctional). *Methods Enzymol.* **142**: 507-512.
- Friden, P. and P. Schimmel** (1988). *LEU3* of *Saccharomyces cerevisiae* activates multiple genes for branched-chain amino acid biosynthesis by binding to a common decanucleotide core sequence. *Mol. Cell. Biol.* **8**: 2690-2697.
- Gerlt, J. A. and P. C. Babbitt** (2001). Divergent evolution of enzymatic function: mechanistically diverse superfamilies and functionally distinct suprafamilies. *Annu. Rev. Biochem.* **70**: 209-246.
- Gibson, F. and J. Pittard** (1968). Pathway of biosynthesis of aromatic amino acids and vitamins and their control in microorganisms. *Bacteriol. Rev.* **32**: 465-492.
- Goosens, A., T. E. Dever, A. Pascual-Ahuir and R. Serrano** (2001). The protein kinase Gcn2p mediates sodium toxicity in yeast. *J. Biol. Chem.* **276**: 30753-30760.
- Graf, R., B. Mehmman and G. H. Braus** (1993). Analysis of feedback-resistant anthranilate synthases from *Saccharomyces cerevisiae*. *J. Bacteriol.* **175**: 1061-8.
- Grant, G. A., D. J. Schuller and L. J. Banaszak** (1996). A model for the regulation of D-3-phosphoglycerate dehydrogenase, a V-max-type allosteric enzyme. *Protein Sci.* **5**: 34-41.

- Gu, W., D. S. Williams, H. C. Aldrich, G. Xie, D. W. Gabriel and R. A. Jensen** (1997). The aroQ and pheA domains of the bifunctional P-protein from *Xanthomonas campestris* in a context of genomic comparison. *Microb. Comp. Genomics* **2**: 141-58.
- Güldener, U., S. Heck, T. Fielder, J. Beinhauer and J. H. Hegemann** (1996). A new efficient gene disruption cassette for repeated use in budding yeast. *Nucleic Acids Res.* **24**: 2519-2524.
- Guthrie, C. and G. R. Fink** (1991). Guide to yeast genetics and molecular biology. *Methods Enzymol.* **194**.
- Hannahan, D.** (1983). Studies on transformation of *Escherichia coli* with plasmids. *J. Mol. Biol.* **166**: 557-580.
- Harris, J., C. Kleanthous, J. R. Coggins, A. R. Hawkins and C. Abell** (1993). Different mechanistic and stereochemical courses for the reactions catalysed by type I and type II dehydroquinases. *J. Chem. Soc., Chem. Commun.* **13**: 1080-1081.
- Hartmann, M.** (2001). *Fungal DAHP Synthases: Evolution and Structure of Differently Regulated Isoenzymes*. Dissertation. Georg-August-University, Göttingen.
- Hartmann, M., T. R. Schneider, A. Pfeil, G. Heinrich, W. N. Lipscomb and G. H. Braus** (2003). Evolution of feedback-inhibited beta /alpha barrel isoenzymes by gene duplication and a single mutation. *Proc. Natl. Acad. Sci. USA* **100**: 862-7.
- Haslam, E.** (1993). *Shikimic Acid. Metabolism and Metabolites*. Chichester, New York, Brisbane, Toronto, Singapore, John Wiley & Sons.
- Haslam, E.** (1993). *Shikimic Acid. Metabolism and Metabolites*. Chichester, New York, Brisbane, Toronto, Singapore: 158.
- Hawkins, A. R., H. K. Lamb, M. Smith, J. W. Keyte and C. F. Roberts** (1988). Molecular organization of the quinic acid utilization (QUT) gene cluster in *Aspergillus nidulans*. *Mol. Gen. Genet.* **214**: 224-231.
- Hawkins, A. R. and M. Smith** (1991). Domain structure and interaction within the pentafunctional arom polypeptide. *Eur. J. Biochem.* **196**: 717-24.
- Helmstaedt, K., G. Heinrich, R. Merkl and G. H. Braus** (2004). Chorismate mutase of *Thermus thermophilus* is a monofunctional AroH class enzyme inhibited by tyrosine. *Arch. Microbiol.* **181**: 195-203.
- Helmstaedt, K., A. Strittmatter, W. N. Lipscomb and G. H. Braus** (2005). Evolution of e-deoxy-D-arabino-heptulosonate-7-phosphate synthase- encoding genes in the yeast *Saccharomyces cerevisiae*. *Proc Natl Acad Sci U S A* **102**: 9784-9789.
- Henn-Sax, M., R. Thoma, S. Schmidt, M. Henning, K. Kirschner and R. Sterner** (2002). Two (betaalpha)(8)-barrel enzymes of histidine and tryptophan biosynthesis have similar reaction mechanisms and common strategies for protecting their labile substrates. *Biochemistry* **41**: 12032-12042.

- Herrmann, K. M. and L. M. Weaver** (1999). The Shikimate pathway. *Annu. Rev. Plant Physiol. Plant Mol. Biol.* **50**: 473-503.
- Hinnebusch, A. G.** (1985). A hierarchy of trans-acting factors modulates translation of the activator of general amino acid control in *Saccharomyces cerevisiae*. *Mol. Cell. Biol.* **5**: 2349-2360.
- Hinnebusch, A. G.** (1988). Mechanism of gene regulation in the general control of amino acid biosynthesis in *Saccharomyces cerevisiae*. *Microbiol. Rev.*
- Hinnebusch, A. G.** (2000). *Mechanism and regulation of initiator methionyl-tRNA binding to ribosomes*. New York, Cold Spring Harbor Laboratory Press: 185-243.
- Hinnebusch, A. G. and K. Natarajan** (2002). Gcn4p, a master regulator of gene expression, is controlled at multiple levels by diverse signals of starvation and stress. *Euk. Cell* **1**: 22-32.
- Holmes, D. S. and M. Quigley** (1981). A rapid boiling method for the preparation of bacterial plasmids. *Anal. Biochem.* **114**: 193-197.
- Hsu, S. K., L. L. Lin, H.-H. Lo and W. H. Hsu** (2004). Mutational analysis of feedback inhibition and catalytic sites of prephenate dehydratase from *Corynebacterium glutamicum*. *Arch. Microbiol.* **181**: 237-244.
- Inglede, W. M. and C. C. Tai** (1972). Quinate metabolism in *Pseudomonas aeruginosa*. *Can. J. Biochem.* **18**: 1817-1824.
- Inglede, W. M., M. E. F. Tresguerres and J. L. Canovas** (1971). Regulation of the enzymes of the hydroaromatic pathway in *Acinetobacter calcoaceticus*. *J. Gen. Microbiol.* **68**: 273-282.
- Inoue, H., H. MNojima and H. Okayama** (1990). High efficiency transformation of *Escherichia coli* with plasmids. *Gene* **96**: 23-28.
- Irniger, S. and G. H. Braus** (2003). Controlling transcription by destruction: the regulation of yeast Gcn4p stability. *Curr. Genet.* **44**: 8-18.
- Ito, H., Y. Fukuda, K. Murata and A. Kimura** (1983). Transformation of intact yeast cells treated with alkali cations. *J. Bacteriol.* **153**: 163-8.
- Izui, K., H. Matsumura, T. Furumoto and Y. Kai** (2004). Phosphoenolpyruvate Carboxylase: A New Era of Structural Biology. *Annu. Rev. Plant Biol.* **55**: 69-84.
- Jensen, R. A., G. Xie, D. H. Calhoun and C. A. Bonner** (2002). The correct phylogenetic relationship of KdsA (3-deoxy-d-manno-octulosonate 8-phosphate synthase) with one of two independently evolved classes of AroA (3-deoxy-d-arabino-heptulosonate 7-phosphate synthase). *J. Mol. Evol.* **54**: 416-23.
- Jimenez, N., F. Gonzales-Candelas and F. J. Silva** (2000). Prephenate dehydratase from the aphid endosymbiont (*Buchnera*) displays changes in the regulatory domain that

- suggest its desensitization to inhibition by phenylalanine. *J. Bacteriol.* **182**: 2967-2969.
- Jones, D. G., U. Reusser and G. H. Braus** (1991). Molecular cloning, characterization and analysis of the regulation of the *ARO2* gene, encoding chorismate synthase, of *Saccharomyces cerevisiae*. *Mol. Microbiol.* **5**: 2143-2152.
- Jones, E. W. and G. R. Fink** (1982). *Regulation of amino acid and nucleic acid biosynthesis in yeast*. New York, Cold Spring Harbor Laboratory Press: 181-299.
- Kahan, F. M., J. S. Kahan, P. J. Cassidy and H. Kropp** (1974). The mechanism of action of fosfomycin (phosphomycin). *Ann. NY Acad. Sci.* **235**: 364-386.
- Kai, Y., H. Matsumura and K. Izui** (2003). Phosphoenolpyruvate carboxylase: three-dimensional structure and molecular mechanisms. *Arch Biochem Biophys* **414**: 170-179.
- Kellis, M., N. Patterson, M. Endrizzi, B. Birren and E. S. Lander** (2003). Sequencing and comparison of yeast species to identify genes and regulatory elements. *Nature* **423**: 241-254.
- Kleanthous, C., R. Deka, K. Davis, S. M. Kelly, A. Cooper, S. E. Harding, N. C. Price, A. R. Hawkins and J. R. Coggins** (1992). A comparison of the enzymological and biophysical properties of two distinct classes of dehydroquinase enzymes. *Biochem. J.* **282**: 687-695.
- Knaggs, A. R.** (1999). The biosynthesis of shikimate metabolites. *Nat. Prod. Rep.* **16**: 525-560.
- Knaggs, A. R.** (2001). The biosynthesis of shikimate metabolites. *Nat. Prod. Rep.* **18**: 334-355.
- Knaggs, A. R.** (2003). The biosynthesis of shikimate metabolites. *Nat. Prod. Rep.* **20**: 119-136.
- Kohen, A., R. Berkovich, V. Belakhov and T. Baasov** (1993). Stereochemistry of the KDO8P synthase. An efficient synthesis of the 3-fluoro analogues of KDO8P. *Bioorg. Med. Chem. Lett.* **3**: 1577-1582.
- Kohlhaw, G. B.** (2003). Leucine Biosynthesis in Fungi: Entering Metabolism through the Back Door. *Microbiol. Mol. Biol. Rev.* **67**: 1-15.
- Koll, P., R. Bode and D. Birnbaum** (1988). Regulation of metabolic branch points of aromatic amino acid biosynthesis in *Pichia guilliermondii*. *J. Basic Microbiol.* **28**: 619-27.
- König, V.** (2002). *Kristallstrukturuntersuchungen zum Katalyse- und Regulationsmechanismus der Tyrosin-regulierten 3-Deoxy-D-arabino-Heptulose-7-Phosphat-Synthase aus Saccharomyces cerevisiae*. Dissertation. Georg-August-Universität, Göttingen.

- König, V., A. Pfeil, G. H. Braus and T. R. Schneider** (2004). Substrate and metal complexes of 3-deoxy-D-arabino-heptulosonate-7-phosphate synthase from *Saccharomyces cerevisiae* provide new insights into the catalytic mechanism. *J. Mol. Biol.* **337**: 675-90.
- Krappmann, S.** (2000). *Biosynthesis of Aromatic Amino Acids in Yeast and Aspergillus - Mechanisms Controlling the Flux of Chorismate*. Dissertation. Georg-August-Universität, Göttingen.
- Krappmann, S., K. Helmstaedt, T. Gerstberger, S. Eckert, B. Hoffmann, M. Hoppert, G. Schnappauf and G. H. Braus** (1999). The *aroC* gene of *Aspergillus nidulans* codes for a monofunctional, allosterically regulated chorismate mutase. *J. Biol. Chem.* **274**: 22275-82.
- Krappmann, S., W. N. Lipscomb and G. H. Braus** (2000). Coevolution of transcriptional and allosteric regulation at the chorismate metabolic branch point of *Saccharomyces cerevisiae*. *Proc. Natl. Acad. Sci. USA* **97**: 13585-90.
- Laemmli, U. K.** (1970). Cleavage of structural proteins during the assembly of the head of the bacteriophage T4. *Nature* **227**: 680-685.
- Lang, D., R. Thoma, M. Henn-Sax, R. Sterner and M. Wilmanns** (2000). Structural evidence for evolution of the beta/alpha barrel scaffold by gene duplication and fusion. *Science* **289**: 1546-1550.
- Lee, A. Y., P. A. Karplus, B. Ganem and J. Clardy** (1995). Atomic structure of the buried catalytic pocket of Escherichia-coli chorismate mutase. *J. Am. Chem. Soc.* **117**: 3627-3628.
- Li, Z., K. A. Sau, S. Chen, C. Whitehouse, T. Baasov and K. S. Anderson** (2003). A Snapshot of Enzyme Catalysis Using Electrospray Ionization Mass Spectrometry. *J. Am. Chem. Soc.* **125**: 9938-9939.
- Liberles, J. S., M. Thórólfsson and A. Martínez** (2005). Allosteric mechanisms in ACT domain containing enzymes involved in amino acid metabolism. *Amino Acids*.
- Luque, I. and F. E.** (2000). Structural Stability of Binding Sites: Consequences for Binding Affinity and Allosteric Effects. *Proteins: Structure, Function, and Genetics Suppl* **4**: 63-71.
- Maes, D., J. P. Zeelen, N. Thanki, N. Beaucamp, M. Alvarez, M. H. Thi, J. Backmann, J. A. Martial, L. Wyns, R. Jaennicke and R. K. Wierenga** (1999). The crystal structure of trisphosphate isomerase (TIM) from *Thermotoga maritima*: a comparative thermostability structural analysis of ten different TIM structures. *Proteins* **37**: 441-453.

- Mannhaupt, G., R. Stucka, U. Pilz, C. Schwarzlose and H. Feldmann** (1989). Characterization of the prephenate dehydrogenase-encoding gene, *TYR1*, from *Saccharomyces cerevisiae*. *Gene* **85**: 303-311.
- Massant, J. and N. Glansdorff** (2004). Metabolic channelling of carbamoyl phosphate in the hyperthermophilic archaeon *Pyrococcus furiosus*: dynamic enzyme-enzyme interactions involved in the formation of the channelling complex. *Biochem. Soc. Trans.* **32**: 306-309.
- Meimoun, A., T. Holtzman, Z. Weissman, H. McBride, D. J. Stillman and D. Kornitzer** (2000). Degradation of the Transcription Factor Gcn4 Requires the Kinase Pho85 and the SCF<sup>CDC4</sup> Ubiquitin-Ligase Complex. *Mol. Biol. Cell* **11**: 915-927.
- Meusdoerffer, F. and G. R. Fink** (1983). Structure and expression of two aminoacyl-tRNA synthetase genes from *Saccharomyces cerevisiae*. *J. Biol. Chem.* **258**: 6293-6299.
- Miozzari, G., P. Niederberger and R. Hütter** (1978). Tryptophan biosynthesis in *Saccharomyces cerevisiae*: control of the flux through the pathway. *J. Bacteriol.* **134**: 48-59.
- Moesch, H. U., B. Scheier, R. Lahti, P. Mantsala and G. H. Braus** (1991). Transcriptional activation of yeast nucleotide biosynthetic gene *ADE4* by *GCN4*. *J. Biol. Chem.* **266**: 20453-20456.
- Mumberg, D., R. Muller and M. Funk** (1994). Regulatable promoters of *Saccharomyces cerevisiae*: comparison of transcriptional activity and their use for heterologous expression. *Nucleic Acids Res.* **22**: 5767-8.
- Nagano, N., E. G. Hutchinson and J. M. Thornton** (1999). Barrel structures in proteins: automatic identification and classification including a sequence analysis of TIM barrels. *Protein Sci.* **8**: 2072-2084.
- Natarajan, K., M. R. Meyer, B. M. Jackson, D. Slade, C. Roberts, A. G. Hinnebusch and M. J. Marton** (2001). Transcriptional profiling shows that Gcn4p is a master regulator of gene expression during amino acid starvation in yeast. *Mol. Biol. Cell* **21**.
- O'Callaghan, D., D. Maskell, F. Y. Liew, C. S. Easmon and G. Dougan** (1988). Characterization of aromatic- and purine-dependent *Salmonella typhimurium*: attenuation, persistence, and ability to induce protective immunity in BALB/c mice. *Infect. Immun.* **56**: 419-423.
- Paravicini, G., T. Schmidheini and G. Braus** (1989). Purification and properties of the 3-deoxy-D-arabino-heptulosonate-7-phosphate synthase (phenylalanine-inhibitable) of *Saccharomyces cerevisiae*. *Eur. J. Biochem.* **186**: 361-6.
- Park, H., J. L. Hilsenbeck, H. J. Kim, W. A. Shuttleworth, Y. H. Park, J. N. Evans and C. Kang** (2004). Structural studies of *Streptococcus pneumoniae* EPSP synthase in

- unliganded state, tetrahedral intermediate-bound state and S3P-GLP-bound state. *Mol. Microbiol.* **51**: 963-971.
- Pereira, S. A., J. S. de Oliveira, F. Canduri, M. V. Dias, M. S. Palma, L. A. Basso, W. F. J. de Azevedo and D. S. Santos** (2004). Interaction of shikimic acid with shikimate kinase. *Biochem. Biophys. Res. Commun.* **325**: 10-17.
- Pereira, S. A., J. S. de Oliveira, F. Canduri, M. V. Dias, M. S. Palma, L. A. Basso, D. S. Santos and W. F. J. de Azevedo** (2004). Structure of shikimate kinase from *Mycobacterium tuberculosis* reveals the binding of shikimic acid. *Acta Cryst.* **D60**: 2310-2319.
- Piotrowska, M.** (1980). Cross-pathway regulation of ornithine carbamoyltransferase synthesis in *Aspergillus nidulans*. *J. Gen. Microbiol.* **116**: 336-339.
- Pohnert, G., S. Zhang, A. Husain, D. B. Wilson and B. Ganem** (1999). Regulation of phenylalanine biosynthesis. Studies on the mechanism of phenylalanine binding and feedback inhibition in the *Escherichia coli* P-protein. *Biochemistry* **38**: 12212-12217.
- Prantl, F., A. Strasser, M. Aebi, R. Furter, P. Niederberger, K. Kirschner and R. Hütter** (1985). Purification and characterization of the indole-3-glycerolphosphate synthase/antranilate synthase complex of *Saccharomyces cerevisiae*. *Eur. J. Biochem.* **146**: 95-100.
- Radaev, S., P. Dastidar, M. Patel, R. W. Woodard and D. L. Gatti** (2000). Structure and mechanism of 3-deoxy-D-manno-octulosonate 8-phosphate synthase. *J. Biol. Chem.* **275**: 9476-84.
- Raychaudhuri, S., F. Younas, P. A. Karplus, C. H. Faerman and D. R. Ripoll** (1997). Backbone makes significant contribution to the electrostatics of alpha/beta barrel proteins. *Protein Sci.* **6**: 1849-1857.
- Roberts, F., C. W. Roberts, J. J. Johnson, D. E. Kyle, T. Krell, J. R. Coggins, G. H. Coombs, W. K. Milhous, S. Tzipori, D. J. P. Ferguson, D. Chakrabarti and R. McLeod** (1998). Evidence for the shikimate pathway in apicomplexan parasites. *Nature* **393**: 801-805.
- Romero, R. M., M. F. Roberts and J. D. Phillipson** (1995). Chorismate mutase in microorganisms and plants. *Phytochemistry* **40**: 1015-1025.
- Roszak, A. W., D. A. Robinson, T. Krell, I. S. Hunter, M. Fredereickson, C. Abell, J. R. Coggins and A. J. Laphorn** (2002). The structure and mechanism of type II dehydroquinase from *Streptomyces coelicolor*. *Structure* **10**: 493-503.
- Sambrook, J., E. F. Fritsch and T. Maniatis** (1989). *Molecular cloning. A laboratory manual*. Cold Spring Harbor, New York, Cold Spring Harbor Laboratory Press.

- Schagger, H. and G. von Jagow** (1991). Blue native electrophoresis for isolation of membrane protein complexes in enzymatically active form. *Anal. Biochem.* **199**: 223-31.
- Schmidheini, T., H. U. Mösch, R. Graf and G. H. Braus** (1990). A GCN4 protein recognition element is not sufficient for GCN4-dependent regulation of transcription in the *ARO7* promoter of *Saccharomyces cerevisiae*. *Mol. Gen. Genet.* **224**: 57-64.
- Schnappauf, G., M. Hartmann, M. Künzler and G. H. Braus** (1998). The two 3-deoxy-D-arabino-heptulosonate-7-phosphate synthase isoenzymes from *Saccharomyces cerevisiae* show different kinetic modes of inhibition. *Arch. Microbiol.* **169**: 517-24.
- Schnappauf, G., S. Krappmann and G. H. Braus** (1998). Tyrosine and tryptophan act through the same binding site at the dimer interface of yeast chorismate mutase. *J. Biol. Chem.* **273**: 17012-7.
- Schönbrunn, E., S. Eschenberg, F. Krekel, K. Luger and N. Amrhein** (2000). Role of the loop containing residue 115 in the induced-fit mechanism of the bacterial cell wall biosynthetic enzyme MurA. *Biochemistry* **39**: 2164-2173.
- Schönbrunn, E., S. Eschenberg, W. A. Shuttleworth, J. V. Schloss, N. Amrhein, J. N. Evans and W. Kabsch** (2001). Interaction of the herbicide glyphosate with its target enzyme 5-enolpyruvylshikimate 3-phosphate synthase in atomic coil. *Proc. Natl. Acad. Sci. USA* **98**: 1376-1380.
- Schoner, R. and K. M. Herrmann** (1976). 3-Deoxy-D-arabino-heptulosonate 7-phosphate synthase. Purification, properties, and kinetics of the tyrosine-sensitive isoenzyme from *Escherichia coli*. *J. Biol. Chem.* **251**: 5440-7.
- Shevchenko, A., M. Wilm, O. Vorm and M. Mann** (1996). Mass spectrometric sequencing of proteins from silver-stained polyacrylamide gels. *Anal. Chem.* **68**: 850-858.
- Shumilin, I. A., P. A. Bauerle, J. Wu, R. W. Woodard and R. Kretsinger** (2004). Crystal Structure of the Reaction Complex of 3-Deoxy-D-arabino-heptulosonate-7-Phosphate Synthase from *Thermotoga maritima* Refines the Catalytic Mechanism and Indicates a New Mechanism of Allosteric Regulation. *J. Mol. Biol.* **341**: 455-466.
- Shumilin, I. A., R. Bauerle and R. H. Kretsinger** (2003). The high-resolution structure of 3-deoxy-D-arabino-heptulosonate-7-phosphate synthase reveals a twist in the plane of bound phosphoenolpyruvate. *Biochemistry* **42**: 3766-76.
- Shumilin, I. A., R. H. Kretsinger and R. H. Bauerle** (1999). Crystal structure of phenylalanine-regulated 3-deoxy-D-arabino-heptulosonate-7-phosphate synthase from *Escherichia coli*. *Structure Fold Des.* **7**: 865-75.
- Shumilin, I. A., C. Zhao, R. Bauerle and R. H. Kretsinger** (2002). Allosteric inhibition of 3-deoxy-D-arabino-heptulosonate-7-phosphate synthase alters the coordination of both substrates. *J. Mol. Biol.* **320**: 1147-56.

- Simpson, R. J. and B. E. Davidson** (1976). Studies on 3-deoxy-D-arabinoheptulosonate-7-phosphate synthetase(phe) from *Escherichia coli* K12. 1.Purification and subunit structure. *Eur J Biochem* **70**: 493-500.
- Skerra, A. and T. G. M. Schmidt** (2000). Use of the *strep*-tag and streptavidin for detection and purification of recombinant proteins. *Methods Enzymol.* **326**: 271-304.
- Sprinson, D. B.** (1961). The biosynthesis of aromatic compounds from D-glucose. *Adv. Carbohydr. Chem.* **15**: 235-270.
- Subramaniam, P. S., G. Xie, T. Xia and R. A. Jensen** (1998). Substrate ambiguity of 3-deoxy-D-manno-octulosonate 8-phosphate synthase from *Neisseria gonorrhoeae* in the context of its membership in a protein family containing a subset of 3-deoxy-D-arabino-heptulosonate 7-phosphate synthases. *J. Bacteriol.* **180**: 119-27.
- Takahashi, M. and W. W. Chan** (1971). Separation and properties of isozymes of 3-deoxy-D-arabino-heptulosonate-7-phosphate synthetase from *Saccharomyces cerevisiae*. *Can. J. Biochem.* **49**: 1015-25.
- Terpe, K.** (2003). Overview of tag protein fusions: from molecular and biochemical fundamentals to commercial systems. *Appl. Microbiol. Biotechnol.* **60**: 523-533.
- Teshiba, S., R. Furter, P. Niederberger, G. Braus, G. Paravicini and R. Hütter** (1986). Cloning of the *ARO3* gene of *Saccharomyces cerevisiae* and its regulation. *Mol. Gen. Genet.* **205**: 353-7.
- Valenzuela, L., C. Aranda and A. Gonzales** (2001). TOR modulates *GCN4*-dependent expression of genes turned on by nitrogen limitation. *J. Bacteriol.* **183**: 2331-2334.
- Voss, H., V. Benes, M. A. Andrade, A. Valencia, S. Rechmann, C. Teodoru, C. Schwager, V. Paces, C. Sander and W. Ansorge** (1997). DNA sequencing and analysis of 130 kb from yeast chromosome XV. *Yeast* **13**: 1641-1648.
- Wagner, T., R. H. Kretsinger, R. Bauerle and W. D. Tolbert** (2000). 3-Deoxy-D-manno-octulosonate-8-phosphate synthase from *Escherichia coli*. Model of binding of phosphoenolpyruvate and D-arabinose-5-phosphate. *J. Mol. Biol.* **301**: 233-8.
- Wagner, T., I. A. Shumilin, R. Bauerle and R. H. Kretsinger** (2000). Structure of 3-deoxy-D-arabino-heptulosonate-7-phosphate synthase from *Escherichia coli*: comparison of the Mn(2+)\*2-phosphoglycolate and the Pb(2+)\*2-phosphoenolpyruvate complexes and implications for catalysis. *J. Mol. Biol.* **301**: 389-99.
- Walker, G. E., B. Dunbar, I. S. Hunter, G. A. Nimmo and J. R. Coggins** (1996). Evidence for a novel class of microbial 3-deoxy-D-arabino-heptulosonate-7-phosphate synthase in *Streptomyces coelicolor* A32(2), *Streptomyces rimosus* and *Neurospora crassa*. *Microbiology* **142**: 1973-1982.

- Wang, J., H. S. Duetzel, R. W. Woodard and D. L. Gatti** (2001). Structures of *Aquifex aeolicus* KDO8P synthase in complex with R5P and PEP, and with a bisubstrate inhibitor: role of active site water in catalysis. *Biochemistry* **40**: 15676-83.
- Weber, K. and M. Osborn** (1969). The reliability of molecular weight determinations by dodecylsulfate polyacrylamide electrophoresis. *J. Mol. Biol.* **244**: 61-68.
- Weiss, U. and J. M. Edwards** (1980). *The Biosynthesis of Aromatic Amino Acids*. New York, USA, John Wiley & Sons Inc.
- Wierenga, R. K.** (2001). The TIM-barrel fold: a versatile framework for efficient enzymes. *FEBS Lett.* **492**: 193-198.
- Wilmanns, M., C. C. Hyde, D. R. Davies, K. Kirschner and J. N. Jansonius** (1991). Structural conservation in parallel beta/alpha-barrel enzymes that catalyze three sequential reactions in the pathway of tryptophan biosynthesis. *Biochemistry* **30**: 9161-9169.
- Winzler, E. A., D. D. Shoemaker, A. Astromoff, H. Liang, K. Anderson, B. Andre, R. Bangham, R. Benito, J. D. Boeke, H. Bussey, A. M. Chu, C. Connelly, K. Davis, F. Dietrich, S. W. Dow, M. El Bakkoury, F. Foury, S. H. Friend, E. Gentalen, G. Giaver, J. H. Hegemann, T. Jones, M. Laub, H. Liao and R. W. Davis** (1999). Functional characterization of the *S. cerevisiae* genome by gene deletion and parallel analysis. *Science* **285**: 901-906.
- Wise, E. L. and I. Rayment** (2004). Understanding the Importance of Protein Structure to Nature's Routes for Divergent Evolution in TIM barrel Enzymes. *Acc. Chem. Res.* **37**: 149-158.
- Woycechowsky, K. J. and D. Hilvert** (2004). Deciphering enzymes - Genetic selection as a probe of structure and mechanism. *Eur. J. Biochem.* **271**: 1630-1637.
- Xia, T., J. Song, G. Zhao, H. C. Aldrich and R. A. Jensen** (1993). The *aroQ*-encoded monofunctional chorismate mutase (CM-F) protein is a periplasmic enzyme in *Erwinia herbicola*. *J. Bacteriol.* **175**: 4729-4737.
- Xue, Y., W. N. Lipscomb, R. Graf, G. Schnappauf and G. H. Braus** (1994). The crystal structure of allosteric chorismate mutase at 2.2-Å resolution. *Proc. Natl. Acad. Sci. USA* **91**: 10814-10818.
- Yang, R., S. A. Wek and R. C. Wek** (2000). Glucose limitation induces GCN4 translation by activation of Gcn2p protein kinase. *Mol. Cell. Biol.*: 2706-2717.
- Zhang, S., G. Pohnert, P. Kongsaree, D. B. Wilson, J. Clardy and B. Ganem** (1998). Chorismate Mutase-Prephenate Dehydratase from *Escherichia coli*. *J. Biol. Chem.* **273**: 6248-6253.

**Zhang, S., D. B. Wilson and B. Ganem** (2000). Probing the catalytic mechanism of prephenate dehydratase by site-directed mutagenesis of the *Escherichia coli* P-protein dehydratase domain. *Biochemistry* **9**: 4722-4728.

## Danksagung

An dieser Stelle möchte ich mich bei Prof. Dr. Gerhard Braus für die Ermöglichung des selbständigen Arbeitens, für die Überlassung des Themas, für das entgegengebrachte Vertrauen, für die Supervisionen und für die Hilfe beim Suchen und Finden von Geschichten. Danke für eine sehr lehrreiche Zeit.

Herrn PD Dr. Stefan Irniger möchte ich für die freundliche Übernahme des Korreferates danken und für die nette gemeinsame Zeit in der AG Braus.

Ein riesengroßes Dankeschön geht an Christina Munderloh und ihr großes Engagement während ihrer Diplomarbeit. Es hat viel Spaß gemacht, zusammen mit Dir zu arbeiten.

Verena sei herzlichst gedankt für die tolle Zusammenarbeit und den regen Gedankenaustausch über *unsere* DAHP Synthese bei dem ein oder anderen Kaffee und für vieles mehr...

Thomas Schneider möchte ich danken für Ideen zur DAHPS.

Ein großer Dank gilt Virginia Korte, Linda Ebermann, Beate Kellert, Karen Meng und Peter Grzeganeck für ihre Hilfe während ihrer Laborpraktika.

Kerstin Helmstaedt danke ich für die Hilfe und Tricks bei Protein-Fragen (FPLC, Silicon, ...). Sven Krappmann möchte ich danken für die Einführung in den „Phe-Effekt“. Ein Dank geht an Markus Hartmann für die kleine Einführung in die DAHP Synthese. Kerstin und Sven möchte ich auch für das sorgfältige Korrekturlesen der Arbeit danken.

Oliver Valerius und Verena Pretz danke ich für die massenspektrometrischen Auswertungen.

Arnim Wiezer und Jarek Sobkowiak für die große Hilfe an der SGI. Und für die schnellen Reparaturen von PCR-Blöcken und dem Fermenter-Rührantrieb danke ich der Werkstattcrew Olaf Waase, Patrick Regin und Gerhard Birke.

Für das Korrekturlesen geht auch ein riesengroßes Dankeschön an Anke und Peter.

Der wechselnden Labor- und Büro-Crew aus L.146/148 danke ich für eine unvergessliche Zeit. Danke Gaby, Olli, Markus, Axel, Tim, Claudia, Lilly, Stefan, Christina, Aleks, Nico, Stephan, Silke, Kerstin, Krystyna und Elke.

Meinen Eltern, Großeltern, Christina, Julia und Peter danke ich für die immerwährende Unterstützung. Danke, dass es Euch gibt.



## Lebenslauf

<b>Name</b>	Andrea Grzeganeck, geb. Pfeil
<b>Geburtstag</b>	18. April 1975
<b>Geburtsort</b>	Stade
<b>Familienstand</b>	verheiratet
<b>Staatsangehörigkeit</b>	deutsch
<b>Ausbildung</b>	
Sommer 2004 bis Ende 2004	Wissenschaftliche Mitarbeiterin in der Abteilung Neurologie unter PD Dr. Markus Otto an der Medizinischen Fakultät der Georg-August-Universität in Göttingen Bindungsstudien von Prionen (human, murin, Hamster) am Biacore 2000.
Sommer 2000 - Sommer 2004	Wissenschaftliche Mitarbeiterin in der Abteilung für Molekulare Mikrobiologie unter Prof. Dr. Gerhard Braus am Institut für Mikrobiologie und Genetik der Georg-August-Universität in Göttingen mit dem Ziel der Promotion Thema der Dissertation The tyrosine regulated DAHP synthase and the biosynthetic pathway of aromatic amino acids in <i>Saccharomyces cerevisiae</i> .
März 1999 – April 2000	Diplomarbeit unter Prof. Dr. Gerhard Gottschalk am Institut für Mikrobiologie und Genetik der Universität Göttingen Titel der Diplomarbeit: Untersuchungen zur Expression von Genen der F <sub>420</sub> H <sub>2</sub> -Dehydrogenase aus <i>Methanosarcina mazei</i> Gö1 und <i>Achaeeoglobus fulgidus</i>
Februar 1999	Diplomprüfungen in Physikalischer Chemie, Biochemie und Mikrobiologie
Oktober 1996	Diplomvorprüfungen in Anorganischer Chemie, Physikalischer Chemie, Botanik und Mikrobiologie
Oktober 1994 – April 2000	Studium der Biologie an der Georg-August-Universität in Göttingen
Sommer 1987 – Sommer 1994	Gymnasium Vincent-Lübeck-Schule in Stade
Sommer 1985 – Sommer 1987	Besuch der Orientierungsstufe an der Grund- und Hauptschule mit Orientierungsstufe in Grünendeich/Steinkirchen
Sommer 1981 – Sommer 1985	Grundschule Hollern-Twielenfleth